



UNICAMP

**UNIVERSIDADE ESTADUAL DE CAMPINAS
FACULDADE DE ENGENHARIA DE ALIMENTOS**

Carolina Siqueira Franco Picone

**FORMAÇÃO DE NANOPARTÍCULAS POR ASSOCIAÇÃO
DE BIOPOLÍMEROS E SURFACTANTES**

Orientadora/Supervisor: Profa. Dra. Rosiane Lopes da Cunha

**FORMATION OF NANOPARTICLES BY
BIOPOLYMER - SURFACTANT ASSOCIATION**

**Tese de Doutorado apresentada à Faculdade de
Engenharia de Alimentos – UNICAMP, para a
obtenção do título de Doutora em Engenharia de
Alimentos**

**Doctorate thesis presented to the Faculty of
Food Engineering of the University of Campinas
to obtain the Ph.D. grade in Food Engineering**

Este exemplar corresponde à versão final da tese de doutorado defendida por Carolina Siqueira Franco Picone, aprovada pela comissão julgadora em 26/06/2012 e orientada pela Profa. Dra. Rosiane Lopes da Cunha

Profa. Dra. Rosiane Lopes da Cunha

CAMPINAS, 2012

FICHA CATALOGRÁFICA ELABORADA POR
CLAUDIA AP. ROMANO DE SOUZA – CRB8/5816 - BIBLIOTECA DA FACULDADE DE
ENGENHARIA DE ALIMENTOS – UNICAMP

P588f Picone, Carolina Siqueira Franco, 1983-
Formação de nanopartículas por associação de
biopolímeros e surfactantes / Carolina Siqueira Franco
Picone. -- Campinas, SP: [s.n], 2012.

Orientador: Rosiane Lopes da Cunha.
Tese (doutorado) – Universidade Estadual de
Campinas, Faculdade de Engenharia de Alimentos.

1. Nanopartículas. 2. Surfactantes. 3. Gelana. 4.
Quitosana. I. Cunha, Rosiane Lopes. II. Universidade
Estadual de Campinas. Faculdade de Engenharia de
Alimentos. III. Título.

Informações para Biblioteca Digital

Título em inglês: Formation of nanoparticles by biopolymer - surfactant
association

Palavras-chave em inglês:

Nanoparticles

Surfactants

Gellan gum

Chitosan

Área de concentração: Engenharia de Alimentos

Titulação: Doutor em Engenharia de Alimentos

Banca examinadora:

Rosiane Lopes da Cunha [Orientador]

Ângelo Luiz Fazani Cavallieri

Fernanda Yumi Ushikubo

Lucimara Gaziola de la Torre

Vânia Regina Nicoletti Telis

Data da defesa: 26/06/2012

Programa de Pós-Graduação: Engenharia de Alimentos

BANCA EXAMINADORA

Profa. Dra. Rosiane Lopes da Cunha

(Orientadora) – Depto. de Engenharia de Alimentos/FEA/UNICAMP

Profa. Dra. Ana Silvia Prata Soares

(Membro titular) – Faculdade de Ciências Aplicadas/ UNICAMP

Prof. Dr. Ângelo Luiz Fazani Cavallieri

(Membro titular) – Depto. de Tecnologia de Alimentos/UFG

Profa. Dra. Lucimara Gaziola de la Torre

(Membro titular) – Depto. de Processos Biotecnológicos/FEQ/UNICAMP

Profa. Dra. Vânia Regina Nicolleti

(Membro titular) – Depto. de Engenharia e Tecnologia de Alimentos/IBILCE/UNESP

Dra. Fernanda Yumi Ushikubo

(Membro Suplente) – Depto. de Engenharia de Alimentos/FEA/UNICAMP

Profa. Dra. Flávia Maria Neto

(Membro Suplente) – Depto. de Alimentos e Nutrição/FEA/UNICAMP

Profa. Dra. Jane Selia dos Reis Coimbra

(Membro Suplente) – Depto. de Tecnologia de Alimentos/UFV

Um cientista é como um explorador de matas, cujo trabalho é desbravar uma floresta sobre a qual pouco se sabe. Seu objetivo é descobrir as maravilhas naturais nela escondida. Em seu dia-a-dia muitas vezes ele se perde, desvia do que acha ser o caminho certo. Mas isso também faz parte, ele é um explorador. Nesses desvios outras coisas podem ser encontradas, muitas das vezes tão ou mais interessantes que as que desejava encontrar inicialmente.

(Autor desconhecido)

AGRADECIMENTOS

À Faculdade de Engenharia de Alimentos, em especial ao Departamento de Engenharia de Alimentos, por possibilitar a realização deste trabalho.

Ao CNPq, Capes e Fapesp pelo apoio financeiro.

À Prof^ª Rosiane Lopes da Cunha pela valiosa orientação e por despertar em mim a paixão pela ciência.

À banca examinadora pelas sugestões para conclusão deste trabalho.

A todos os professores que durante toda minha vida acadêmica contribuíram para minha formação.

Aos meus pais, Taís e Salvador e à minha irmã, Fernanda.

Ao Guilherme pelo companheirismo, conselhos e paciência.

A todos os colegas e amigos do laboratório e departamento.

À Prof^ª Maria Helena A. Santana (FEQ/Unicamp) e ao Prof. Watson Loh (IQ/Unicamp) pelas colaborações.

A todas as pessoas não mencionadas, que direta ou indiretamente contribuíram para a realização desse trabalho.

SUMÁRIO

<i>Capítulo 1: Introdução e Objetivos</i>	1
1. Introdução.....	3
2. Objetivos.....	5
2.1. Objetivos específicos.....	5
3. Organização da tese em capítulos.....	6
4. Revisão Bibliográfica.....	7
<i>Capítulo 2: Revisão Bibliográfica</i>	9
1. Complexos polieletrólitos.....	11
2. Quitosana.....	14
3. Goma gelana.....	19
4. Surfactantes.....	23
5. Interações polímero – surfactante.....	28
6. Referências Bibliográficas.....	31
<i>Capítulo 3: Influence of pH on formation and properties of gellan gels</i>	43
Abstract.....	45
1. Introduction.....	45
2. Material and methods.....	47
2.1. Material.....	47
2.2. Preparation of the gellan solutions.....	47
2.3. Oscillatory rheology.....	48
2.4. Thermal behaviour.....	48
2.5. Compression testing.....	49
2.6. Scanning electron microscopy.....	50
2.7. Statistical analyses.....	50
3. Results.....	50
3.1. Thermal scanning rheology.....	50
3.2. DSC.....	54
3.3. Compression testing.....	58
3.4. Microscopy.....	59

4. Discussion.....	61
5. Conclusion.....	63
6. Acknowledgements.....	64
7. References.....	64
<i>Capítulo 4: Polysorbates-chitosan association</i>	67
<i>Study of polysorbates - chitosan association to the formation of nano and microstructures</i>	69
Abstract.....	69
1. Introduction.....	70
2. Experimental.....	72
2.1 Materials.....	72
2.2. Preparation of systems.....	72
2.3. Electrical conductivity, zeta potential and particle size distribution.....	73
2.4. Rheological measurements.....	73
2.4.1. Flow curves.....	73
2.4.2. Oscillatory measurements.....	74
2.5. Polarizing microscopy.....	74
2.6. Statistical analysis.....	74
3. Results.....	75
3.1. Effect of length of polysorbate hydrophobic tail.....	75
3.2. Effect of pH on the self-assembly of polysorbate-20.....	85
3.3. Polysorbate-chitosan association.....	87
4. Conclusions.....	95
5. References.....	95
<i>Capítulo 5: Chitosan-Gellan electrostatic complexes</i>	99
<i>Chitosan-Gellan electrostatic complexes: influence of polysaccharide ratio, preparation conditions and surfactant presence</i>	101
Abstract	101
1. Introduction.....	102
2. Materials.....	104
3. Methods.....	105

3.1. Preparation of stock solutions.....	105
3.2. Sample preparation.....	105
3.3. Particle size, zeta potential and quantity of particles.....	106
3.4. Particles stability.....	107
3.5. Statistical analysis.....	107
4. Results.....	107
4.1. Effect of polysaccharide concentration on chitosan-gellan complexation	107
4.2. Particle stability.....	113
4.3. Effect of PEC preparation on its properties.....	118
4.4. Influence of surfactant	121
5. Conclusion.....	126
6. References.....	126
<i>Capítulo 6: Conclusões Gerais.....</i>	<i>131</i>
<i>Apêndice 1: Ensaios preliminares de dissolução dos polissacarídeos.....</i>	<i>135</i>
1. Objetivos.....	137
2. Métodos.....	137
3. Resultados.....	137
4. Referências Bibliográficas.....	139
<i>Apêndice 2: Caracterização reológica da quitosana a diferentes temperaturas.....</i>	<i>141</i>
1. Objetivo.....	143
2. Métodos.....	143
2.1. Preparação das soluções.....	143
2.2. Ensaios reológicos.....	143
2.2.1. Curvas de escoamento.....	143
2.2.2. Ensaios oscilatórios.....	144
3. Resultados e Discussão.....	145
3.1. Curvas de escoamento.....	145
3.2. Ensaios oscilatórios.....	149
4. Conclusões.....	150
5. Referências Bibliográficas.....	150

ÍNDICE DE TABELAS
Capítulo 2

Tabela 1. Estrutura, massa molar e balanço hidrofílico-lipofílico (HLB) dos surfactantes não-iônicos mais comumente empregados em alimentos (Hait & Moulik, 2001).....	25
--	----

Capítulo 3

Table 1. Transition temperatures of the complex viscosity changes for 1.5% (w/w) gellan solutions at pH 3.5, 5.3 and 7.0 during consecutive cooling – heating cycles.....	53
Table 2. Temperatures of G' and G'' crossover for 1.5% (w/w) gellan solutions at pH 3.5, 5.3 and 7.0 during consecutive cooling – heating cycles.....	54
Table 3. Peak temperatures of thermograms for 1.5% (w/w) gellan solutions at pH 3.5, 5.3 and 7.0 during consecutive cooling – heating cycles.....	57
Table 4. Enthalpy values for 1.5% (w/w) gellan solutions at pH 3.5, 5.3 and 7.0 during consecutive cooling – heating cycles. Negative sign means exothermic transition.....	57

Capítulo 4

Table 1. Rheological parameters of samples composed of polysorbate-20 or polysorbate-80 and water at pH 6.7.....	75
Table 2. Gelation temperature of polysorbate-80/water samples during cooling.....	77
Table 3. Size range of polysorbate samples at different surfactant concentrations.....	81
Table 4. Viscosity at 70 s ⁻¹ , electrical conductivity and size range of polysorbate-20/water (pH 6.7) and polysorbate-20/acetate buffer (pH 3) at 25°C.....	86
Table 5. Rheological parameters of non-Newtonian chitosan-polysorbate-20 systems.....	88
Table 6. Size range of polysorbate-chitosan systems.....	91

Capítulo 5

Table 1. Composition of chitosan (CH):gellan (GN) systems.....	105
Table 2. Composition of chitosan (CH):gellan (GN):surfactant (ST) ternary systems.....	106
Table 3. Range of diameters of the particles formed with different chitosan:gellan ratios.....	111
Table 4. Range in diameter of the chitosan:gellan particles with storage time at 25 °C...117	
Table 5. Count rate and zeta potential of samples prepared in 2 steps: properties of the samples during the first and second mixing steps.....	119

Apêndice 2

Tabela 1. Parâmetros reológicos da lei da potência para solução de quitosana 0,2 % (m/m) em diferentes temperaturas.....147

ÍNDICE DE FIGURAS

Capítulo 2

Figura 1. Representação esquemática do efeito do pH no grau de ionização dos polieletrólitos e conseqüente estrutura dos complexos. Adaptado de Berger et al. (2004).....	13
Figura 2. Representação esquemática do processo de desacetilação da quitina e formação da quitosana.....	14
Figura 3. Representação esquemática das mudanças químicas induzidas pela redução de pH da solução de quitosana. Adaptado de Farris et al. (2011).....	16
Figura 4. Unidade tetramérica da gelana desacilada (Ogawa et al. 2006).....	19
Figura 5. Representação esquemática do processo de transição conformacional da gelana (Miyoshi et al., 1996).....	21
Figura 6. Estrutura molecular dos surfactantes não-iônicos mais comumente empregados em alimentos. A) Tweens, B) Spans.....	24
Figura 7. Parâmetros de empacotamento, estrutura geométrica dos surfactantes e respectivas estruturas dos agregados formados. Adaptado de Holmberg et al. (2003).....	27

Capítulo 3

Figure 1. Complex viscosity (η^*) and $\tan(\delta)$ in heating – cooling cycles (20 – 90 °C) of gellan gum 1.5 % (w/w) at different pH values: (A) and (B) pH 3.5; (C) and (D) pH 5.3; and (E) and (F) pH 7.0. (- · - ·) transition temperatures on cooling; (- - -) transition temperatures on heating. I. First cooling, II. Heating, III. Second cooling. The inset shows the method used to determine the transitions.....	52
Figure 2. DSC-thermograms of gellan 1.5% (w/w) A) pH 3.5, B) pH 5.3 and C) pH 7.0. Temperature rate of 1 °C/min.....	56
Figure 3: Typical strain – stress curves for 1.5% (w/w) gellan gels at pH 3.5, 5.3 and 7.0.....	58
Figure 4. Mechanical properties of gels of 1.5% (w/w) gellan gum at pH 3.5, 5.3 and 7.0. A) Stress at fracture (σ_r), B) Strain at fracture (ϵ_r) and C) Young's modulus (E). Means and error bars were calculated from triplicates of each sample. Means with different letters show statistically significant differences at $p < 0.05$	59
Figure 5. SEM micrographs of 1.5% (w/w) gellan gum gels at pH 3.5, 5.3 and 7.0. Scale bar = 10 μ m.....	60

Capítulo 4

Figure 1. Molecular structure of polysorbates.....	72
Figure 2. Complex viscosity of polysorbate-80/water systems during cooling from 60 to 25 °C.....	76
Figure 3. Elastic (G' , full symbols) and loss modulus (G'' , empty symbols) of polysorbate-80/water systems during cooling.....	78
Figure 4. Electrical conductivity (mS/cm) of polysorbate/water systems at 25 °C, pH 6.7..	79
Figure 5. Size distribution by intensity of polysorbate-20 or 80 and water at different surfactant concentration. A) 10% (w/v), B) 20% (w/v), C) 30% (w/v), D) 40% (w/v), E) 50% (w/v) and D) 60% (w/v).....	82
Figure 6. Visual appearance of polysorbate/water systems at 25 °C. A) Polysorbate-20 and B) Polysorbate-80. The micrographies show the birefringence of samples under cross light.....	84
Figure 7. Viscosity at 100 s^{-1} of chitosan-polysorbate-20 systems formed by different chitosan concentrations: \diamond 0% (w/v), \blacktriangle 0.01% (w/v), \times 0.10% (w/v), \blacksquare 0.50% (w/v) and \circ 1.00% (w/v).....	88
Figure 8. Electrical conductivity (mS/cm) of chitosan-polysorbate-20 assembled systems at 25 °C and different chitosan concentrations: \diamond 0% (w/v), \blacktriangle 0.01% (w/v), \times 0.10% (w/v), \blacksquare 0.50% (w/v) and \circ 1.00% (w/v). The zoom highlights the effect of 0.01% (w/v) in 40 - 50% (w/v) polysorbate mixed systems.....	89
Figure 9. Size distribution by intensity of chitosan and chitosan-polysorbate-20 systems at different polysorbate concentrations: A) 0% (w/v), B) 10% (w/v), C) 20% (w/v), D) 30% (w/v), E) 40% (w/v), F) 50% (w/v), G) 60% (w/v).....	92
Figure 10. Schematic representation of complexation between polymers and surfactants. A) Surfactant adsorption along polymer molecule and B) Surfactant adsorption in the form of discrete micelles.....	93

Capítulo 5

Figure 1. Zeta potential of 0.01% (w/v) gellan and 0.01% (w/v) chitosan solutions at different pH values.....	108
Figure 2. Zeta potential of chitosan:gellan systems at pH 4.5 and different polysaccharide ratios.....	109
Figure 3. Volume-weighted size distribution of chitosan (1C:0G), gellan (0C:1G) and mixed samples at different chitosan:gellan ratios. The illustrations show the hypothetical interactions between the polysaccharides.....	112
Figure 4. Zeta potential of samples 1C:9G, 2C:8G and 3C:7G during storage at 25 °C..	114
Figure 5. Count rate of 3C:7G, 2C:8G and 1C:9G samples during storage at 25 °C. The inset graph shows the count rate in the first 5 hours after mixing the polysaccharides.....	115

Figure 6. Volume-weighted size distribution of the 3C:7G, 2C:8G and 1C:9G samples during storage at 25°C.....	118
Figure 7. Illustration of PEC formation in the M20:80 sample	120
Figure 8. Volume-weighted size distribution of the 3C:7G and 2C:8G samples with added 0.0001% (w/v) polysorbate-20 during 48 hours of storage at 25 °C. A) 3C:7G:0.1S and b) 2C:8G:0.1S.....	122
Figure 9. Influence of the addition of polysorbate (0.0001% w/v) on the zeta potential of the 3C:7G and 2C:8G samples during 48 hours of storage at 25 °C.....	123
Figure 10. Volume-weighted size distribution of the 3C:7G and 2C:8G samples with added polysorbate-20: 0.00005, 0.0001, 0.0002, 0.0005 and 0.0010% (w/v).....	125

Apêndice 2

Figura 1. Curva de escoamento típica de uma solução de quitosana 0,2 % (m/m) a 10, 20, 30, 50 e 80°C.....	145
Figura 2. Viscosidade em estado estacionário (η) versus taxa de deformação de soluções de quitosana 0,2 % (m/m) em diferentes temperaturas.....	146
Figura 3. Efeito da temperatura sobre a viscosidade aparente ($50 \cdot s^{-1}$) de solução de quitosana 0,2 % (m/m).....	148
Figura 4. Viscosidade Complexa (η^*) durante o aquecimento (símbolos fechados) e resfriamento (símbolos abertos) de soluções de quitosana 0,2 % (m/m).....	150

RESUMO

As nano partículas possuem grande potencial para a liberação controlada de bioativos, porém ainda são pouco exploradas na área de alimentos. Neste trabalho foi estudada a formação de nanopartículas a partir da autoagregação de surfactantes, associação surfactante-polissacarídeo e complexação eletrostática entre diferentes polissacarídeos, no caso, quitosana e gelana. A compreensão das interações moleculares responsáveis pela formação das partículas e o conhecimento das variáveis que afetam sua formação permitem prever e controlar suas propriedades. Tais interações dependem fortemente das características de cada macromolécula, como flexibilidade, estado conformacional e densidade de cargas que são diretamente afetadas pelas condições físico-químicas do meio como pH, força iônica e temperatura. Por isso, este trabalho foi dividido em três etapas. (I) Inicialmente foi avaliado o comportamento em solução dos polissacarídeos utilizados posteriormente para a formação de complexos. Os efeitos do pH e da temperatura nas características reológicas e no estado conformacional de soluções puras de gelana e quitosana foram estudados. A agregação da gelana foi mais sensível às alterações do meio que a quitosana. (II) Na segunda etapa, nanopartículas foram formadas por autoassociação de polissorbatos na presença de quitosana. A influência do comprimento da cauda hidrofóbica do surfactante e do pH do meio nas propriedades das partículas foi estudada por espalhamento de luz, reologia, condutivimetria e microscopia de luz polarizada. O tamanho e estrutura das partículas formadas pelo surfactante de menor cadeia hidrofóbica foram mais favoráveis à associação com a quitosana. O pH do meio (3,0 ou 6,7) não influenciou de maneira significativa as características das partículas. O efeito da concentração de quitosana na estrutura e tamanho de partículas foi analisado. Maiores concentrações levaram a viscosidades mais elevadas, impedindo a agregação das micelas e formando partículas

menores. (III) No terceiro estudo, nanopartículas foram obtidas pela complexação eletrostática de gelana e quitosana. Os efeitos da razão de concentração de cada polissacarídeo, do tempo de estocagem a 25 °C e da presença de um surfactante não-iônico (polissorbato) no tamanho, carga e quantidade de partículas formadas foram avaliados. Devido à menor densidade de carga e flexibilidade da gelana, maior quantidade deste polissacarídeo foi necessária para obtenção de partículas neutras. De forma geral, as partículas apresentaram aumento de tamanho ao longo das primeiras 100 horas após o preparo e não foram observadas mudanças significativas das propriedades das partículas devido à adição de surfactante. O método de preparo das amostras também foi estudado. Partículas preparadas pela mistura das soluções de polissacarídeos em dois passos foram consideravelmente maiores que as preparadas pela mistura em uma única etapa. Este trabalho confirmou a possibilidade de formação de nanopartículas promissoras para a encapsulação de bioativos em alimentos a partir da associação de biopolímeros e surfactantes, cujas propriedades poderiam ser moduladas em função da composição e condições de processo.

ABSTRACT

Nanoparticles are promising vehicles for bioactive delivery, but their potential has not been fully explored by the food industry. This work studied the formation of nanoparticles by self-assembly of surfactants, polysaccharide-surfactant association, and electrostatic complexes formed by different polysaccharides, especially chitosan and gellan gum. The knowledge of molecular interactions and the variables that affect particle formation allows predicting and controlling the properties of nanoparticles. These interactions depend on the characteristics of each macromolecule such as conformation, charge density and flexibility, which are affected by the physico-chemical properties of the solution, such as pH, ionic strength and temperature. This work was divided in three parts: (I) Firstly it was studied the behaviour of each polysaccharide alone. The influence of the pH and temperature on the rheological properties and structural conformation of the pure gellan and chitosan samples was determined. Gellan aggregation was more strongly affected by such variables than chitosan. (II) In the second part, nanoparticles were obtained by polysorbate-chitosan association. The effect of the length of surfactant tail and the solution pH on the particle properties was studied by dynamic light scattering, rheological and conductivity measurements and polarizing microscopy. The size and structure of nanoparticles composed by the shorter surfactant were more appropriated to chitosan assembly. The pH (6.7 or 3.0) did not affect significantly the particle properties. The effects of chitosan concentration on particle structure and size were studied. Greater chitosan concentration led to smaller particles due to the increase in viscosity values which prevented micelles aggregation. (III) In the third study nanoparticles were produced by electrostatic complexation of chitosan and gellan gum. Particle size, charge density, stability and complexes number were evaluated as a function of polysaccharide concentration, chitosan:gellan ratio and the presence of a non-ionic surfactant. Due to the

stiffness and low charge density of gellan gum, a greater amount of such polysaccharide was necessary to obtain neutral particles. Overall particles showed an increase in size during 100 hours of storage at 25 °C, but no significant changes on particle properties were observed due to surfactant addition. The methodology of particle preparation was also evaluated. Particles prepared by 2 mixing steps were markedly larger than those prepared by mixing polysaccharides in a single step (all together). This work showed that it is possible to produce nanoparticles with promising application on bioactive delivery by biopolymer-surfactant association, since their properties could be modulated as a function of composition and process conditions.

– CAPÍTULO 1 –

Introdução e Objetivos

1. Introdução

Devido à instabilidade de compostos bioativos durante o processamento e armazenamento de produtos alimentícios, a tecnologia de nanoencapsulação, anteriormente explorada apenas pela indústria farmacêutica, vem sendo recentemente aplicada à indústria de alimentos (Luo et al., 2011). As nanopartículas oferecem a vantagem de não afetar a palatabilidade do alimento ao qual são incorporadas, além de apresentar uma considerável área superficial, que é um importante fator relacionado à biodisponibilidade de substâncias (Cheong et al., 2008). A habilidade das nanopartículas em encapsular e promover a liberação controlada de compostos funcionais depende de suas características moleculares e físico-químicas como composição, estrutura interna, polaridade, tamanho, estabilidade, hidrofobicidade e carga elétrica (McClements et al., 2009). Portanto, é de interesse estabelecer a relação entre as características das moléculas presentes, o processo de formação e as propriedades finais das nanopartículas.

Sob condições físico-químicas apropriadas, certos tipos de componentes alimentícios se organizam espontaneamente formando estruturas bem definidas. A força precursora para a associação é a redução da energia livre do sistema. A interação entre vários componentes para a formação de uma estrutura organizada reduz a entropia da mistura, o que é termodinamicamente desfavorável. No entanto há uma contribuição entálpica e/ou entrópica que se sobrepõe a esta condição. A natureza dessa contribuição favorável depende do sistema, mas normalmente envolve ligações de hidrogênio, interações hidrofóbicas e eletrostáticas (McClements et al., 2009). A associação de surfactantes é o tipo mais comum de estruturas auto-organizadas em alimentos (Mezzenga et al., 2005). A força motriz para a formação das estruturas é o caráter

anfílico de sua estrutura molecular. O efeito hidrofóbico da cauda do surfactante faz com que as moléculas se auto-organizem de forma a minimizar o contato desfavorável entre a cauda apolar do surfactante e o meio hidrofílico. O tipo de estrutura formada e seu tamanho podem ser controlados pela seleção cuidadosa do surfactante de acordo com a carga da sua fração hidrofílica e comprimento da cauda hidrofóbica, e o controle das condições do meio como pH, força iônica e temperatura (Lawrence, 1994).

Nanoestruturas também podem ser obtidas através de complexos eletrostáticos. Neste caso, as forças precursoras são interações eletrostáticas entre moléculas de cargas opostas. A maneira mais comum de variar o sinal e força das interações eletrostáticas intermoleculares é através do controle do pH do sistema, o qual afeta diretamente a densidade de carga dos compostos (Berger et al., 2004). Os polissacarídeos são ingredientes alimentícios promissores para a formação de complexos eletrostáticos devido à grande diversidade de estruturas e cargas. Dentre eles destaca-se a quitosana, que vem sendo muito estudada para a formação de sistemas de liberação controlada devido à sua abundância e propriedade mucoadesiva, a qual aumenta a absorção dos bioativos pela mucosa intestinal (Dash et al., 2011; Gåserød et al., 1998). Por outro lado, nanopartículas compostas por quitosana pura são instáveis no pH do estômago, podendo levar à liberação precoce do composto de interesse. A sua complexação com um polissacarídeo resistente a tais condições, como a gelana, pode gerar nanopartículas com grande potencial de encapsulação de bioativos alimentícios. Ao contrário da maioria dos polissacarídeos utilizados em alimentos, a gelana possui a capacidade de formar géis inclusive em baixos valores de pH (Picone & Cunha, 2011; Yamamoto & Cunha, 2007). Assim, a utilização da gelana na composição das nanopartículas proporcionaria a proteção do composto ao baixo pH do estômago, permitindo sua liberação controlada no local de absorção.

2. Objetivos

Este trabalho teve como objetivo estudar os mecanismos de formação e as características de diferentes nanopartículas formadas pela associação de biopolímeros e surfactantes, com potencial aplicação em encapsulação de bioativos alimentícios.

2.1. Objetivos específicos

- Compreender o comportamento em solução dos polissacarídeos utilizados para a formação das nanopartículas. Determinar o efeito do pH e temperatura na conformação e agregação da gelatina e da quitosana.

- Formar nanopartículas por associação de surfactantes (polissorbato) e quitosana. Para isso foram avaliados:

- A influência do comprimento da cadeia hidrofóbica do polissorbato no processo de autoassociação e formação das estruturas e na viscosidade das mesmas, de forma a selecionar o surfactante mais adequado para interação com a quitosana.
- O efeito do pH do meio no processo de autoassociação do surfactante.
- A influência da concentração de quitosana e de surfactante nas propriedades reológicas, tamanho e condutividade elétrica dos sistemas.

- Formar nanopartículas por complexos eletrolíticos quitosana-gelatina. Os objetivos específicos desta etapa foram:

- Entender os mecanismos de formação e a influência da razão de polieletrólitos e condições de mistura nas características dos complexos (tamanho e estabilidade durante a estocagem).
- Compreender o efeito da adição de surfactante na formação e propriedades destes complexos.

3. Organização da tese em capítulos

Os mecanismos de interação entre biopolímeros (no caso polissacarídeos) e surfactantes são muito complexos e dependem não apenas das características de cada componente, mas também das condições do meio. O pH e a temperatura da solução, por exemplo, podem ocasionar alterações estruturais nos polissacarídeos que irão determinar seu mecanismo de agregação e interação com outros compostos. Por isso, inicialmente foi realizado um estudo do comportamento de soluções puras de cada polissacarídeo, no caso gelana e quitosana, frente ao pH e temperatura do meio. Os resultados dos ensaios de dissolução de cada biopolímero são apresentados no Apêndice 1. O comportamento reológico da quitosana e da gelana frente às variações de pH e temperatura do meio são apresentados no Apêndice 2 e Capítulo 3, respectivamente. A partir destes resultados, foram determinadas as condições de trabalho para as próximas etapas.

Abaixo se detalha a estrutura desta tese:

Capítulo 1: Introdução e objetivos

Capítulo 2: Revisão bibliográfica

Capítulo 3: Influence of pH on formation and properties of gellan gels.

Dependendo do estado conformacional da gelana, diferentes interações são observadas. Neste capítulo foi estudada a transição conformacional hélice-enovelada da gelana em diferentes valores de pH e temperatura através de ensaios reológicos e microcalorimetria diferencial de varredura. Os resultados foram publicados na *Carbohydrate Polymers* (2011), v. 84, p. 662–668.

Capítulo 4: Polysorbates-chitosan association.

Com o intuito de produzir nanopartículas mistas de surfactante e quitosana, diferentes polissorbatos e condições do meio foram estudadas. Primeiramente foi avaliado o efeito do comprimento da cauda hidrofóbica do surfactante no processo de agregação e

nas estruturas formadas. O polissorbato que apresentou maior compatibilidade para a associação com a quitosana foi escolhido para as próximas etapas. O efeito do pH na estrutura foi avaliado e a associação do polissorbato com quitosana em diferentes concentrações foi estudada.

Capítulo 5: Chitosan-Gellan electrostatic complexes.

Neste capítulo foram formadas nanopartículas por complexos eletrostáticos quitosana-gelana. A razão de concentração entre os polissacarídeos foi analisada em relação ao tamanho dos complexos formados, densidade de carga e quantidade de complexos. A estabilidade dos complexos ao longo do tempo de estocagem a 25 °C foi avaliada, assim como diferentes métodos de preparo (ordens distintas de misturas dos polissacarídeos). O efeito da adição de polissorbato no preparo dos complexos foi estudado visando à redução de tamanho dos mesmos.

Capítulo 6 – Conclusões gerais

Apêndice 1 – Ensaio preliminares de dissolução dos polissacarídeos

Apêndice 2 - Caracterização reológica da quitosana a diferentes temperaturas.

4. Revisão Bibliográfica

- Berger, J., Reist, M., Mayer, J. M., Felt, O., & Gurny, R. (2004). Structure and interactions in chitosan hydrogels formed by complexation or aggregation for biomedical applications. *European Journal of Pharmaceutics and Biopharmaceutics*, 57(1), 35-52.
- Cheong, J. N., Tan, C. P., Man, Y. B. C., & Misran, M. (2008). alpha-tocopherol nanodispersions: Preparation, characterization and stability evaluation. *Journal of Food Engineering*, 89(2), 204-209.
- Dash, M., Chiellini, F., Ottenbrite, R. M., & Chiellini, E. (2011). Chitosan—A versatile semi-synthetic polymer in biomedical applications. *Progress in Polymer Science*, 36(8), 981-1014.
- Gåserød, O., Jolliffe, I. G., Hampson, F. C., Dettmar, P. W., & Skjåk-Bræk, G. (1998). The enhancement of the bioadhesive properties of calcium alginate gel beads by coating with chitosan. *International Journal of Pharmaceutics*, 175(2), 237-246.

- Lawrence, M. J. (1994). Surfactant systems: their use in drug delivery. *Chemical Society Reviews*, 23(6), 417-424.
- Luo, Y., Zhang, B., Whent, M., Yu, L., & Wang, Q. (2011). Preparation and characterization of zein/chitosan complex for encapsulation of α -tocopherol, and its in vitro controlled release study. *Colloids and Surfaces B: Biointerfaces*, 85(2), 145-152.
- McClements, D. J., Decker, E. A., Park, Y., & Weiss, J. (2009). Structural design principles for delivery of bioactive components in nutraceuticals and functional foods. *Critical Reviews in Food Science and Nutrition*, 49(6), 577-606.
- Mezzenga, R., Schurtenberger, P., Burbidge, A., & Michel, M. (2005). Understanding foods as soft materials. *Nature Materials*, 4(10), 729-740.
- Picone, C. S. F., & Cunha, R. L. (2011). Influence of pH on formation and properties of gellan gels. *Carbohydrate Polymers*, 84(1), 662-668.
- Yamamoto, F., & Cunha, R. L. (2007). Acid gelation of gellan: Effect of final pH and heat treatment conditions. *Carbohydrate Polymers*, 68(3), 517-527.

- CAPÍTULO 2 -
Revisão Bibliográfica

1. Complexos polieletrólíticos

Complexos macromoleculares de diferentes polímeros podem ser formados via ligações intermoleculares como ligações de hidrogênio, forças de Coulomb, van der Waals e forças de transferência. De acordo com a natureza das forças, os complexos formados recebem diferentes nomenclaturas: complexos polieletrólíticos, complexos de transferência de carga, complexos de ligações de hidrogênio e estero-complexos (Dumitriu & Chornet, 1998).

Complexos polieletrólíticos (PECs) consistem na complexação de dois polímeros de cargas opostas, um aniônico e outro catiônico em um meio aquoso (Lee et al., 1997). Eles apresentam propriedades físicas e químicas particulares, pois as interações eletrostáticas no PEC são consideravelmente mais fortes que outras interações secundárias (Lee et al., 2003). Sua aplicação na encapsulação é feita pela incorporação do princípio ativo em uma das soluções de polieletrólito antes da formação do complexo ou pela formação de uma matriz polimérica contendo o bioativo a qual é recoberta por outro polímero para se controlar a taxa de liberação do material encapsulado (Simsek-Ege et al., 2003).

Assim como as propriedades de hidrogéis são determinadas pela densidade de ligações, as características dos PECs são governadas pelo grau de interação entre os polímeros. A quantidade de interações depende essencialmente da densidade de carga de cada polieletrólito e determina sua proporção relativa no complexo. Quanto menor a densidade de carga relativa do polímero, maior sua proporção no PEC visto que maior quantidade de cadeias é necessária para interagir com o outro polieletrólito (Berger et al., 2004). A razão entre os biopolímeros é um dos principais fatores que determinam as propriedades dos complexos, as quais podem ser moldadas pelo controle da reação de complexação (Takahashi et al., 1990). Os fatores mais importantes a serem controlados

nesta reação é o pH da solução, temperatura e força iônica do meio (Argüelles-Monal et al., 1993; Chavasit et al., 1988; Lee et al., 1997). O pH determina o grau de ionização dos polieletrólitos e para que eles estejam ionizados com cargas opostas, é necessário que o pH da solução esteja entre o pKa de ambos polissacarídeos (Lee et al., 1999). A Figura 1 apresenta as mudanças estruturais do PEC geradas por alterações no pH de soluções de polieletrólitos de cargas opostas. Em baixos valores de pH, o polieletrólito catiônico apresenta alta densidade de carga, porém o polieletrólito aniônico está pouco ionizado e portanto, um baixo número de interações é observado. Em altos valores de pH, o polieletrólito catiônico apresenta baixa densidade de carga e novamente, pequena quantidade de interações é estabelecida. A faixa ideal de pH para formação do PEC é observada em valores intermediários de pH, onde ambos polieletrólitos encontram-se fortemente carregados com cargas opostas (Figura 1).

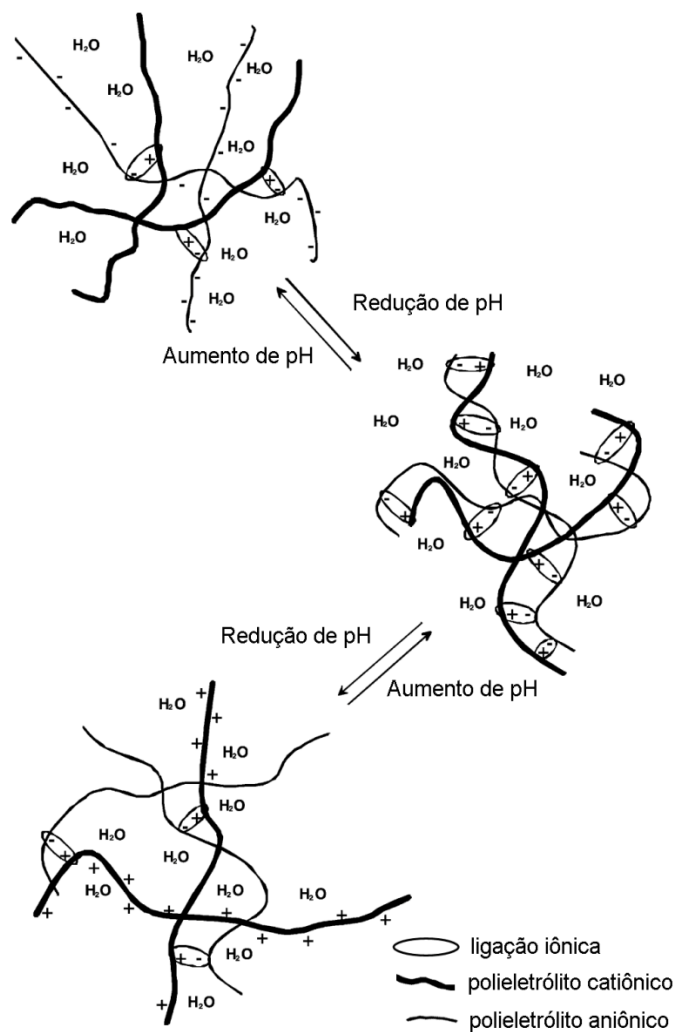


Figura 1. Representação esquemática do efeito do pH no grau de ionização dos polieletrólitos e consequente estrutura dos complexos. Adaptado de Berger et al. (2004).

A ordem e razão de mistura dos polímeros também devem ser observadas durante a complexação (Fukuda & Kikuchi, 1978), assim como fatores característicos de cada polieletrólito, como a densidade de carga, massa molar, distribuição dos sítios ionizáveis ao longo da estrutura, flexibilidade, variação do estado conformacional, grau de ionização e de substituição do polímero (Bartkowiak & Hunkeler, 1999; Berger et al., 2004; Bhattarai et al., 2010; Etrych et al., 2005; Hamman, 2010; li'ina & Varlamov, 2005; Park et al., 2010).

Quando os polieletrólitos são misturados em uma razão na qual há excesso de carga (tanto positiva, como negativa), um complexo não estequiométrico é formado, o qual normalmente é solúvel devido à repulsão eletrostática entre as partículas. Por outro lado, um complexo polieletrólito estequiométrico é formado quando há quantidades iguais de cargas opostas, ou seja, a carga final da partícula é neutra. Neste caso, os complexos são insolúveis, gerando precipitados (Berret, 2007; Kramarenko et al., 2006; Lima Vidal et al., 2005).

A quitosana, o alginato, a carboximetilcelulose, a λ -carragena e a sulfato-dextrana são os polissacarídeos naturais mais estudados na formação dos complexos polieletrólíticos (Argin-Soysal et al., 2009; Barck & Butler, 2005; Bartkowiak & Hunkeler, 1999; Berger et al., 2004; Briones & Sato, 2010; Dev et al., 2010). Neste trabalho, estudou-se a formação de complexos entre a gelana e a quitosana, cujas características são detalhadas a seguir (seção 2 e 3).

2. Quitosana

A quitosana é um polissacarídeo catiônico derivado da quitina (Figura 2).

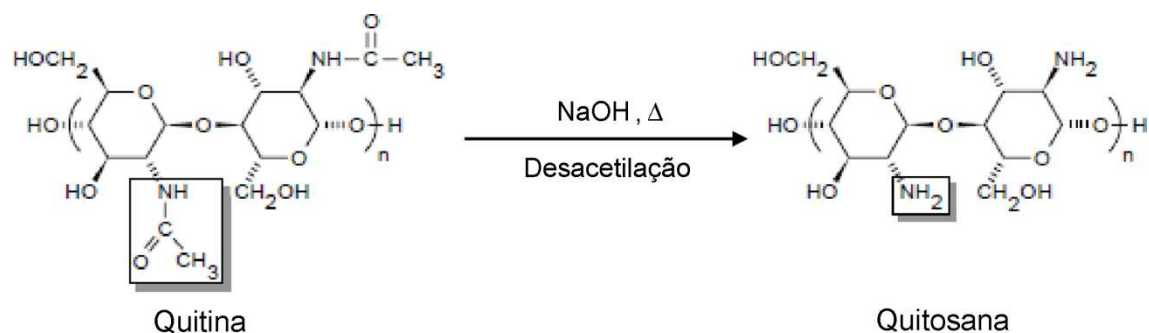


Figura 2. Representação esquemática do processo de desacetilação da quitina e formação da quitosana.

Ela apresenta uma estrutura linear muito semelhante à celulose (Berth et al., 2002), sendo composta por três grupos funcionais reativos: um grupo amino na posição

C-2 ($pK_a \approx 6,3 - 7,0$) e grupos hidroxilas primários e secundários nas posições C-3 e C-6, respectivamente (Claesson & Ninham, 1992; Shahidi et al., 1999). Os grupos aminas, quando protonados, são potenciais sítios de ligações com outros compostos via interações eletrostáticas (Gomez et al., 2006).

As propriedades da quitosana em solução dependem da sua massa molar, grau de desacetilação, pH e força iônica do meio. O grau de desacetilação típico de quitosanas comerciais varia entre 70 e 95% e a massa molar entre 10 e 1000 kDa (George & Abraham, 2006). A dimensão da cadeia de quitosana e seu volume hidrodinâmico dependem do caráter semi-rígido das cadeias, o que está relacionado ao grau de acetilação do polissacarídeo (Rinaudo, 2006). Quanto maior a desacetilação da cadeia, maior sua flexibilidade (Anthonsen et al., 1993; Pedroni et al., 2003). A configuração β -1,4 confere à cadeia da quitosana seu aspecto rígido e caráter linear, enquanto que a abundância de grupos hidroxila (uma hidroxila primária e uma secundária) e o grupo amino altamente reativo explicam a tendência de formar ligações de hidrogênio intra e intermoleculares (Farris et al., 2011).

Em solução, a quitosana se comporta como um polieletrólito “*wormlike*” (Payne & Raghavan, 2007) e seu comprimento de persistência é reportado como 4,2 nm para moléculas 15% acetiladas (Yamakawa & Fujii, 1974), 5 nm para moléculas com grau de acetilação entre 2 e 21% (Rinaudo et al., 1993) e 22 nm para moléculas 42% acetiladas (Terbojevich et al., 1991). O comprimento de persistência (L_p) pode ser obtido a partir da equação de Benoit-Doty que é válida para cadeias “*wormlike*” e monodispersas (equação 1) (Benoit & Doty, 1953):

$$R_{G,\theta}^2 = \frac{LL_p}{3} - L_p^2 + \frac{2L_p^3}{L} - \frac{2L_p^4}{L^2} (1 - e^{-L/L_p}) \quad (1)$$

Onde R_G é o raio de giro da molécula e L é o comprimento de contorno total da cadeia polimérica.

Em valores de pH < 5,5, a forte repulsão eletrostática inter e intramolecular ocasionada pelos grupos amino protonados faz com que as moléculas de quitosana adotem uma conformação estendida o que resulta no aumento de sua solubilidade (Peng et al., 2010; Thongngam & McClements, 2004; Martínez et al., 2004) e torna sua estrutura mais rígida (Pa & Yu, 2001). Em valores de pH intermediários (4 – 6), o raio de giro da quitosana permanece relativamente constante (Schatz et al., 2003). Já em valores de pH acima de 6 ela perde suas cargas e tende a precipitar devido à desprotonação dos grupos amino (Claesson & Ninham, 1992; Thongngam & McClements, 2004) que diminui a repulsão eletrostática entre as moléculas e favorece as ligações de hidrogênio intra e intermoleculares (Figura 3).

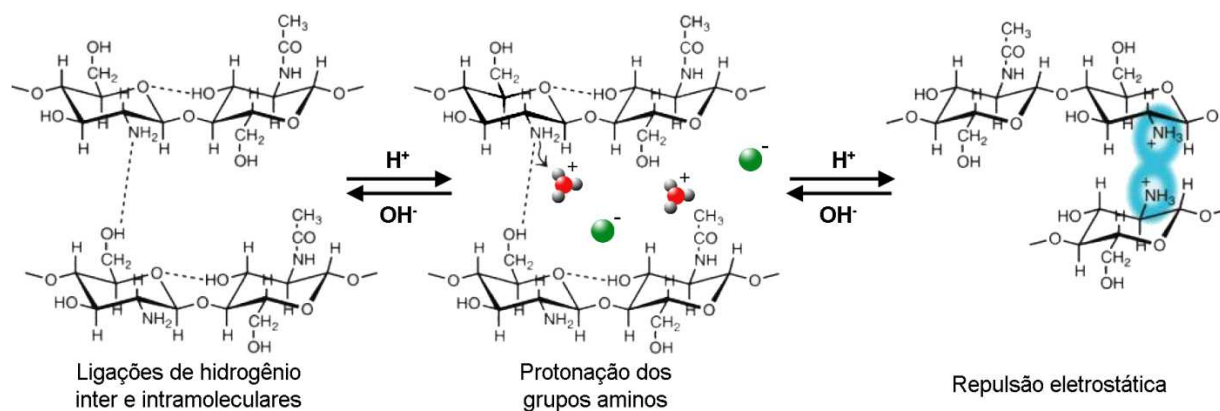


Figura 3. Representação esquemática das mudanças químicas induzidas pela redução de pH da solução de quitosana. Adaptado de Farris et al. (2011).

A flexibilidade rotacional das moléculas de quitosana é relativamente grande para um polieletrólito (Claesson & Ninham, 1992) e aumenta com o aumento do grau de desacetilação do polissacarídeo (Pedroni et al., 2003). No entanto, detalhes sobre sua

conformação estrutural ainda não são bem conhecidos e os trabalhos publicados são contraditórios (Payne & Raghavan, 2007). Pedroni et al. (2003) sugerem que, em solução, as moléculas de quitosana se organizam em blocos de cadeias alongadas, interceptadas por agregados esféricos formados pela aglomeração da fração acetilada do polissacarídeo. Segundo eles, cadeias com alto grau de desacetilação apresentam conformação estendida devido à repulsão eletrostática entre os grupos $-NH_3^+$. Já Vårum et al. (1991) propõem que a quitosana se organiza de forma enovelada. Tsaih e Chen (1997) afirmam que quando a quitosana apresenta massa molar igual ou superior a 223 kDa sua estrutura é enovelada, enquanto massas molares iguais ou menores que 148 kDa correspondem a moléculas com formato de bastão. No entanto, segundo os autores, a densidade de carga do polissacarídeo é muito mais relevante que sua massa molar. Em condições onde os grupos amino estão protonados, a repulsão eletrostática entre eles causa a expansão das cadeias, resultando em uma estrutura enovelada, enquanto que quando os grupos amino são neutralizados observa-se a compactação da estrutura.

Quitosanas com 88% de desacetilação, quando em meio ácido e completamente ionizadas, apresentam 5,85 Å de distância entre os sítios iônicos ao longo da cadeia (Babak et al., 2000).

O uso de quitosana como material de recobrimento de microcápsulas para liberação controlada de compostos tem recebido grande atenção após a descoberta de sua mucoadesividade. Estudos *in vitro* revelam que a quitosana tem a capacidade de aderir à mucosa gástrica de porcos, aumentando a absorção de compostos bioativos (Gåserød et al., 1998). O mecanismo principal de interação entre a quitosana e a mucosa são ligações eletrostáticas entre os grupos aminos positivos da quitosana e a camada mucosa negativamente carregada (mucina) (Deacon et al., 2000; Fiebrig et al., 1995; He

et al., 1998). O aumento da massa molar da quitosana resulta em maior adesão a esses tecidos (Lehr et al., 1992).

Hidrogéis de quitosana são obtidos apenas por intermédio de agentes de ligação como tripolifosfato ou glutaraldeído (George & Abraham, 2006; Gomaa et al., 2010). No entanto, sua complexação com polissacarídeos aniônicos também pode resultar na formação de gel sem que seja necessário o uso de agentes reticulantes. Além disso, a complexação pode conferir às partículas maior resistência a baixos valores de pH, visto que a maior limitação do uso de hidrogéis de quitosana em sistemas de liberação controlada é a sua dissolução em baixos valores de pH, como os encontrados no estômago (~1,2). Dentre os polissacarídeos aniônicos, o alginato é o mais estudado para a formação de complexos (George & Abraham, 2006). Sua complexação com a quitosana é irreversível e se dá através de ligações iônicas entre os grupos $-NH_3^+$ e $-COO^-$ da quitosana e do alginato, respectivamente (Bartkowiak & Hunkeler, 1999). Tal interação previne a dissolução dos complexos em baixos valores de pH. Além de melhorar a resistência das partículas à digestão, a formação de complexos permite modelar suas propriedades. Estudos revelam que a complexação entre a quitosana e o alginato reduz a porosidade de cápsulas de alginato, diminuindo a perda do bioativo encapsulado durante a armazenagem e o processo digestivo (Huguet et al., 1996; Sezer & Akbuga, 1999).

O principal tipo de interação entre a quitosana e polissacarídeos aniônicos são as forças eletrostáticas atrativas entre os grupos amino catiônicos da quitosana e os grupos aniônicos do outro polieletrólito (Berger et al., 2004). No entanto, interações secundárias adicionais também podem ocorrer como ligações amida (Nge et al., 2002) e ligações de hidrogênio (Daly & Knorr, 1988; Taravel & Domard, 1995).

Como a quitosana tem uma estrutura rígida, estéreo-regular e com volumosos anéis de piranose (Yao et al., 1997), a formação de complexos polieletrólíticos pode

induzir mudanças conformacionais no outro polieletrólito caso sua estrutura seja menos rígida (Berger et al., 2004), como a da α -keratose (Park et al., 1996), ácido poliacrílico (PAA) (Cerrai et al., 1996), xilana (Gabriellii et al., 2000) ou colágeno (Taravel & Domard, 1995).

3. Goma gelana

A gelana é um polissacarídeo aniônico extracelular, produzido pela bactéria *Sphingomonas elodea*. O produto direto da fermentação é o polissacarídeo em sua forma altamente acilada, cuja repulsão estérica impede a gelificação. O tratamento com álcali resulta na forma desacilada, que é a normalmente comercializada e possui elevado poder gelificante. Em sua forma desacilada, a gelana apresenta uma sequência complexa de tetrassacarídeos (Figura 4) que se repetem: β -D- glucose, β -D- ácido glucurônico e α -L- ramnose na proporção molar de 2: 1: 1, e um grupo lateral carboxílico em cada unidade tetramérica repetida (Milas & Rinaudo, 1996; Miyoshi et al., 1996; Sanderson, 1990). Sua densidade de carga é relativamente baixa quando comparada a de outros polissacarídeos como as pectinas e carragenas, sendo de 0,25 mol de cargas negativas/mol de monossacarídeo (de Jong & van de Velde, 2007).

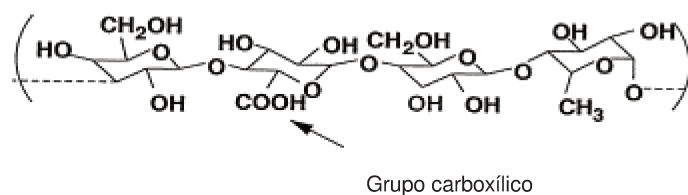


Figura 4. Unidade tetramérica da gelana desacilada (Ogawa et al., 2006).

A gelana possui alto poder gelificante, e tem a capacidade de formar gel inclusive em baixas concentrações (Rodríguez-Hernández et al., 2003). Diferentemente de outros polissacarídeos tradicionalmente utilizados em alimentos, como agarose e carragenas, a gelana forma géis rígidos, translúcidos e resistentes a baixos valores de pH (Moritaka et

al., 1995; Picone & Cunha, 2011; Yamamoto & Cunha, 2007). A resistência ao baixo pH confere à gelana um potencial uso como agente encapsulante, visto que um dos principais desafios nessa área é o desenvolvimento de um material de parede que ofereça proteção às severas condições de pH do estômago.

Em solução aquosa (sol), a gelana apresenta repulsão eletrostática intra e intermolecular entre seus grupos carboxílicos laterais, o que impede tanto a formação quanto a agregação das hélices para a formação de gel. A gelificação de soluções de gelana pode ser induzida pela mudança da força iônica do meio, por alterações de pH, tratamento térmico ou aumento da concentração do polímero (Rodríguez-Hernández et al., 2003). Dois modelos são propostos na literatura para explicar a gelificação da goma gelana (Robinson et al., 1991), o fibroso e o de domínios. Eles são bem similares, mas diferem entre si na descrição dos agregados. O modelo mais comumente aceito é o de domínios, o qual sugere que a altas temperaturas, a gelana se apresenta em estado desordenado (cadeias simples) e na conformação enovelada. Assim, resfriando-se a solução em condições não gelificantes, os novelos se convertem reversivelmente em duplas-hélices (estado ordenado) e a associação dessas duplas-hélices por forças de van der Waals leva à gelificação macroscópica (transição sol – gel), como pode ser observado na Figura 5. Com a redução do pH e/ou na presença de cátions, conjuntos de duplas-hélices se associam formando a rede de gel (Miyoshi et al., 1996; Nickerson et al., 2003; Robinson et al., 1991; Rodríguez-Hernández et al., 2003).

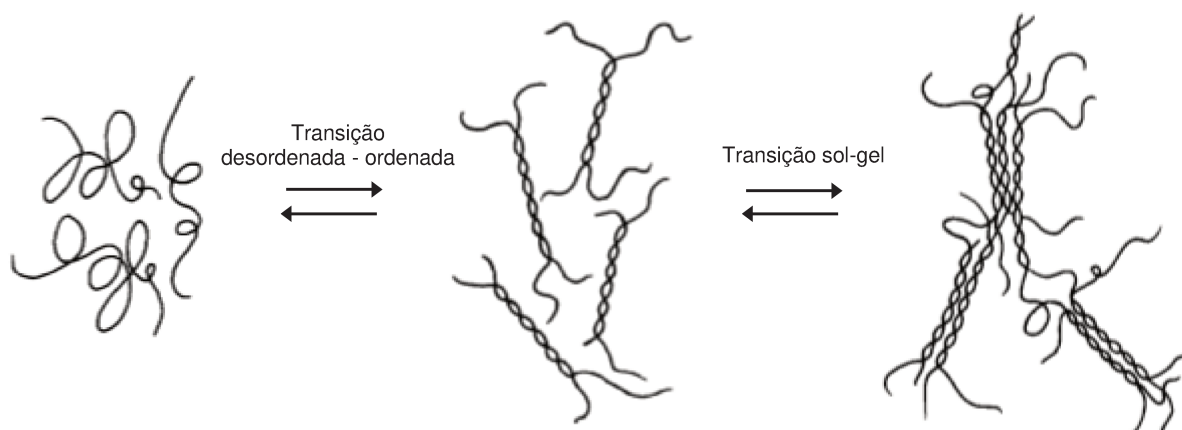


Figura 5. Representação esquemática do processo de transição conformacional da gelana (Miyoshi et al., 1996).

A temperatura de transição conformacional da gelana varia entre 30 e 50 °C, dependendo da concentração do polímero e da composição do solvente (principalmente pH e presença de sais) (Giavasis et al., 2000; Ikeda et al., 2004; Kasapis et al., 1999; Lau et al., 2000; Ogawa et al., 2002; Rodríguez-Hernández et al., 2003), tal como ocorre com a goma xantana (Ikeda et al., 2004; Lee & Brant, 2002). Assim como a xantana, em diferentes trabalhos afirma-se que essa mudança conformacional é reversível (Miyoshi et al., 1996; Nakajima et al., 1996).

O pH natural de uma solução típica de gelana contendo íons cálcio em concentrações de 1,5 a 60 mM está em torno de 5,0 (Sanderson, 1990). Em pH alcalino e sob aquecimento ocorre desacilação das moléculas de gelana (Kang et al., 1982), o que favorece a agregação e contribui para a formação de géis mais fortes que em pH natural, como observado por Moritaka et al. (1995). A redução de pH de dispersões de gelana até valores próximos a 4 também resulta no aumento da força dos géis, independentemente do tipo de acidificação empregada (Moritaka et al., 1995; Yamamoto & Cunha, 2007), visto que nestas condições a repulsão eletrostática entre as moléculas é reduzida e a formação de zonas de junção é favorecida. No entanto, em valores de pH próximos a 2,

dois comportamentos distintos são relatados na literatura. Moritaka e colaboradores (1995) observaram que soluções de gelana acidificadas de forma direta com adição de HCl até pH 2 apresentam aspecto turvo e separação de fases que possivelmente estariam relacionados à hidrólise ácida das moléculas. Já Yamamoto e Cunha (2007) estudaram a acidificação indireta de soluções de gelana a partir da adição de GDL e obtiveram elevados valores de tensão de ruptura em sistemas formados em pH 2. Aparentemente, a acidificação indireta não provoca hidrólise das moléculas de gelana mesmo a baixos valores de pH. O decréscimo do pH também reduz a mobilidade das cadeias de gelana, facilitando a agregação e gelificação. Sabe-se que a redução do pH gera dissociação dos grupos carboxílicos laterais das moléculas de gelana, tornando-a um polieletrólito menos aniônico. A redução da repulsão eletrostática intermolecular favorece a formação de duplas-hélices pela associação de duas moléculas, com a presença de ligações de hidrogênio entre o ácido glucurônico de uma cadeia e a glicose e a ramnose de outra cadeia. Além disso, íons H^+ se ligam à superfície das hélices individuais e diminuem sua densidade de carga, reduzindo a barreira eletrostática para a agregação das hélices e possibilitando a formação de “zonas de junção”. Interações secundárias, incluindo ligações de hidrogênio, ligam as cadeias às zonas de junção, o que resulta na gelificação macroscópica (transição sol – gel) (Giavasis et al., 2000; Horinaka et al., 2004; Ikeda et al., 2004; Kani et al., 2005; Kasapis et al., 1999; Lau et al., 2000; Mao et al., 1999; Moritaka et al., 1995; Nickerson et al., 2003; Ogawa et al., 2002; Rodríguez-Hernández et al., 2003).

Segundo Dentini et al. (1988), em solução a gelana se comporta como um típico polieletrólito “*wormlike*”. Suas cadeias apresentam grande rigidez devido à estrutura volumosa intrínseca da molécula (Takahashi et al., 2004), porém seu tamanho não se altera inclusive em condições de baixa repulsão intramolecular (Horinaka et al., 2004). O

comprimento vertical das duplas hélices de gelana desacilada é reportado como 0,5 nm por “small-angle X-ray diffraction” (Yuguchi et al., 1999). Apesar de ser um polissacarídeo extensivamente estudado, sua complexação com outros polissacarídeos ainda é pouco conhecida.

4. Surfactantes

O termo “surfactante” é usado para designar moléculas relativamente pequenas, com ação superficial e características anfifílicas. Os surfactantes são compostos por uma cabeça hidrofílica e uma cauda hidrofóbica (Hasenhuettl, 2008; McClements, 2004; Myers, 2006), sendo que suas propriedades funcionais dependem das características de cada fração. O grupo hidrofóbico normalmente consiste de uma ou duas cadeias carbônicas contendo entre 10 e 20 átomos de carbono por cadeia. As cadeias carbônicas podem ser saturadas ou insaturadas, lineares ou ramificadas, alifáticas e/ou aromáticas, mas a maioria dos surfactantes alimentícios possui uma ou duas cadeias alifáticas saturadas ou insaturadas (McClements et al., 2009). Já a cabeça hidrofílica do surfactante pode ser catiônica, aniônica, zwitteriônica ou não-iônica. Os surfactantes alimentícios são predominantemente aniônicos (como os sais de ácidos graxos), zwitteriônicos (como a lecitina) ou não-iônicos (monoglicerídeos e polissorbatos como o Tween e o Span) (McClements et al., 2009). Enquanto surfactantes não-iônicos interagem com a fase aquosa via ligações dipolo e ligações de hidrogênio, surfactantes iônicos interagem também por ligações iônicas e covalentes. Portanto sistemas estabilizados por surfactantes iônicos são muito mais instáveis a alterações de força iônica e pH do meio que sistemas compostos por surfactantes não-iônicos (Narang et al., 2007). Devido a isso e à maior toxicidade dos surfactantes iônicos (como o dodecil sulfato de sódio (SDS) que possui carácter aniônico), o emprego de surfactantes não-iônicos, tais como polissorbatos

(Tweens) e ésteres sorbitanos (Spans) (Figura 6) é a mais recomendável em alimentos, além da lecitina de carácter zwitteriônico. Os polissorbatos são derivados de sorbitana esterificados com ácidos graxos (Tabela 1, Figura 6). Dependendo do tipo de ácido graxo presente na molécula, o polissorbato recebe uma numeração, por exemplo: 20 para o monolaurato e 60 para o monoestearato (Tabela 1) (Hait & Moulik, 2001).

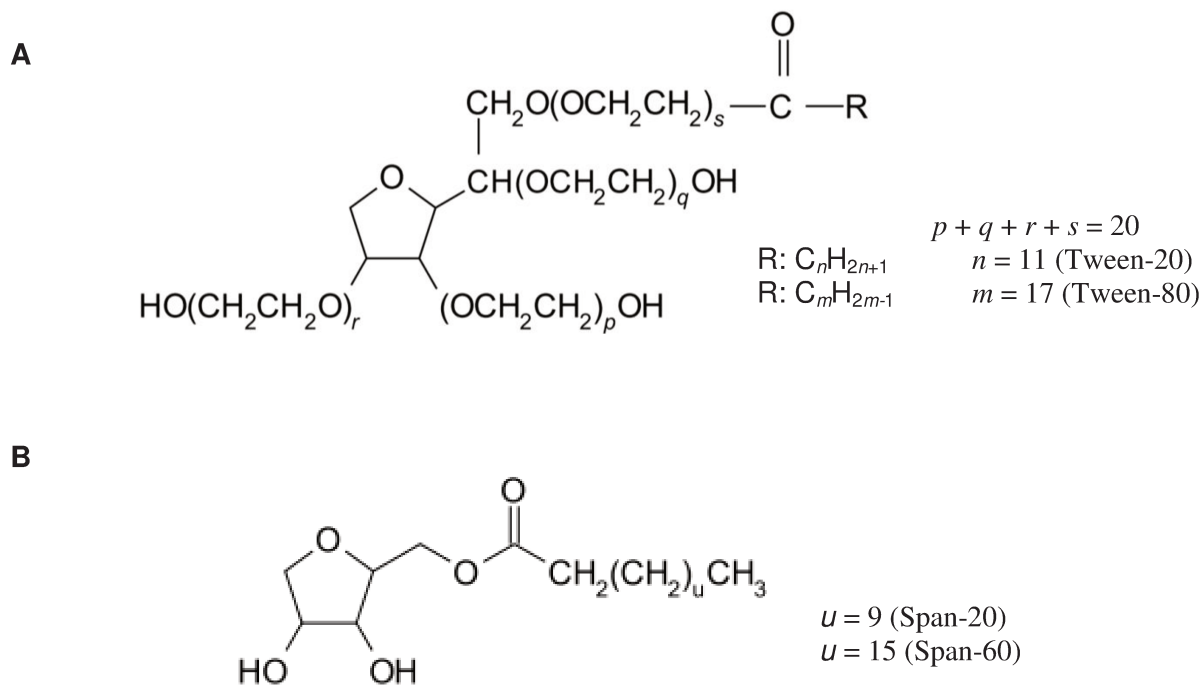


Figura 6. Estrutura molecular dos surfactantes não-iônicos mais comumente empregados em alimentos. A) Tweens, B) Spans.

Tabela 1. Estrutura, massa molar e balanço hidrofílico-lipofílico (HLB) dos surfactantes não-iônicos mais comumente empregados em alimentos (Hait & Moulik, 2001).

Nome comercial	Estrutura	Massa molar (Da)	HLB
Tween 20	Monolaurato de polioxietileno (20) de sorbitana	1227,54	16,7
Tween 60	Monoestearato de polioxietileno (20) de sorbitana	1311,70	14,9
Tween 80	Monooleato de polioxietileno (20) de sorbitana	1309,68	15,0
Span 20	Monolaurato de sorbitana	346,46	8,6
Span 40	Monopalmitato de sorbitana	402,56	6,7
Span 60	Monoestearato de sorbitana	430,62	4,7
Span 80	Monooleato de sorbitana	428,61	4,3

O número 20 em parênteses se refere ao número total de grupos oxietileno presentes na molécula.

Apesar das interações do surfactante com substâncias aquosas estarem relacionadas à característica da sua fração hidrofílica, de forma geral as interações do surfactante com outras moléculas do meio dependem da proporção entre sua parte hidrofílica e hidrofóbica, ou HLB (balanço hidrofílico-lipofílico). Este balanço é fundamental na determinação de suas propriedades, especialmente no caso de autoassociação de surfactantes não-iônicos (Hait & Moulik, 2001). Surfactantes com $HLB > 10$ são predominantemente hidrofílicos e são mais adequados para a dispersão de moléculas hidrofóbicas em meios aquosos que surfactantes com $HLB < 10$ (predominantemente hidrofóbicos) (Narang et al., 2007).

Para surfactantes não-iônicos com grupos polietileno (como os Tweens) o HLB pode ser obtido pela equação 2 (Becher, 1967):

$$HLB = \frac{(\%mol \text{ de grupos hidrofílicos})}{5} \quad (2)$$

Desse modo, o HLB máximo de um surfactante não-iônico não substituído seria 20 (Becher, 1967). Várias maneiras empíricas para a determinação de HLB são propostas na

literatura. Chun e Martin (1961) encontraram uma relação linear entre o HLB de agentes surfactantes e a tensão interfacial das amostras. As amostras foram compostas por soluções contendo 10% do agente surfactante e recobertas por tolueno antes da análise de tensão interfacial. Já Schulz et al. (1998) mediram o HLB de soluções de um biopolímero (quitosana 1% em ácido acético) pela comparação do diâmetro de uma gota de tolueno sobre a solução de quitosana, com o diâmetro obtido pelo gotejamento em soluções de mesma concentração de surfactante cujo HLB já era previamente conhecido.

Como já comentado anteriormente, o HLB é essencial para a determinação do comportamento do surfactante em uma solução. No caso de surfactantes com alto HLB (maior que 10) adicionados a uma solução hidrofílica, a tendência é que ele se mantenha na interface água-ar com a fração hidrofóbica voltada para a parte externa à solução e a parte hidrofílica envolta na fase aquosa, reduzindo dessa maneira a tensão interfacial água-ar. Com o aumento da concentração de surfactante em solução, a tensão interfacial tende a se reduzir até que o filme de surfactante na interface seja rompido pela migração de parte do surfactante para o corpo da solução, este ponto é denominado concentração micelar crítica (CMC). A CMC dos polissorbatos 20 e 80 é 0,07% e 0,015% (m/v), respectivamente (Cottrell & Peij, 2007).

Devido à forte repulsão eletrostática entre a fração hidrofóbica do surfactante e a solução aquosa, as moléculas surfactantes tendem a se auto-organizar formando estruturas termodinamicamente estáveis denominados colóides de associação, com dimensão média entre 1 nm e 1 μ m (Figura 7). O tipo de estrutura formada (Figura 7) depende de diversos fatores como a estrutura e concentração do surfactante, a composição do meio aquoso e a temperatura (McClements et al., 2009) e pode ser estimada a partir do parâmetro de empacotamento (P) do surfactante (equação 3) (Myers, 2006):

$$P = \frac{v}{a \cdot l} \quad (3)$$

onde v e l são o volume e o comprimento da fração hidrofóbica, respectivamente, e a é a área ocupada pelo grupo hidrofílico do surfactante.




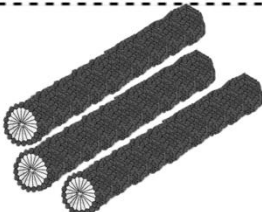

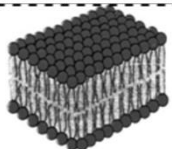
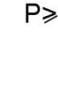
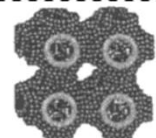


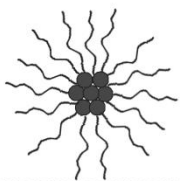
Estrutura geométrica	Estrutura dos agregados	Denominação da fase
$1/3 < P < 1/2$ 		Micelar
	Estruturas intermediárias	Cúbica
$P < 1/3$ 		Hexagonal
	Estruturas intermediárias	Cúbica
$P \approx 1$ 		Lamelar
$P \geq 1$ 		Cúbica
$P > 1$ 		Hexagonal reversa
	Estruturas intermediárias	Cúbica
		Micelar reversa

Figura 7. Parâmetros de empacotamento, estrutura geométrica dos surfactantes e respectivas estruturas dos agregados formados. Adaptado de Holmberg et al. (2003).

A formação dessas estruturas vem sendo estudada por diversas técnicas, incluindo condutivimetria (Zhai et al., 2005), microscopia de luz polarizada (Varade et al., 2007), reologia (Zhao et al., 2011), espalhamento de luz (Herve et al., 1993; Tomašić et al., 2005) e de raio-X (Sagar et al., 2007; Varade et al., 2007), calorimetria (Nibu et al., 1997), fluorescência, espectroscopia, espectrofotometria e ressonância magnética nuclear (NMR) (Hait & Moulik, 2001).

Fases isotrópicas, como as fases micelares e cúbicas são límpidas e transparentes e não apresentam birrefringência quando observadas por microscopia de luz polarizada (Holmberg et al., 2003; Lawrence, 1994). No entanto, a fase micelar apresenta baixa viscosidade, enquanto a fase cúbica é extremamente viscosa (Lawrence, 1994). Já estruturas anisotrópicas como os cristais líquidos apresentam birrefringência e possuem aspecto opaco e/ou translúcido. A fase hexagonal é menos viscosa que a fase cúbica, mas é consideravelmente mais viscosa que a lamelar (Holmberg et al., 2003; Lawrence, 1994).

5. Interações polímero – surfactante

A presença de um polímero pode alterar significativamente a agregação de surfactantes, aumentar a estabilidade térmica das estruturas formadas e ampliar a faixa de concentração da fase micelar (Chevalier & Zemb, 1990).

Quando o polieletrólito e o surfactante apresentam cargas opostas, uma forte associação cooperativa entre ambos é observada enquanto interações mais fracas são observadas entre polímeros não-iônicos e surfactantes iônicos (Sarrazin-Cartalas et al., 1994). Interações entre polímeros iônicos e surfactantes não-iônicos são reportadas em casos em que há uma expressiva quantidade de ligações de hidrogênio entre ambas moléculas (Saito & Taniguch, 1973). Os mecanismos de interação entre essas moléculas

não é completamente compreendido, mas sabe-se que interações hidrofóbicas também são de grande importância. A associação de polímeros e surfactantes é fortalecida quando o polímero possui uma fração de grupos fortemente hidrofóbicos que tendem a interagir com a cauda hidrofóbica do surfactante (Diab et al., 2007). Em alguns casos, as interações hidrofóbicas se sobrepõem inclusive à repulsão eletrostática entre polieletrólitos e surfactantes de mesma carga, levando à associação dos mesmos (Sarrazin-Cartalas et al., 1994). Polímeros com características estruturais específicas também podem apresentar maior afinidade por surfactantes neutros (Diab et al., 2007) como, por exemplo, o ácido poliacrílico (PAA) que se associa à cabeça polar de surfactantes neutros através de ligações de hidrogênio (Ladhe et al., 2006).

As interações entre polímeros e surfactantes dependem de vários fatores como a concentração e razão molar entre os componentes, a força iônica da solução, a natureza do solvente, temperatura, presença de aditivos (Barreiro-Iglesias et al., 2003; Tomašić et al., 2005; Tsianou & Alexandridis, 1999) e características específicas inerentes ao polieletrólito e ao surfactante como o carácter iônico de ambos, a hidrofobicidade do polímero e da cauda apolar do surfactante (Marques et al., 1999; Rosen et al., 1998), a conformação estrutural e flexibilidade do polímero (Barreiro-Iglesias et al., 2003; Ritacco et al., 2000), a massa molar do polímero e sua densidade de carga e o comprimento da cadeia hidrofóbica do surfactante (Goddard, 2002; Holmberg et al., 2003; Pepić et al., 2009; Taylor et al., 2007).

Na presença de um polímero, a associação de surfactantes induzida pelo aumento de sua concentração ocorre de maneira distinta que em meios aquosos puros. Ao migrar para o corpo da solução, as moléculas de surfactante tendem a interagir primeiramente com os sítios de ligação do polímero por interações hidrofóbicas e/ou eletrostáticas, caso ambos tenham cargas opostas, formando complexos polímero-surfactante. A

concentração mínima de surfactante em que essa interação se inicia é denominada concentração de agregação crítica (CAC), a qual é utilizada como uma medida da força de interação entre polímero-surfactante (Kong et al., 2007). Com o aumento da concentração de surfactante, atinge-se o ponto de saturação do polímero, denominado PSP (Silva et al., 2011). Somente após este ponto é que as moléculas de surfactante irão se autoassociar em micelas. Portanto, a CMC em sistemas contendo polímeros é observada em maiores concentrações de surfactante. O aumento da quantidade de átomos de carbono da cauda hidrofóbica do surfactante aumenta a quantidade de interações hidrofóbicas e conseqüentemente o valor da CAC, ocasionando mudanças na estrutura dos complexos formados (Kogej et al., 2001; Thunemann, 2002).

Diferentes mecanismos de interação são propostos para sistemas polímero-surfactante. Barreiro-Iglesias et al. (2003) sugerem que as interações dependem da proporção de cada componente (Goldraich et al., 1997; Guerrini et al., 1998). Abaixo da concentração de agregação crítica (CAC) não ocorre nenhuma interação expressiva entre ambas moléculas. Entre a CAC e a CMC, se a concentração de polímero é menor que a concentração de agregação, a adição de surfactante irá favorecer interações intrapoliméricas (cada agregado envolvendo apenas uma molécula), o que causará o enovelamento da cadeia do polímero e a redução da viscosidade da solução (Goddard, 1993). Para concentrações de polímero maiores que a concentração de agregação, o surfactante age como uma ponte de ligação entre diferentes cadeias poliméricas (complexação interpolimérica), promovendo a formação de uma estrutura tridimensional e o aumento da viscosidade. Acima da CAC o surfactante forma micelas que solubilizam as regiões hidrofóbicas do polímero, reduzindo a quantidade de interações interpoliméricas e conseqüentemente, a viscosidade do sistema (Hansson & Lindman, 1996).

Já Groot (2000) sugere que a adsorção de surfactantes em polímeros pode ocorrer de duas maneiras: a adsorção pode ocorrer ao longo de toda a cadeia do polímero, ou na forma de micelas. O primeiro mecanismo acontece quando a interação polímero-surfactante ocorre predominantemente devido a interações hidrofóbicas entre a cauda do surfactante e sítios hidrofóbicos do polímero. A adsorção na forma de micelas é observada quando a interação polímero-surfactante ocorre predominante pela fração hidrofílica do surfactante. Neste caso, o tamanho das micelas diminui com o aumento da quantidade de sítios hidrofóbicos do polímero (Groot, 2000).

A interação da quitosana com surfactantes aniônicos acontece através de interações eletrostáticas de forte intensidade (Onesippe & Lagerge, 2008; Thongngam & McClements, 2005). Já as interações entre a quitosana e surfactantes não-iônicos são de natureza fraca como associação íon-dipolo, ligações de hidrogênio e interações hidrofóbicas (Goddard, 2002; Taylor et al., 2007). Complexos quitosana - ésteres de sorbitana, por exemplo, são formados por ligações de hidrogênio entre os grupos carboxílicos e hidroxilas do éster de sorbitana e aminas, íons amônio e grupos hidroxilas da quitosana. Além disso, interações hidrofóbicas entre a cauda apolar do éster e sítios hidrofóbicos da quitosana são de grande relevância (Grant et al., 2006). Apesar das interações entre a quitosana e ésteres de sorbitana serem conhecidas (Grant et al., 2006; Grant et al., 2008), não existem estudos sobre seu comportamento frente a outros surfactantes não-iônicos utilizados em alimentos, como os polissorbatos.

6. Referências Bibliográficas

- Anthonsen, M. W., Vårum, K. M., & Smidsrød, O. (1993). Solution properties of chitosans: conformation and chain stiffness of chitosans with different degrees of N-acetylation. *Carbohydrate Polymers*, 22(3), 193-201.
- Argin-Soysal, S., Kofinas, P., & Lo, Y. M. (2009). Effect of complexation conditions on xanthan-chitosan polyelectrolyte complex gels. *Food Hydrocolloids*, 23(1), 202-209.

- Argüelles-Monal, W., Hechavarria, O. L., Rodriguez, L., & Peniche, C. (1993). Swelling of membranes from the polyelectrolyte complex between chitosan and carboxymethyl cellulose. *Polymer Bulletin*, 31(4), 471-478.
- Babak, V. G., Merkovich, E. A., Desbrières, J., & Rinaudo, M. (2000). Formation of an ordered nanostructure in surfactant-polyelectrolyte complexes formed by interfacial diffusion. *Polymer Bulletin*, 45(1), 77-81.
- Barck, K., & Butler, M. F. (2005). Comparison of morphology and properties of polyelectrolyte complex particles formed from chitosan and polyanionic biopolymers. *Journal of Applied Polymer Science*, 98(4), 1581-1593.
- Barreiro-Iglesias, R., Alvarez-Lorenzo, C., & Concheiro, A. (2003). Poly(acrylic acid) microgels (carbopol® 934)/surfactant interactions in aqueous media: Part I: Nonionic surfactants. *International Journal of Pharmaceutics*, 258(1-2), 165-177.
- Bartkowiak, A., & Hunkeler, D. (1999). Alginate–Oligochitosan Microcapsules: A Mechanistic Study Relating Membrane and Capsule Properties to Reaction Conditions. *Chemistry of Materials*, 11(9), 2486-2492.
- Becher, P. (1967). *Non ionic surfactants*. New York: Dekker.
- Benoit, H., & Doty, P. (1953). Light Scattering from Non-Gaussian Chains. *The Journal of Physical Chemistry*, 57(9), 958-963.
- Berger, J., Reist, M., Mayer, J. M., Felt, O., & Gurny, R. (2004). Structure and interactions in chitosan hydrogels formed by complexation or aggregation for biomedical applications. *European Journal of Pharmaceutics and Biopharmaceutics*, 57(1), 35-52.
- Berret, J. F. (2007). Stoichiometry of Electrostatic Complexes Determined by Light Scattering. *Macromolecules*, 40(12), 4260-4266.
- Berth, G., Colfen, H., & Dautzenberg, H. (2002). Physicochemical and chemical characterisation of chitosan in dilute aqueous solution. In Borchard, E. S. A. *Analytical Ultracentrifugation Vi* pp. 50-57.
- Berth, G., & Dautzenberg, H. (1999). Solution behavior of some selected polysaccharides studied preferentially by static light scattering. *Recent Research Developments in Macromolecules Research*, 3(1), 225-248.
- Bhattarai, N., Gunn, J., & Zhang, M. (2010). Chitosan-based hydrogels for controlled, localized drug delivery. *Advanced Drug Delivery Reviews*, 62(1), 83-99.
- Briones, A. V., & Sato, T. (2010). Encapsulation of glucose oxidase (GOD) in polyelectrolyte complexes of chitosan–carrageenan. *Reactive and Functional Polymers*, 70(1), 19-27.

- Cerrai, P., Guerra, G. D., Tricoli, M., Maltinti, S., Barbani, N., & Petarca, L. (1996). Polyelectrolyte complexes obtained by radical polymerization in the presence of chitosan. *Macromolecular Chemistry and Physics*, 197(11), 3567-3579.
- Chavasit, V., Kienzle-Sterzer, C., & Antonio Torres, J. (1988). Formation and characterization of an insoluble polyelectrolyte complex: Chitosan-polyacrylic acid. *Polymer Bulletin*, 19(3), 223-230.
- Chevalier, Y., & Zemb, T. (1990). The structure of micelles and microemulsions. *Reports on Progress in Physics*, 53(3), 279-371.
- Chun, A. H. C., & Martin, A. N. (1961). Measurement of hydrophile-lipophile balance of surface-active agents. *Journal of Pharmaceutical Sciences*, 50(9), 732-736.
- Claesson, P. M., & Ninham, B. W. (1992). Ph-Dependent Interactions between Adsorbed Chitosan Layers. *Langmuir*, 8(5), 1406-1412.
- Cottrell, T., & Peij, J. V. (2007). Sorbitan Esters and Polysorbates. In Whitehurst, R. J. *Emulsifiers in Food Technology* pp. 162-185: Blackwell Publishing
- Daly, M. M., & Knorr, D. (1988). Chitosan-alginate complex coacervate capsules: Effects of calcium chloride, plasticizers, and polyelectrolytes on mechanical stability. *Biotechnology Progress*, 4(2), 76-81.
- de Jong, S., & van de Velde, F. (2007). Charge density of polysaccharide controls microstructure and large deformation properties of mixed gels. *Food Hydrocolloids*, 21(7), 1172-1187.
- Deacon, M. P., McGurk, S., Roberts, C. J., Williams, P. M., Tendler, S. J., Davies, S. J., Davis, S. S., & Harding, S. E. (2000). Atomic force microscopy of gastric mucin and chitosan mucoadhesive systems. *Biochemical Journal*, 348(3), 557-563.
- Dentini, M., Coviello, T., Burchard, W., & Crescenzi, V. (1988). Solution properties of exocellular microbial polysaccharides. 3. Light scattering from gellan and from the exocellular polysaccharide of *Rhizobium trifolii* (strain TA-1) in the ordered state. *Macromolecules*, 21(11), 3312-3320.
- Dev, A., Mohan, J. C., Sreeja, V., Tamura, H., Patzke, G. R., Hussain, F., Weyeneth, S., Nair, S. V., & Jayakumar, R. (2010). Novel carboxymethyl chitin nanoparticles for cancer drug delivery applications. *Carbohydrate Polymers*, 79(4), 1073-1079.
- Diab, C., Winnik, F. M., & Tribet, C. (2007). Enthalpy of interaction and binding isotherms of non-ionic surfactants onto micellar amphiphilic polymers (amphipols). *Langmuir*, 23(6), 3025-3035.
- Dumitriu, S., & Chornet, E. (1998). Inclusion and release of proteins from polysaccharide-based polyion complexes. *Advanced Drug Delivery Reviews*, 31(3), 223-246.
- Etrych, T., Leclereq, L., Boustta, M., & Vert, M. (2005). Polyelectrolyte complex formation and stability when mixing polyanions and polycations in salted media: A model

- study related to the case of body fluids. *European Journal of Pharmaceutical Sciences*, 25(2-3), 281-288.
- Farris, S., Mora, L., Capretti, G., & Piergiovanni, L. (2011). Charge Density Quantification of Polyelectrolyte Polysaccharides by Conductometric Titration: An Analytical Chemistry Experiment. *Journal of Chemical Education*, 89(1), 121-124.
- Fiebrig, I., Harding, S. E., Rowe, A. J., Hyman, S. C., & Davis, S. S. (1995). Transmission electron microscopy studies on pig gastric mucin and its interactions with chitosan. *Carbohydrate Polymers*, 28(3), 239-244.
- Fukuda, H., & Kikuchi, Y. (1978). In vitro clot formation on the polyelectrolyte complexes of sodium dextran sulfate with chitosan. *Journal of Biomedical Materials Research*, 12(4), 531-539.
- Gabriellii, I., Gatenholm, P., Glasser, W. G., Jain, R. K., & Kenne, L. (2000). Separation, characterization and hydrogel-formation of hemicellulose from aspen wood. *Carbohydrate Polymers*, 43(4), 367-374.
- Gåserød, O., Jolliffe, I. G., Hampson, F. C., Dettmar, P. W., & Skjåk-Bræk, G. (1998). The enhancement of the bioadhesive properties of calcium alginate gel beads by coating with chitosan. *International Journal of Pharmaceutics*, 175(2), 237-246.
- George, M., & Abraham, T. E. (2006). Polyionic hydrocolloids for the intestinal delivery of protein drugs: Alginate and chitosan — a review. *Journal of Controlled Release*, 114(1), 1-14.
- Giavasis, I., Harvey, L. M., & McNeil, B. (2000). Gellan Gum. *Critical Reviews in Biotechnology*, 20(3), 177-211.
- Goddard, E. D. (1993). Polymer-surfactant interactions. In Goddard, E. D., & Ananthapadmanabhan, K. P. *Interactions of surfactants with polymers and proteins* pp. 123-169. Boca Raton: CRC Press.
- Goddard, E. D. (2002). Polymer/Surfactant Interaction: Interfacial Aspects. *Journal of Colloid and Interface Science*, 256(1), 228-235.
- Goldraich, M., Schwartz, J. R., Burns, J. L., & Talmon, Y. (1997). Microstructures formed in a mixed system of a cationic polymer and an anionic surfactant. *Colloids and Surfaces a-Physicochemical and Engineering Aspects*, 125(2-3), 231-244.
- Gomaa, Y. A., El-Khordagui, L. K., Boraiei, N. A., & Darwish, I. A. (2010). Chitosan microparticles incorporating a hydrophilic sunscreen agent. *Carbohydrate Polymers*, 81(2), 234-242.
- Gomez, L., Ramirez, H. L., Neira-Carrillo, A., & Villalonga, R. (2006). Polyelectrolyte complex formation mediated immobilization of chitosan-invertase neoglycoconjugate on pectin-coated chitin. *Bioprocess Biosyst Eng*, 28(6), 387-395.

- Grant, J., Cho, J., & Allen, C. (2006). Self-assembly and physicochemical and rheological properties of a polysaccharide–surfactant system formed from the cationic biopolymer chitosan and nonionic sorbitan esters. *Langmuir*, 22(9), 4327-4335.
- Grant, J., Lee, H., Liu, R. C. W., & Allen, C. (2008). Intermolecular Interactions and Morphology of Aqueous Polymer/Surfactant Mixtures Containing Cationic Chitosan and Nonionic Sorbitan Esters. *Biomacromolecules*, 9(8), 2146-2152.
- Groot, R. D. (2000). Mesoscopic simulation of polymer–surfactant aggregation. *Langmuir*, 16(19), 7493-7502.
- Guerrini, M. M., Negulescu, II, & Daly, W. H. (1998). Interactions of aminoalkylcarbamoyl cellulose and sodium dodecyl sulfate. I. Surface tension. *Journal of Applied Polymer Science*, 68(7), 1091-1097.
- Hait, S., & Moulik, S. (2001). Determination of critical micelle concentration (CMC) of nonionic surfactants by donor-acceptor interaction with Iodine and correlation of CMC with hydrophile-lipophile balance and other parameters of the surfactants. *Journal of Surfactants and Detergents*, 4(3), 303-309.
- Hamman, J. H. (2010). Chitosan based polyelectrolyte complexes as potential carrier materials in drug delivery systems. *Marine Drugs*, 8(4), 1305-1322.
- Hansson, P., & Lindman, B. (1996). Surfactant-polymer interactions. *Current Opinion in Colloid & Interface Science*, 1(5), 604-613.
- Hasenhuettl, G. L. (2008). Overview of Food Emulsifiers. In Hasenhuettl, G. L., & Hartel, R. W. *Food Emulsifiers and Their Applications* pp. 1-9. New York: Springer
- He, P., Davis, S. S., & Illum, L. (1998). In vitro evaluation of the mucoadhesive properties of chitosan microspheres. *International Journal of Pharmaceutics*, 166(1), 75-88.
- Herve, P., Roux, D., Bellocq, A. M., Nallet, F., & Gulikkrzywicki, T. (1993). Dilute and concentrated phases of vesicles at thermal-equilibrium. *Journal De Physique II*, 3(8), 1255-1270.
- Holmberg, K., Jönsson, B., Kronberg, B., & Lindman, B. (2003). *Surfactants and polymers in aqueous solution*. West Sussex: John Wiley & Sons.
- Horinaka, J., Kani, K., Hori, Y., & Maeda, S. (2004). Effect of pH on the conformation of gellan chains in aqueous systems. *Biophysical Chemistry*, 111(3), 223-227.
- Huguet, M. L., Neufeld, R. J., & Dellacherie, E. (1996). Calcium alginate beads coated with polycationic polymers: Comparison of chitosan and DEAE-dextran. *Process Biochemistry*, 31(4), 347-353.
- Iliina, A. V., & Varlamov, V. P. (2005). Chitosan-based polyelectrolyte complexes: A review. *Applied Biochemistry and Microbiology*, 41(1), 5-11.

- Ikeda, S., Nitta, Y., Temsiripong, T., Pongsawatmanit, R., & Nishinari, K. (2004). Atomic force microscopy studies on cation-induced network formation of gellan. *Food Hydrocolloids*, 18(5), 727-735.
- Kang, K. S., Veeder, G. T., Mirrasoul, P. J., Kaneko, T., & Cottrell, I. W. (1982). Agar-like polysaccharide produced by a *Pseudomonas* species - Production and basic properties. *Applied and Environmental Microbiology*, 43(5), 1086-1091.
- Kani, K., Horinaka, J., & Maeda, S. (2005). Effects of monovalent cation and anion species on the conformation of gellan chains in aqueous systems. *Carbohydrate Polymers*, 61(2), 168-173.
- Kasapis, S., Giannouli, P., Hember, M. W. N., Evageliou, V., Poulard, C., Tort-Bourgeois, B., & Sworn, G. (1999). Structural aspects and phase behaviour in deacylated and high acyl gellan systems. *Carbohydrate Polymers*, 38(2), 145-154.
- Kogej, K., Evmenenko, G., Theunissen, E., Berghmans, H., & Reynaers, H. (2001). Investigation of structures in polyelectrolyte/surfactant complexes by X-ray scattering. *Langmuir*, 17(11), 3175-3184.
- Kong, L., Cao, M., & Hai, M. (2007). Investigation on the interaction between sodium dodecyl sulfate and cationic polymer by dynamic light scattering, rheological, and conductivity measurements. *Journal of Chemical and Engineering Data*, 52(3), 721-726.
- Kramarenko, E. Y., Khokhlov, A. R., & Reineker, P. (2006). Stoichiometric polyelectrolyte complexes of ionic block copolymers and oppositely charged polyions. *Journal of Chemical Physics*, 125(19).
- Ladhe, A. R., Radomyselski, A., & Bhattacharyya, D. (2006). Ethoxylated nonionic surfactants in hydrophobic solvent: Interaction with aqueous and membrane-immobilized poly(acrylic acid). *Langmuir*, 22(2), 615-621.
- Lau, M. H., Tang, J., & Paulson, A. T. (2000). Texture profile and turbidity of gellan/gelatin mixed gels. *Food Research International*, 33(8), 665-671.
- Lawrence, M. J. (1994). Surfactant systems: their use in drug delivery. *Chemical Society Reviews*, 23(6), 417-424.
- Lee, H.-C., & Brant, D. A. (2002). Rheology of Concentrated Isotropic and Anisotropic Xanthan Solutions: 3. Temperature Dependence. *Biomacromolecules*, 3(4), 742-753.
- Lee, J. W., Kim, S. Y., Kim, S. S., Lee, Y. M., Lee, K. H., & Kim, S. J. (1999). Synthesis and characteristics of interpenetrating polymer network hydrogel composed of chitosan and poly(acrylic acid). *Journal of Applied Polymer Science*, 73(1), 113-120.

- Lee, K. Y., Park, W. H., & Ha, W. S. (1997). Polyelectrolyte complexes of sodium alginate with chitosan or its derivatives for microcapsules. *Journal of Applied Polymer Science*, 63(4), 425-432.
- Lee, S. B., Lee, Y. M., Song, K. W., & Park, M. H. (2003). Preparation and properties of polyelectrolyte complex sponges composed of hyaluronic acid and chitosan and their biological behaviors. *Journal of Applied Polymer Science*, 90(4), 925-932.
- Lehr, C.-M., Bouwstra, J. A., Schacht, E. H., & Junginger, H. E. (1992). In vitro evaluation of mucoadhesive properties of chitosan and some other natural polymers. *International Journal of Pharmaceutics*, 78(1-3), 43-48.
- Lima Vidal, R. R., Pereira Fagundes, F., Cabral de Menezes, S. M., Machado da Silva Ruiz, N., & Balaban Garcia, R. (2005). Solution properties of partially hydrolysed polyacrylamide and chitosan mixed solutions. *Macromolecular Symposia*, 229(1), 118-126.
- Mao, R. S., Tang, J. M., & Swanson, B. G. (1999). Effect of pH buffers on mechanical properties of gellan gels. *Journal of Texture Studies*, 30(2), 151-166.
- Marques, E. F., Regev, O., Khan, A., Miguel, M. D., & Lindman, B. (1999). Interactions between cationic vesicles and oppositely charged poly electrolytes-phase behavior and phase structure. *Macromolecules*, 32(20), 6626-6637.
- McClements, D. J. (2004). *Food Emulsions: principles, practices and techniques*. Boca Raton: CRC Press.
- McClements, D. J., Decker, E. A., Park, Y., & Weiss, J. (2009). Structural design principles for delivery of bioactive components in nutraceuticals and functional foods. *Critical Reviews in Food Science and Nutrition*, 49(6), 577-606.
- Milas, M., & Rinaudo, M. (1996). The gellan sol-gel transition. *Carbohydrate Polymers*, 30(2-3), 177-184.
- Miyoshi, E., Takaya, T., & Nishinari, K. (1996). Rheological and thermal studies of gel-sol transition in gellan gum aqueous solutions. *Carbohydrate Polymers*, 30(2-3), 109-119.
- Moritaka, H., Nishinari, K., Taki, M., & Fukuba, H. (1995). Effects of pH, potassium chloride, and sodium chloride on the thermal and rheological properties of gellan gum gels. *Journal of Agricultural and Food Chemistry*, 43(6), 1685-1689.
- Myers, D. (2006). *Surfactant science and technology*. Hoboken: John Wiley & Sons.
- Nakajima, K., Ikehara, T., & Nishi, T. (1996). Observation of gellan gum by scanning tunneling microscopy. *Carbohydrate Polymers*, 30(2-3), 77-81.
- Narang, A. S., Delmarre, D., & Gao, D. (2007). Stable drug encapsulation in micelles and microemulsions. *International Journal of Pharmaceutics*, 345(1-2), 9-25.

- Nge, T. T., Yamaguchi, M., Hori, N., Takemura, A., & Ono, H. (2002). Synthesis and characterization of chitosan/poly(acrylic acid) polyelectrolyte complex. *Journal of Applied Polymer Science*, 83(5), 1025-1035.
- Nibu, Y., Suemori, T., & Inoue, T. (1997). Phase behavior of binary mixture of heptaethylene glycol decyl ether and water: Formation of phase compound in solid phase. *Journal of Colloid and Interface Science*, 191(1), 256-263.
- Nickerson, M. T., Paulson, A. T., & Speers, R. A. (2003). Rheological properties of gellan solutions: effect of calcium ions and temperature on pre-gel formation. *Food Hydrocolloids*, 17(5), 577-583.
- Ogawa, E., Matsuzawa, H., & Iwahashi, M. (2002). Conformational transition of gellan gum of sodium, lithium, and potassium types in aqueous solutions. *Food Hydrocolloids*, 16(1), 1-9.
- Ogawa, E., Takahashi, R., Yajima, H., & Nishinari, K. (2006). Effects of molar mass on the coil to helix transition of sodium-type gellan gums in aqueous solutions. *Food Hydrocolloids*, 20(2-3), 378-385.
- Onesippe, C., & Lagerge, S. (2008). Studies of the association of chitosan and alkylated chitosan with oppositely charged sodium dodecyl sulfate. *Colloids and Surfaces A-Physicochemical and Engineering Aspects*, 330(2-3), 201-206.
- Pa, J.-H., & Yu, T. L. (2001). Light scattering study of chitosan in acetic acid aqueous solutions. *Macromolecular Chemistry and Physics*, 202(7), 985-991.
- Park, J. H., Saravanakumar, G., Kim, K., & Kwon, I. C. (2010). Targeted delivery of low molecular drugs using chitosan and its derivatives. *Advanced Drug Delivery Reviews*, 62(1), 28-41.
- Park, W. H., Lee, K. Y., & Ha, W. S. (1996). Insoluble polyelectrolyte complex formed from chitosan and α -keratose: conformational change of α -keratose. *Macromolecular Chemistry and Physics*, 197(7), 2175-2183.
- Payne, G. F., & Raghavan, S. R. (2007). Chitosan: a soft interconnect for hierarchical assembly of nano-scale components. *Soft Matter*, 3(5), 521-527.
- Pedroni, V. I., Schulz, P. C., Gschaidner, M. E., & Andreucetti, N. (2003). Chitosan structure in aqueous solution. *Colloid & Polymer Science*, 282(1), 100-102.
- Pepić, I., Filipović-Grčić, J., & Jalšenjak, I. (2009). Bulk properties of nonionic surfactant and chitosan mixtures. *Colloids and Surfaces A: Physicochemical and Engineering Aspects*, 336(1-3), 135-141.
- Picone, C. S. F., & Cunha, R. L. (2011). Influence of pH on formation and properties of gellan gels. *Carbohydrate Polymers*, 84(1), 662-668.
- Rinaudo, M. (2006). Chitin and chitosan: Properties and applications. *Progress in Polymer Science*, 31(7), 603-632.

- Rinaudo, M., Milas, M., & Ledung, P. (1993). Characterization of chitosan - Influence of ionic-strength and degree of acetylation on chain expansion. *International Journal of Biological Macromolecules*, 15(5), 281-285.
- Ritacco, H., Albouy, P. A., Bhattacharyya, A., & Langevin, D. (2000). Influence of the polymer backbone rigidity on polyelectrolyte-surfactant complexes at the air/water interface. *Physical Chemistry Chemical Physics*, 2(22), 5243-5251.
- Robinson, G., Manning, C. E., & Morris, E. R. (1991). Conformation and Physical Properties of the Bacterial Polysaccharides Gellan, Welan, and Rhamsan. In Dickinson, E. *Food Polymers, Gels and Colloids* pp. 22-33. Cambridge: Royal Society of Chemistry.
- Rodríguez-Hernández, A. I., Durand, S., Garnier, C., Tecante, A., & Doublier, J. L. (2003). Rheology-structure properties of gellan systems: evidence of network formation at low gellan concentrations. *Food Hydrocolloids*, 17(5), 621-628.
- Rosen, O., Sjostrom, J., & Piculell, L. (1998). Responsive polymer gels based on hydrophobically modified cellulose ethers and their interactions with ionic surfactants. *Langmuir*, 14(20), 5795-5801.
- Sagar, G. H., Arunagirinathan, M. A., & Bellare, J. R. (2007). Self-assembled surfactant nano-structures important in drug delivery: A review. *Indian Journal of Experimental Biology*, 45(2), 133-159.
- Saito, S., & Taniguchi, T. (1973). Effect of nonionic surfactants on aqueous polyacrylic acid solutions. *Journal of Colloid and Interface Science*, 44(1), 114-120.
- Sanderson, G. R. (1990). Gellan gum. In Harris, P. *Food gels* pp. 201-233. New York: Elsevier Applied Science.
- Sarrazin-Cartalas, A., Iliopoulos, I., Audebert, R., & Olsson, U. (1994). Association and thermal gelation in mixtures of hydrophobically modified polyelectrolytes and nonionic surfactants. *Langmuir*, 10(5), 1421-1426.
- Schatz, C., Viton, C., Delair, T., Pichot, C., & Domard, A. (2003). Typical Physicochemical Behaviors of Chitosan in Aqueous Solution. *Biomacromolecules*, 4(3), 641-648.
- Schulz, P. C., Rodríguez, M. S., Del Blanco, L. F., Pistonesi, M., & Agulló, E. (1998). Emulsification properties of chitosan. *Colloid & Polymer Science*, 276(12), 1159-1165.
- Sezer, A. D., & Akbuga, J. (1999). Release characteristics of chitosan treated alginate beads: II. Sustained release of a low molecular drug from chitosan treated alginate beads. *Journal of Microencapsulation*, 16(6), 687-696.
- Shahidi, F., Arachchi, J. K. V., & Jeon, Y. J. (1999). Food applications of chitin and chitosans. *Trends in Food Science & Technology*, 10(2), 37-51.

- Silva, S. M. C., Antunes, F. E., Sousa, J. J. S., Valente, A. J. M., & Pais, A. A. C. C. (2011). New insights on the interaction between hydroxypropylmethyl cellulose and sodium dodecyl sulfate. *Carbohydrate Polymers*, 86(1), 35-44.
- Simsek-Ege, F. A., Bond, G. M., & Stringer, J. (2003). Polyelectrolyte complex formation between alginate and chitosan as a function of pH. *Journal of Applied Polymer Science*, 88(2), 346-351.
- Takahashi, R., Tokunou, H., Kubota, K., Ogawa, E., Oida, T., Kawase, T., & Nishinari, K. (2004). Solution properties of gellan gum: Change in chain stiffness between single- and double-stranded chains. *Biomacromolecules*, 5(2), 516-523.
- Takahashi, T., Takayama, K., Machida, Y., & Nagai, T. (1990). Characteristics of polyion complexes of chitosan with sodium alginate and sodium polyacrylate. *International Journal of Pharmaceutics*, 61(1-2), 35-41.
- Taravel, M. N., & Domard, A. (1995). Collagen and its interaction with chitosan: II. Influence of the physicochemical characteristics of collagen. *Biomaterials*, 16(11), 865-871.
- Taylor, D. J. F., Thomas, R. K., & Penfold, J. (2007). Polymer/surfactant interactions at the air/water interface. *Advances in Colloid and Interface Science*, 132(2), 69-110.
- Terbojevich, M., Cosani, A., Conio, G., Marsano, E., & Bianchi, E. (1991). Chitosan: chain rigidity and mesophase formation. *Carbohydrate Research*, 209(0), 251-260.
- Thongngam, M., & McClements, D. J. (2004). Characterization of Interactions between Chitosan and an Anionic Surfactant. *Journal of Agricultural and Food Chemistry*, 52(4), 987-991.
- Thongngam, M., & McClements, D. J. (2005). Influence of pH, ionic strength, and temperature on self-association and interactions of sodium dodecyl sulfate in the absence and presence of chitosan. *Langmuir*, 21(1), 79-86.
- Thunemann, A. F. (2002). Polyelectrolyte-surfactant complexes (synthesis, structure and materials aspects). *Progress in Polymer Science*, 27(8), 1473-1572.
- Tomašić, V., Tomašić, A., Šmit, I., & Filipović-Vinceković, N. (2005). Interactions in mixed cationic surfactants and dextran sulfate aqueous solutions. *Journal of Colloid and Interface Science*, 285(1), 342-350.
- Tsaih, M. L., & Chen, R. H. (1997). Effect of molecular weight and urea on the conformation of chitosan molecules in dilute solutions. *International Journal of Biological Macromolecules*, 20(3), 233-240.
- Tsianou, M., & Alexandridis, P. (1999). Control of the rheological properties in solutions of a polyelectrolyte and an oppositely charged surfactant by the addition of cyclodextrins. *Langmuir*, 15(23), 8105-8112.

- Varade, D., Ushiyama, K., Shrestha, L. K., & Aramaki, K. (2007). Wormlike micelles in Tween-80/CmEO3 mixed nonionic surfactant systems in aqueous media. *Journal of Colloid and Interface Science*, 312(2), 489-497.
- Vårum, K. M., Antohonsen, M. W., Grasdalen, H., & Smidsrød, O. (1991). Determination of the degree of N-acetylation and the distribution of N-acetyl groups in partially N-deacetylated chitins (chitosans) by high-field n.m.r. spectroscopy. *Carbohydrate Research*, 211(1), 17-23.
- Yamakawa, H., & Fujii, M. (1974). Intrinsic-viscosity of wormlike chains - Determination of shift factor. *Macromolecules*, 7(1), 128-135.
- Yamamoto, F., & Cunha, R. L. (2007). Acid gelation of gellan: Effect of final pH and heat treatment conditions. *Carbohydrate Polymers*, 68(3), 517-527.
- Yao, K. D., Tu, H., Cheng, F., Zhang, J. W., & Liu, J. (1997). pH-sensitivity of the swelling of a chitosan-pectin polyelectrolyte complex. *Die Angewandte Makromolekulare Chemie*, 245(1), 63-72.
- Yuguchi, Y., Urakawa, H., Kitamura, S., Wataoka, I., & Kajiwara, K. (1999). The sol-gel transition of gellan gum aqueous solutions in the presence of various metal salts. *Progress in Colloid and Polymer Science*, 114, 41-47.
- Zhai, L., Zhang, J., Shi, Q., Chen, W., & Zhao, M. (2005). Transition from micelle to vesicle in aqueous mixtures of anionic/zwitterionic surfactants studied by fluorescence, conductivity, and turbidity methods. *Journal of Colloid and Interface Science*, 284(2), 698-703.
- Zhao, J., Wang, Z. N., Wei, X. L., Liu, F., Zhou, W., Tang, X. L., & Wu, T. H. (2011). Phase behaviour and rheological properties of the lamellar liquid crystals formed in dodecyl polyoxyethylene polyoxypropylene ether/water system. *Indian Journal of Chemistry - A*, 50A(5), 641-649.

– CAPÍTULO 3 –

***Influence of pH on formation and properties
of gellan gels***

INFLUENCE OF PH ON FORMATION AND PROPERTIES OF GELLAN GELSPICONE, Carolina Siqueira Franco¹ & CUNHA, Rosiane Lopes^{1*}

¹ Department of Food Engineering, Faculty of Food Engineering, University of Campinas (UNICAMP), 13083-862, Campinas-SP, Brazil

*Phone: +55 19 3521- 4047 FAX: +55 19 3521-4027 email: rosiane@fea.unicamp.br

In: Carbohydrate Polymers (2011), v. 84, p. 662–668.

Abstract

The effect of pH (3.5, 5.3 and 7.0) on the formation of deacylated gellan gels was studied using oscillatory shear measurements and microcalorimetric trials in heating-cooling cycles at 1 °C·min⁻¹. In addition, the mechanical properties and structure of the gels formed at the different pH values were evaluated by uniaxial compression and scanning electron microscopy, respectively. An increase in pH led to an increase in temperature and decrease in enthalpy of the coil-helix transition. These results were attributed to a decreased formation of junction zones at higher pH values due to greater electrostatic repulsion between the gellan molecules. As a consequence, gels formed at neutral pH were more fragile and deformable than acid gels. All the samples showed thermo-reversible rheological behavior, presenting the same rheological properties at 20 °C, before and after heating to 90 °C.

Keywords: gellan gum, acidification, rheology, coil-helix transition

1. Introduction

Gellan gum is a linear anionic heteropolysaccharide produced by *Sphingomonas elodea* (Nishinari, 1999), which has been a subject of interest since its discovery in 1980 due to its ability to form transparent gels even at low concentrations (Rodriguez-Hernandez, Durand, Garnier, Tecante & Doublier, 2003). In addition, traditional gelling

agents such as agarose and carrageenan show reduced gelling capacity at low pH, whereas gellan gum can form strengthened gels (Moritaka, Nishinari, Taki & Fukuba, 1995; Yamamoto & Cunha, 2007).

As with other polysaccharides, gellan molecules undergo a coil to double-helix transition with decreasing temperature, which may lead to gel formation depending on the ionic strength and pH of the solution. The gelation process is known to consist of two steps (Milas & Rinaudo, 1996). Firstly the gellan coil molecules form double helices with the reduction in temperature, and secondly, these helices aggregate forming junction zones, resulting in system gelation (Yuguchi, Urakawa & Kajiwara, 1997). In water, at low ionic strength and neutral pH, aggregation of the helices is impeded by the electrostatic repulsion between negatively charged carboxylic groups on the gellan. The addition of salt or reduction in pH decreases intermolecular repulsion between the helices enhancing junction zone formation and consequently, the gel strength (Funami et al., 2008; Yamamoto & Cunha, 2007). The role of salt ions in gel formation has been widely studied (Fukada, Takahashi, Kitamura, Yuguchi, Urakawa & Kajiwara, 2002; Funami et al., 2008; Milas & Rinaudo, 1996; Miyoshi, Takaya & Nishinari, 1996; Moritaka, Nishinari, Nakahama & Fukuba, 1992; Moritaka, Nishinari, Taki & Fukuba, 1995). In the presence of salt ions, the gelling and melting temperatures of gellan gels shift to higher temperatures and the number of junction zones is enhanced. This makes the gel more heat resistant and leads to an increase in the gel elastic modulus and rigidity. However, only a small number of studies (Horinaka, Kani, Hori & Maeda, 2004; Mao, Tang & Swanson, 1999; Moritaka, Nishinari, Taki & Fukuba, 1995; Yamamoto & Cunha, 2007) was concerned about the effect of pH on the gel properties. The aim of the present work was to study the effect of pH on the gellan coil-helix transition using rheological and calorimetric techniques, so as to evaluate any influence on the mechanical and structural properties of the gels.

2. Material and methods

2.1. Material

Deacylated gellan gum powder (Kelcogel[®] F) (3.42 % w/w moisture content) was kindly donated by Kelco Biopolymers (San Diego, CA). The ions content of the gellan, as determined by Inductively Coupled Plasma (ICP) Emission Spectroscopy (Perkin Elmer – Optima 3000 DV, Waltham, MA, USA) was (% w/w): $K^+ = 4.13$, $Na^+ = 0.43$ and $Ca^{2+} = 0.18$. The stoichiometric equivalence to the carboxyl groups for 1.5 % (w/w) gellan solution was (%): $K^+ = 38.36$, $Na^+ = 6.52$ and $Ca^{2+} = 3.74$. Lactic acid was purchased from Merck (Germany).

2.2. Preparation of the gellan solutions

The solution of 1.5 % w/w gellan gum was prepared by stirring the gellan powder in deionized water at 80 °C for 30 minutes in a jacketed vessel. The pH was adjusted to 7.0 ± 0.2 and 3.5 ± 0.2 by the addition of 0.02 M NaOH or 0.2 M lactic acid, respectively. Solutions at the natural pH (5.3 ± 0.2) were also evaluated. The content of Na^+ ions added was much lower than the ion content of the raw material. The content of K^+ was kept constant since gellan concentration was the same for all the samples. The potassium concentration in the raw material probably contributed to a partial network formation, but not for the further differences observed in rheological and DSC thermal behaviour between the samples.

For the thermal and rheological measurements, the solutions were analyzed just after preparation at 80 °C. For the analyses of the mechanical properties and microstructure, the gellan solutions were poured into cylindrical plastic tubes previously lubricated with silicon oil (21 mm inner diameter x 21 mm height) and Petri dishes, which

were cooled to 10 °C in an ice bath. The gels were then maintained at the same temperature (10 °C) for 24 hours in order to assure complete gel formation.

2.3. Oscillatory rheology

The rheological behavior of the samples was evaluated by oscillatory shear measurements in a stress-controlled rheometer (Carri – Med CSL² 500, TA Instruments, UK) equipped with a stainless steel cone and plate geometry (cone angle = 1.59°; cone diameter = 60 mm). The samples were transferred onto the rheometer plate (which was preheated at 60 °C) immediately after the heat treatment, and were then quickly heated to 90 °C using a Peltier unit. To avoid sample evaporation, the cone and plate was surrounded by a fine layer of silicon oil. The samples were then homogenized by pre-shearing at 100 s⁻¹ for 2 minutes and allowed to rest for 5 minutes prior to the measurements. As the samples were totally liquid at such temperature, no rim instability or structure damage was observed in the samples. Three sweeps (cooling-heating-cooling) were carried out between 20 and 90 °C at 1 °C·min⁻¹, 0.1 Hz and 0.5 Pa. Changes in the slope of complex viscosity vs temperature curves were maximized from the derivation of the data using the Savitzky & Golay filter (Savitzky & Golay, 1964). The temperatures of rheological transitions were determined by the maxima in the (absolute) slope of log (η^*). The contribution of the elastic (G') and loss (G'') moduli on these rheological changes were evaluated by tan δ (G''/G'). The gel point was determined using the criterion of crossover between the G' and G'' (Yamamoto & Cunha, 2007).

2.4. Thermal behavior

The thermal behavior of samples was measured using a VP-DSC (MicroCal, Northampton, MA) calorimeter equipped with twin 0.542 ml cells for the reference and sample solutions. The samples were loaded at 60 °C and heated to 90 °C before the test.

Four repeated heating-cooling cycles between 5 and 90 °C were carried out at 1 °C·min⁻¹. The reference thermogram was recorded under the same conditions by filling both cells with water. The transition temperature (T_{peak}) was determined as the temperature of the maximum peak, whereas the enthalpy was calculated from the area enclosed by the peak and the baseline.

2.5 Compression testing

The mechanical properties of the gels at the different pH values were determined by uniaxial compression measurements in a TA-XT Plus Texture Analyser (Stable Microsystems Ltd., Surrey, England), equipped with a 40 mm diameter cylindrical acrylic plate lubricated with silicon oil to minimize friction between the sample and the probe. The gels were compressed to 80 % of their original height at 10 °C, using a crosshead speed of 1 mm/s.

Hencky stress (σ_H) and strain (ε_H) were calculated from the force-deformation data according to Eqs. (1) and (2), respectively (Steffe, 1996):

$$\sigma_H = F(t) \left[\frac{H(t)}{H_0 A_0} \right] \quad (1)$$

$$\varepsilon_H = -\ln \left[\frac{H(t)}{H_0} \right] \quad (2)$$

Where $F(t)$ is the force at time t , A_0 and H_0 are the initial sample area and height, respectively, and $H(t)$ is the height at time t .

The stress (σ_R) and strain (ε_R) at fracture were obtained from the maximum point of the stress-strain curve, while the Young's modulus (E) was the slope of the initial linear region of this curve (up to 1 % of deformation).

2.6 Scanning electron microscopy

Pieces of gel (approximately 10 mm x 2 mm x 2 mm) were fixed overnight in 2.5 % glutaraldehyde in cacodylate buffer (0.1 M) at pH 7.2. After rinsing in cacodylate buffer (0.1 M), the samples were fractured in liquid nitrogen, followed by another rinse with cacodylate buffer. The fractured samples were post fixed overnight in 1 % buffered osmium tetroxide and then dehydrated in a graded ethanolic series (30, 50, 70, 90 and 100 % v/v). In order to avoid structural damage, the samples were dried at the CO₂ critical point (Balzers Critical Point Dryer CPD03) and then mounted on aluminum stubs and coated with gold in a SCD 050-Balzer Sputter Coater. At least three images of typical structures were recorded at a magnification of 1.000x using a JEOL JSM 5800 LV (Tokyo, Japan) microscope operating at 10 kV.

2.7. Statistical analyses

The results were evaluated from triplicates of each sample, using the analysis of variance (ANOVA). The significant differences ($p < 0.05$) between different samples were determined by the Tukey procedure, using the software STATISTICA 5.5 (Statsoft Inc., Tulsa, USA).

3. Results

3.1. Thermal scanning rheology

Figure 1 shows the rheological behaviour of sample during heating-cooling cycles. The main points were obtained within the linear viscoelastic region of samples (with no structural damage), except by the points at high temperatures (low viscosity and non gel formation). As the measurements were carried out using stress controlled operation mode and the sample showed great changes in viscosity and elasticity values, part of the test would certainly be out of linear viscoelastic range. However, it did not damaged the

sample structure, since in such case the transition temperatures during cooling and G' G'' crossover should be lower than that determined by DSC, and it did not occur.

A single increase in complex viscosity was observed during cooling (Figure 1), which reflected in a decrease in $\tan(\delta)$ values. Such phenomenon occurred at slightly higher temperatures as the pH increased (Table 1), but the gel point temperature (Table 2) did not vary with the pH in both two cooling cycles. Such temperatures are in agreement with the results obtained by Miyoshi, Takaya and Nishinari (1996).

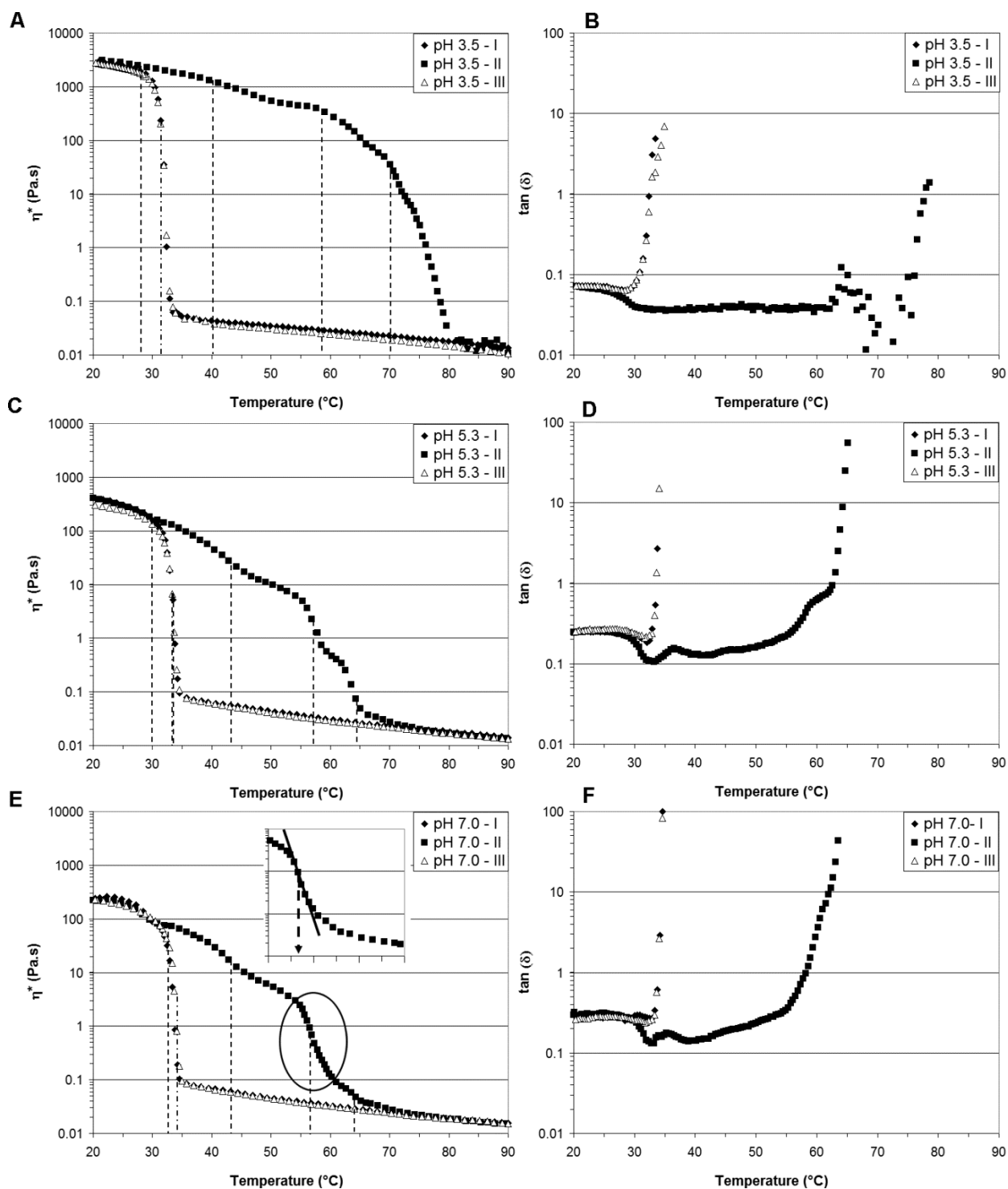


Figure 1. Complex viscosity (η^*) and $\tan(\delta)$ in heating – cooling cycles (20 – 90 °C) of gellan gum 1.5 % (w/w) at different pH values: (A) and (B) pH 3.5; (C) and (D) pH 5.3; and (E) and (F) pH 7.0. (---) transition temperatures on cooling; (---) transition temperatures on heating. I. First cooling, II. Heating, III. Second cooling. The inset shows the method used to determine the transitions.

Table 1: Transition temperatures of the complex viscosity changes for 1.5% (w/w) gellan solutions at pH 3.5, 5.3 and 7.0 during consecutive cooling – heating cycles.

		Transition Temperature (°C)		
Transition		pH 3.5	pH 5.3	pH 7.0
Cooling I	1 st	31.4 ± 0.5 ^{Aa}	33.6 ± 0.9 ^{Ba}	34.2 ± 0.6 ^{Ca}
Heating	1 st	28.1 ± 0.3 ^{Ab}	29.9 ± 0.6 ^{Bb}	32.8 ± 0.6 ^{Ca}
Heating	2 nd	40.1 ± 0.8 ^{Ac}	43.3 ± 0.5 ^{Bc}	43.3 ± 0.6 ^{Bb}
Heating	3 rd	58.6 ± 0.3 ^{Ad}	57.2 ± 0.2 ^{Bd}	56.7 ± 0.3 ^{Cc}
Heating	4 th	70.1 ± 0.5 ^{Ae}	64.7 ± 0.8 ^{Be}	64.1 ± 0.3 ^{Bd}
Cooling II	1 st	31.4 ± 0.5 ^{Aa}	33.4 ± 0.8 ^{Ba}	34.1 ± 0.5 ^{Ba}

($F(17,36)=1915.3$, $p= 0.00$). Different capital letters in the same row and small letters in the same column mean statistically significant differences ($p<0.05$).

However, different complex viscosity profiles were observed on heating, depending on the pH (Figure 1) and relevant hysteresis. Hysteresis is identified as the difference between the ascending (sol to gel transition) and descending (gel to sol transition) curves (Funami et al., 2008). All the curves of η^* presented four slope changes, some of which were very pronounced and others not so easy to identify (Table 1 and Figure 1). At pH 3.5, the increase in temperature led to a decrease in complex viscosity from 3000 Pa·s (at 20 °C) to 0.01 Pa·s near 80 °C. At such pH value, the first transition occurred at a temperature below 30 °C and the last one at 70 °C (temperature variation of about 40 °C) (Table 1 and Figure 1). Increasing the solution pH to 5.3, the first two transitions occurred at higher temperatures than at pH 3.5 whilst the others were observed at lower temperatures. The same tendencies were observed at pH 7.0 (Table 1, Figure 1). Slope changes in the determination of the rheological properties during the thermal scanning analysis were previously reported by Miyoshi, Takaya and Nishinari (1996), who studied the effect of gellan concentration on the rheological properties of gellan gum solutions prepared without variation in pH. They observed only two different slope changes, which were attributed to the helix-coil transition followed by the sol-gel transition.

Table 2: Temperatures of G' and G'' crossover for 1.5% (w/w) gellan solutions at pH 3.5, 5.3 and 7.0 during consecutive cooling – heating cycles.

	Onset Temperature (°C)		
	pH 3.5	pH 5.3	pH 7.0
Cooling I	32.4 ± 0.7	33.3 ± 0.5	33.5 ± 0.3
Cooling II	32.9 ± 0.6	33.4 ± 0.7	34.0 ± 0.5

There is no statistically significant differences between the means ($F(5,12)=1.76$, $p=0.20$).

Overall the $\tan \delta$ showed a decrease around 33 °C on heating which was more pronounced at higher pH values. Such decrease was associated to the higher G'' depression as compared to G'. Above 60 °C $\tan \delta$ increased abruptly, due to the sharp decrease of G' (Figures 1 B, D and F). The hysteresis between the cooling and heating scans (Figure 1) decreased as the pH increased, suggesting that a more lightly cross-linked network was formed with a smaller number of aggregated helices. Previous findings related the increase in hysteresis to the decrease in acyl content of the gellan gum molecules and the presence of gel-promoting cations, which enhance molecular associations (Funami et al., 2008; Gunning, Kirby, Ridout, Brownsey & Morris, 1996; Morris, Kirby & Gunning, 1999). In the present case, the gellan gum used was totally deacylated (NutraSweet, 1996), and thus the changes in hysteresis were associated with interactions promoted by lower pH values and the cations presence. As well as the effect of cation addition, the reduction in pH increased the concentration of positive ions in solution, screening electrostatic repulsion between helices and favoring helix-helix association by way of hydrogen bonds, resulting in an increase in thermal stability or hysteresis of the samples.

3.2. DSC

Figure 2 shows the DSC thermograms of the samples at different pH values. The number of peaks remained the same after consecutive cooling – heating cycles. The

cooling curves showed a single exothermic peak for all pH values, whilst up to four endothermic peaks were observed on the heating curves. These results were in good agreement with those obtained by Moritaka, Nishinari, Taki and Fukuba (1995) and Tanaka and Nishinari (2007). The first endothermic peak appeared in the same temperature range as the exothermic peak observed on cooling, but it was significantly smaller and became larger with the increase in the pH value (Figure 2). An overlap of endothermic peaks was detected around 33 – 50 °C, which became broader as the pH decreased, making it impossible to determine all the peak temperatures and enthalpies at pH 3.5. Two more peaks were detected on heating at higher temperatures, which shifted to lower temperatures as the pH increased. The second endothermic peak also shifted to lower temperatures as the pH increased from 5.3 to 7.0, but the opposite tendency was observed with the first peak. Table 3 shows an increase in the first peak temperature of about 3 °C and Table 4 a strong increase in enthalpy when the pH changed from 3.5 to 7.0. In the same way, the temperature of the exothermic cooling peaks also increased as the pH rose, but no significant changes in enthalpy were observed (Table 4). For all the samples, the sum of the endothermic enthalpy values was slightly lower than the enthalpy of the single exothermic peak observed on cooling (Table 4), especially at the lowest pH. It suggests that the second peak may be partially overlapping the first peak making it difficult to establish the baseline for integration of each peak. Indeed the first peak became broader and presented a reduced enthalpy at lower pH values. Moreover, the small peaks observed at pH 3.5 hinder the establishment of the baseline, which probably masked some part of total enthalpy associated to the thermal transitions.

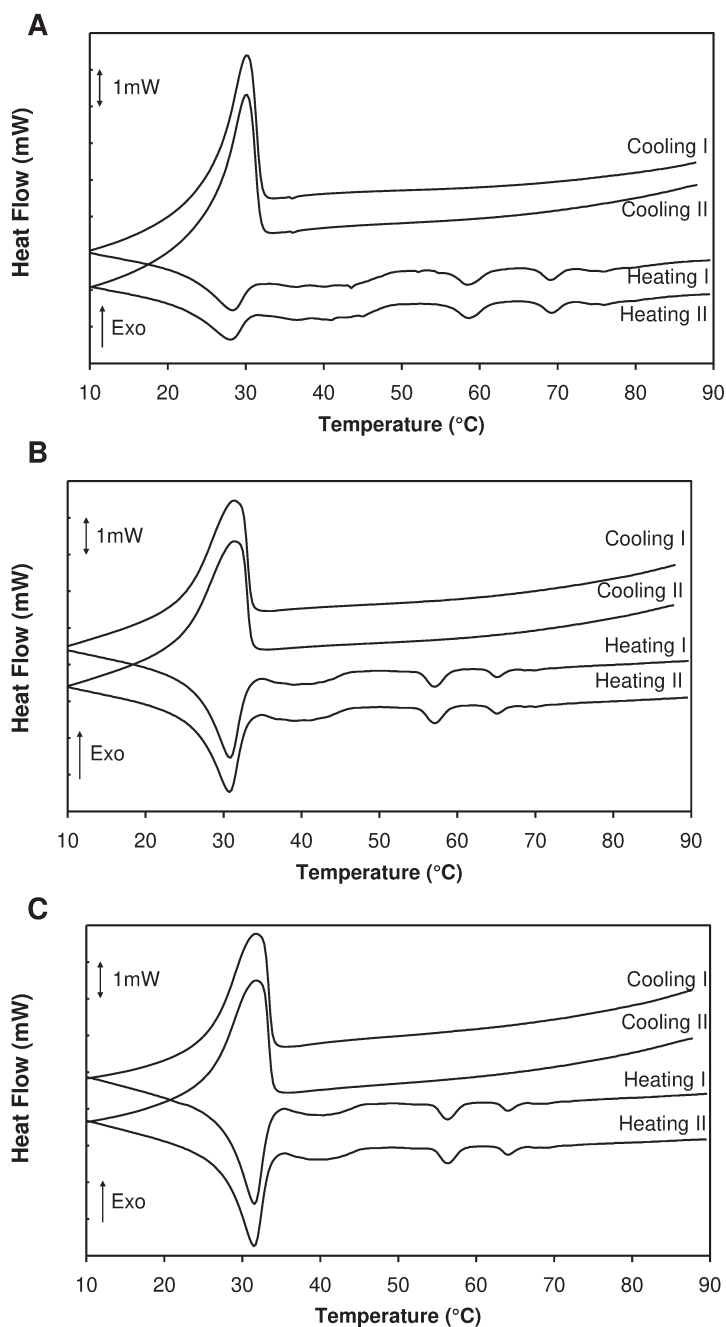


Figure 2. DSC-thermograms of gellan 1.5% (w/w) A) pH 3.5, B) pH 5.3 and C) pH 7.0. Temperature rate of 1 °C/min.

The re-cooling and re-heating did not affect the temperature and enthalpy of the peaks (Tables 3 and 4) showing the thermal reversibility of the gellan gels.

Table 3: Peak temperatures of thermograms for 1.5% (w/w) gellan solutions at pH 3.5, 5.3 and 7.0 during consecutive cooling – heating cycles.

	Peak Temperature (°C)		
	pH 3.5	pH 5.3	pH 7.0
Cooling I	30.29 ± 0.25 ^{Aa}	31.26 ± 0.28 ^{Ba}	31.70 ± 0.04 ^{Bae}
Heating I Peak1	28.45 ± 0.09 ^{Ab}	30.78 ± 0.15 ^{Bab}	31.57 ± 0.01 ^{Ca}
Heating I Peak2	-	40.72 ± 0.05 ^{Ac}	39.83 ± 0.28 ^{Bb}
Heating I Peak3	58.80 ± 0.17 ^{Ac}	57.13 ± 0.19 ^{Bd}	56.33 ± 0.00 ^{Cc}
Heating I Peak4	68.79 ± 0.30 ^{Ad}	64.85 ± 0.19 ^{Be}	64.05 ± 0.00 ^{Cd}
Cooling II	30.35 ± 0.18 ^{Aa}	31.41 ± 0.27 ^{A^{Baf}}	31.77 ± 0.07 ^{Bae}
Heating II Peak 1	28.14 ± 0.10 ^{Ab}	30.63 ± 0.12 ^{Bbf}	31.39 ± 0.07 ^{Ca}
Heating II Peak 2	-	40.81 ± 0.06 ^{Ac}	40.17 ± 0.46 ^{Ab}
Heating II Peak 3	58.75 ± 0.17 ^{Ac}	56.98 ± 0.17 ^{Bd}	56.41 ± 0.08 ^{Bc}
Heating II Peak 4	69.00 ± 0.30 ^{Ad}	64.88 ± 0.26 ^{Be}	64.27 ± 0.05 ^{Bd}

Different capital letters in the same row and small letters in the same column mean statistically significant differences ($p < 0.05$). $F(27,56) = 19,000$; $p = 0.00$.

Overall, peak temperatures showed good agreement with the temperature transitions observed on rheological tests (Table 1 and 3), despite of the different thermal history of both measurements.

Table 4: Enthalpy values for 1.5% (w/w) gellan solutions at pH 3.5, 5.3 and 7.0 during consecutive cooling – heating cycles. Negative sign means exothermic transition.

	Peak Enthalpy (kJ/g)		
	pH 3.5	pH 5.3	pH 7.0
Cooling I	-13.52 ± 0.83 ^{Aa}	-12.03 ± 1.10 ^{Aa}	-12.44 ± 0.36 ^{Aa}
Heating I Peak1	3.07 ± 0.25 ^{Ab}	6.60 ± 0.46 ^{Bb}	6.86 ± 0.14 ^{Bb}
Heating I Peak2	-	2.63 ± 0.26 ^{Ac}	3.38 ± 0.65 ^{Ac}
Heating I Peak3	2.24 ± 0.10 ^{Ac}	0.96 ± 0.52 ^{Bd}	0.67 ± 0.03 ^{Bd}
Heating I Peak4	0.73 ± 0.13 ^{Ad}	0.26 ± 0.03 ^{Bd}	0.32 ± 0.01 ^{Bd}
Cooling II	-12.83 ± 0.47 ^{Aa}	-11.64 ± 0.06 ^{Aa}	-12.94 ± 0.22 ^{Aa}
Heating II Peak 1	2.75 ± 0.13 ^{Abe}	6.59 ± 0.65 ^{Bb}	6.72 ± 0.14 ^{Bb}
Heating II Peak 2	-	2.79 ± 0.34 ^{Ac}	3.41 ± 1.31 ^{Ac}
Heating II Peak 3	2.04 ± 1.24 ^{Ace}	0.68 ± 0.03 ^{Bd}	0.73 ± 0.02 ^{Bd}
Heating II Peak 4	0.57 ± 0.01 ^{Ad}	0.26 ± 0.03 ^{Bd}	0.33 ± 0.00 ^{Bd}

Different capital letters in the same row and small letters in the same column mean statistically significant differences ($p < 0.05$). $F(27,56) = 505,7$; $p = 0.00$.

3.3. Compression testing

The uniaxial compression results showed an increase in gel hardness and elasticity as the pH decreased (Figures 3 and 4 A and C), in agreement with the results obtained by Yamamoto and Cunha (2007). As the pH increased, so the curves became broader (Figure 3) and the rupture stress of the gels at pH 3.5 was more than twice that obtained at the other pH values (Figures 3 and 4). However, the deformation at fracture or deformability showed the opposite tendency (Figures 3 and 4B). The strain at fracture of the gels at pH 3.5 and 5.3 were statistically the same, and both were lower than that at pH 7.0. After the rupture point, the curves presented squelching of the samples. In this region, the gels at pH 3.5 showed a number of small fractures, which decreased as the pH increased.

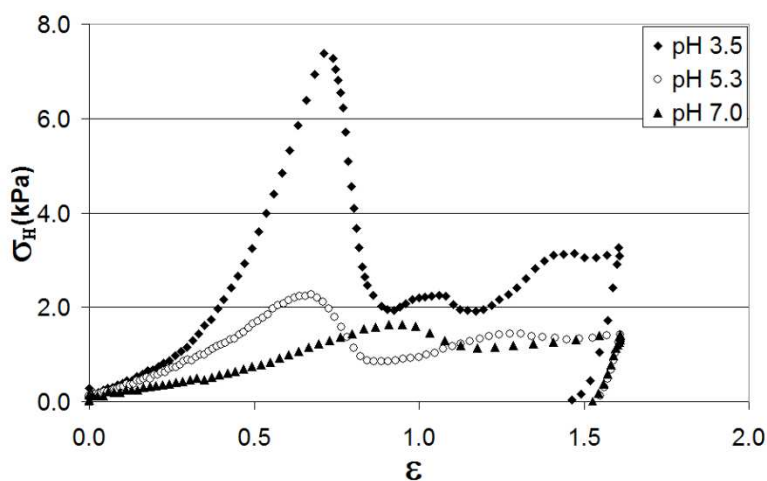


Figure 3: Typical strain – stress curves for 1.5% (w/w) gellan gels at pH 3.5, 5.3 and 7.0.

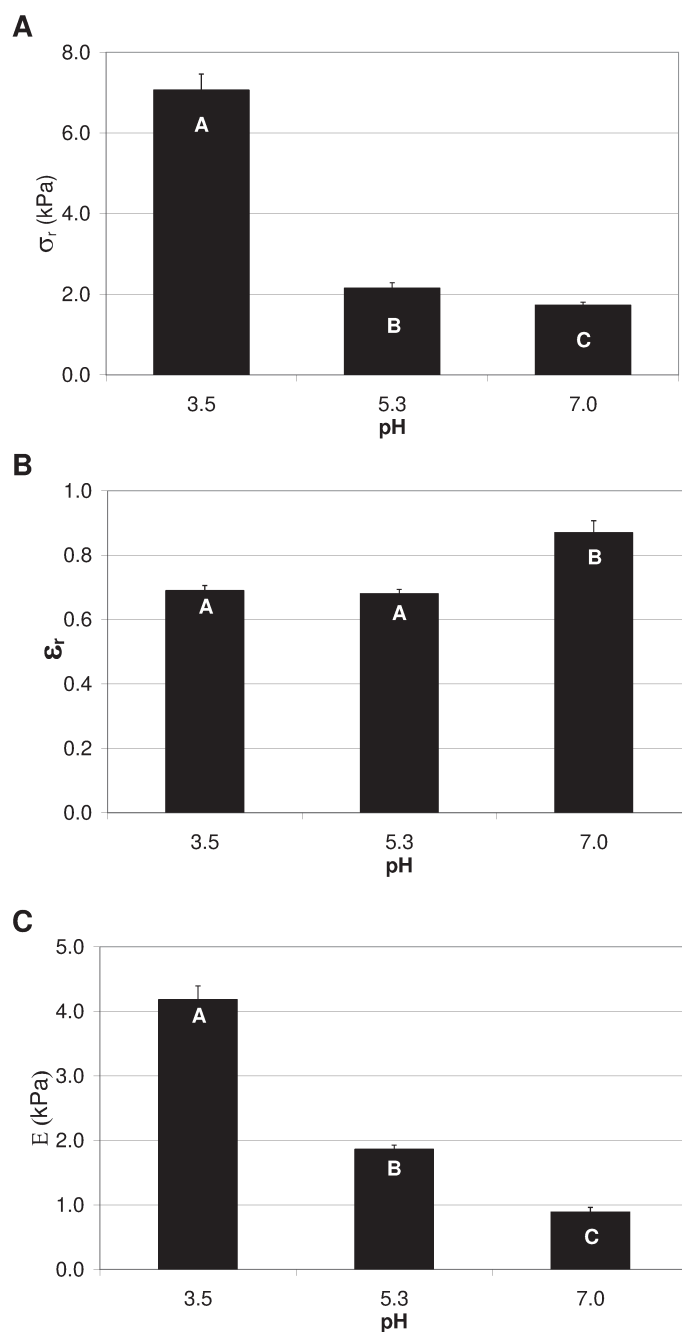


Figure 4. Mechanical properties of gels of 1.5% (w/w) gellan gum at pH 3.5, 5.3 and 7.0. A) Stress at fracture (σ_r), B) Strain at fracture (ϵ_r) and C) Young's modulus (E). Means and error bars were calculated from triplicates of each sample. Means with different letters show statistically significant differences at $p < 0.05$.

3.4. Microscopy

Figure 5 shows the microstructures of the gels at 25 °C and different pH values. Overall the micrographs showed very compact structures with a great number of pores,

typical of gellan gum networks (de Jong & van de Velde, 2007; Picone & Cunha, 2010; Yamamoto & Cunha, 2007). Acidification seemed to close the pore network. The gels at pH 7.0 presented a flat and closed network, while those at pH 5.3 were more continuous and with fewer pores (Figure 5). At pH 3.5 the network was even more continuous and with smaller pores, which were homogeneously distributed throughout the structure (Figure 5).

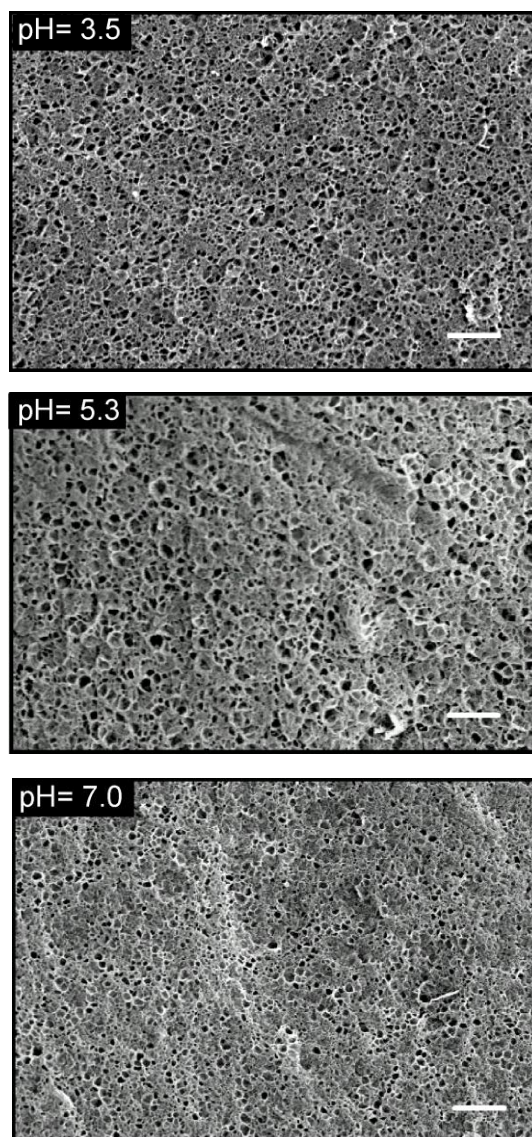


Figure 5. SEM micrographs of 1.5% (w/w) gellan gum gels at pH 3.5, 5.3 and 7.0. Scale bar = 10 μm .

4. Discussion

The gelation of gellan is known to occur during cooling by way of the coil - helix conformational transition followed by an association between the helices, resulting in network formation. Independently of pH, the complex viscosity of the gellan solutions increased in a single step during the cooling ramp (Figure 1), and their transition temperatures were similar to the gel point. This suggests that as soon as the helices were formed, the sol-gel transition took place due to molecular association. The gelation process occurred in a single step, as confirmed by the DSC results in which a single exothermic peak was observed (Figure 2). The rheological and DSC results suggested that such phenomena occurred at slightly lower temperatures at acid pH values (Tables 1 and 3), which was attributed to the more compact and denser gel structure formed at pH 3.5 (Figure 5), requiring more time and energy to complete the network formation. Hysteresis between the cooling – heating rheological scans was also more pronounced at lower pH, which could be associated with the greater stability of the aggregated helices formed under acid conditions, as compared with the isolated double helices. Moreover, hysteresis was previously reported to be related to the continuousness and homogeneity of the gel network structure (Funami et al., 2008), which was confirmed by the more continuous and less porous structure observed at pH 3.5 (Figure 5).

All the samples showed thermo-reversible behavior, since the gel point values were statistically the same after heating and re-cooling, independent of the sample pH value (Table 2). However the calorimetric measurements showed differences in peak shape, temperature and enthalpy (Figure 2), whilst different hysteresis and slopes were observed at similar temperatures in the thermal rheological scans (Figure 1) according to the pH values of the samples. Besides of the different thermal history between the rheological and DSC measurements, the transition temperatures obtained from both techniques showed a

good agreement on cooling and heating, especially at high temperatures. If such difference had affected the structure formation, it would be expected an increase in transition temperatures of DSC measurements as compared to rheological tests. As it did not happened, we considered that the difference in thermal history caused by the decrease up to 5 or 20 °C (with no holding time) did not affect significantly the observed transitions and that the applied shear fields of rheological tests were not strong enough to affect the thermally induced structural changes.

Overall, all the samples showed four peaks in the rheological and DSC scans (Figure 1 and 2), and some authors have suggested that these peaks can be related to the presence of junction zones of different thermo stability (Moritaka, Nishinari, Taki & Fukuba, 1995; Nishinari, 1997). We believe that the first transition on heating (larger peak) corresponded to the melting of non aggregated helices. The enthalpy values increased with increasing pH, indicating that more helices remained non-aggregated and less junction zones had been formed, considering that the electrostatic repulsion between gellan carboxyl groups tended to increase. Such a phenomenon was observed in both techniques at similar temperatures (Figure 1, Table 1). This assumption was confirmed by $\tan \delta$ results that showed a decrease near 30 °C, because of the decrease in G'' (decrease of non aggregated helices density).

The second transition was, in fact an overlapping of peaks resulting from the break of double helix structures. The other peaks observed were related to the melting of these aggregated helices and disruption of junction zones with different thermo stabilities (Figures 1 and 2) formed by the presence of different ions and varied H^+ ions content. The enthalpy and temperature of such peaks decreased with increasing pH (Tables 3 and 4), since less intermolecular interactions were established at higher pH values. As a consequence, slope changes of the complex viscosity as a function of temperature were

also observed at similar temperatures (Table 1). This occurred because the double helical gellan molecules have a higher relative viscosity than the more flexible disordered form, as previously reported by Lee and Brant (2002) for xanthan, a polysaccharide presenting a similar conformational transition (helix-coil).

The higher values for complex viscosity observed at lower pH values and 20°C, resulting from greater molecular association, reflected directly on the gel mechanical properties and microstructure (Figures 3 and 4). During the uniaxial compression measurements the force applied was better distributed along the network structure of the acid gels, showing higher stress at fracture and elasticity modulus values (Figure 4 A and C). However, since the network was more compact, the mobility of the gel strands under the application of force was reduced, resulting in less deformable gels (Figure 4 B).

5. Conclusion

Although the gellan gels were thermo reversible, independently of pH, their formation and mechanical properties were shown to be directly dependent on the solution pH. An increase in pH led to the formation of a reduced number of junction zones and a decrease in molecular aggregation, reducing gel rigidity. On the other hand, this structure increased gel deformability, since the mobility of the strands increased. Thermal scanning showed that the gels were formed by junction zones with different thermal stabilities due to the presence of different H⁺ concentration and the other ions present in the raw material. The disruption of such interactions on heating occurred in four steps, leading to different slopes for the complex viscosity as a function of temperature. The DSC analyses together with the thermal rheological scans were shown to be a powerful tool in understanding the type of gellan network structure, as previously reported for other polysaccharide gels.

6. Acknowledgements

The authors are grateful to Dr. Watson Loh and Dr. Fernanda Rosa Alves for their cooperation in the DSC experiments. This work was supported by The *Fundação de Amparo à Pesquisa e Desenvolvimento de São Paulo – Brazil* (FAPESP, Grant No. 2004/08517-3 and 2006/02390-7) and by The *Conselho Nacional de Desenvolvimento Científico e Tecnológico - Brazil* (CNPq, Grant No. 301869/2006-5).

7. References

- de Jong, S., & van de Velde, F. (2007). Charge density of polysaccharide controls microstructure and large deformation properties of mixed gels. *Food Hydrocolloids*, *21*(7), 1172-1187.
- Fukada, H., Takahashi, K., Kitamura, S., Yuguchi, Y., Urakawa, H., & Kajiwara, K. (2002). Thermodynamics and structural aspect of the gelling process in the gellan gum/metal salt aqueous solutions. *Journal of Thermal Analysis and Calorimetry*, *70*(3), 797-806.
- Funami, T., Noda, S., Nakauma, M., Ishihara, S., Takahashi, R., Al-Assaf, S., Ikeda, S., Nishinari, K., & Phillips, G. O. (2008). Molecular structures of gellan gum imaged with atomic force microscopy in relation to the rheological behavior in aqueous systems in the presence or absence of various cations. *Journal of Agricultural and Food Chemistry*, *56*(18), 8609-8618.
- Gunning, A. P., Kirby, A. R., Ridout, M. J., Brownsey, G. J., & Morris, V. J. (1996). Investigation of gellan networks and gels by atomic force microscopy. *Macromolecules*, *29*(21), 6791-6796.
- Horinaka, J., Kani, K., Hori, Y., & Maeda, S. (2004). Effect of pH on the conformation of gellan chains in aqueous systems. *Biophysical Chemistry*, *111*(3), 223-227.
- Lee, H.-C., & Brant, D. A. (2002). Rheology of Concentrated Isotropic and Anisotropic Xanthan Solutions: 3. Temperature Dependence. *Biomacromolecules*, *3*(4), 742-753.
- Mao, R. S., Tang, J. M., & Swanson, B. G. (1999). Effect of pH buffers on mechanical properties of gellan gels. *Journal of Texture Studies*, *30*(2), 151-166.
- Milas, M., & Rinaudo, M. (1996). The gellan sol-gel transition. *Carbohydrate Polymers*, *30*(2-3), 177-184.

- Miyoshi, E., Takaya, T., & Nishinari, K. (1996). Rheological and thermal studies of gel-sol transition in gellan gum aqueous solutions. *Carbohydrate Polymers*, 30(2–3), 109-119.
- Moritaka, H., Nishinari, K., Nakahama, N., & Fukuba, H. (1992). Effect of potassium-chloride and sodium-chloride on the thermal-properties of gellan gum gels. *Bioscience Biotechnology and Biochemistry*, 56(4), 595-599.
- Moritaka, H., Nishinari, K., Taki, M., & Fukuba, H. (1995). Effects of pH, potassium chloride, and sodium chloride on the thermal and rheological properties of gellan gum gels. *Journal of Agricultural and Food Chemistry*, 43(6), 1685-1689.
- Morris, V., Kirby, A., & Gunning, A. (1999). A fibrous model for gellan gels from atomic force microscopy studies. In K. Nishinari (Ed.). *Physical Chemistry and Industrial Application of Gellan Gum* (Vol. 114, pp. 102-108). Berlin: Springer
- Nishinari, K. (1997). Rheological and DSC study of sol-gel transition in aqueous dispersions of industrially important polymers and colloids. *Colloid and Polymer Science*, 275(12), 1093-1107.
- Nishinari, K. (1999). Physical chemistry and industrial application of gellan gum. Berlin: Springer.
- NutraSweet, K. C. (1996). Gellan gum. San Diego: NutraSweet Kelco Co.
- Picone, C. S. F., & Cunha, R. L. (2010). Interactions between milk proteins and gellan gum in acidified gels. *Food Hydrocolloids*, 24(5), 502-511.
- Rodriguez-Hernandez, A. I., Durand, S., Garnier, C., Tecante, A., & Doublier, J. L. (2003). Rheology-structure properties of gellan systems: evidence of network formation at low gellan concentrations. *Food Hydrocolloids*, 17(5), 621-628.
- Savitzky, A., & Golay, M. J. E. (1964). Smoothing and differentiation of data by simplified squares procedures. *Analytical Chemistry*, 36(8), 1627-1639.
- Steffe, J. F. (1996). *Rheological methods in food process engineering*. East Lansing: Freeman Press.
- Tanaka, S., & Nishinari, K. (2007). Unassociated molecular chains in physically crosslinked gellan gels. *Polymer Journal*, 39(4), 397-403.
- Yamamoto, F., & Cunha, R. L. (2007). Acid gelation of gellan: Effect of final pH and heat treatment conditions. *Carbohydrate Polymers*, 68(3), 517-527.
- Yuguchi, Y., Urakawa, H., & Kajiwara, K. (1997). Structural characteristics of crosslinking domain in gellan gum gel. *Macromolecular Symposia*, 120, 77-89.

– CAPÍTULO 4 –
Polysorbates-Chitosan
Association

**STUDY OF POLYSORBATES - CHITOSAN ASSOCIATION TO THE FORMATION OF NANO AND
MICROSTRUCTURES**

PICONE, Carolina Siqueira Franco¹ & CUNHA, Rosiane Lopes^{1*}

¹ Department of Food Engineering, Faculty of Food Engineering, University of Campinas (UNICAMP), 13083-862, Campinas-SP, Brazil

* Phone: +55 19 3521- 4047 FAX: +55 19 3521-4027 email: rosiane@fea.unicamp.br

To be submitted to *Journal of Colloids and Interface Science*

Abstract

Different environment conditions and polysorbate types were explored to the formation of nano and microstructures by association with chitosan. Systems composed by polysorbates (0 - 90% (w/v)) and aqueous phase (10 - 90% (w/v)) containing or not polysaccharide (0.01 – 1 % (w/v)) were studied. Firstly, the effect of polysorbate hydrophobic tail length on the properties of the self-assembled structures was evaluated in order to determine the best component for chitosan interaction. Then the effect of pH (3 or 6.7) on such structure formation was determined. Finally, the effect of chitosan concentration on the surfactant-polymer association was evaluated. The structures were characterized through rheological and conductivity measurements and optical polarized microscopy. Their size was evaluated by dynamic light scattering. Polysorbate-20 tended to form nanoparticles whilst macrostructures were observed in polysorbate-80 systems. Depending on the polysorbate-80 concentration, a liquid crystalline structure was formed with gel characteristics, which difficult the chitosan association. Thus, the mixed systems were composed by polysorbate-20-chitosan. Structures with similar rheological properties, electrical conductivity and size were obtained with polysorbate-20 at pH 3 or 6.7, therefore mixed samples were prepared at pH 3, where chitosan solubility was higher. Increasing

chitosan concentration in mixed systems resulted in smaller and less polydisperse particles due to the decrease in molecular mobility of systems. These results suggest that nanoparticles with potential use in bioactive delivery can be formed by polysorbate-chitosan association.

Key words: self-assembly, chitosan, surfactant, polysorbates

1. Introduction

Surfactant based delivery systems are promising vehicle for bioactive encapsulation due to the wide range of structures that can be obtained: from nanometric structures, such as micelles, to complex structures, as liquid crystals. This versatility enables their application on distinct products or even in the improvement of product texture. Moreover, the amphiphilic character of surfactants allows the entrapment of either hydrophilic or hydrophobic bioactives increasing their solubilization in the final product [1].

Surfactant self-assembled structures change in size and shape with surfactant concentration, temperature, pH, pressure [2], [3] and in the presence of biopolymers [4], [5]. Chitosan is a polysaccharide with a great potential in the food industry and biotechnology applications due to its biodegradability and biocompatibility [4], [6]. It is an effective material in delivery systems due to its mucoadhesive properties which favors the bioactive adsorption by epithelial tissues [7]. Chitosan is an anionic polyelectrolyte which carries free amino and hydroxyl groups along its backbone. The pKa value of the free amino groups is around 6.5, from which arises its pH dependent solubility [8]. The chitosan deacetylation degree and/or solution conditions have an impact on the charge density along the chains and, therefore, on the chitosan flexibility and conformation [9], [10]. These properties, together with the hydrophobicity of the backbone, play an important role in chitosan-surfactants interactions [11]. Despite the marked importance of chitosan and

nonionic surfactants, very little is known on the assembly and physicochemical properties of these polymer/surfactant pairs. Most of studies reported on polymer/surfactant concern about synthetic polymers and surfactants which cannot be applicable in food products [4], [12], [13].

Polysorbates are non-ionic surfactants widely used in food products. They are derived from PEG-ylated sorbitan (hydrophilic group) esterified with fatty acids (hydrophobic group) with a total of 20 ethylene oxide per molecule. The hydrocarbon chains provide the hydrophobic nature of the polysorbates while the hydrophilic nature is provided by the ethylene oxide subunits [14], [15]. The different polysorbates vary in the length of the polyoxyethylene chain, type of fatty acid, and degree of esterification [16]. Such variances result in different self-assembly mechanisms and structures.

The aim of this work was to explore the conditions and sources of polysorbates to the formation of nano and microstructures by assembly with chitosan. Different concentrations of water (10 - 90 % (w/v), polysaccharide (0.01 – 1 % (w/v)) and surfactants (0 - 90 % (w/v)) were studied. The effect of polysorbate hydrophobic tail length on the properties of the self-assembled structures was initially studied in order to determine the best component for chitosan interaction. Then the effect of pH (3.0 or 6.7) on such structure was determined. Finally, the effect of chitosan concentration on the surfactant-polymer association was evaluated. The structures were characterized through rheological measurements and optical polarized microscopy. The conductivity and size of the structures were evaluated by dynamic light scattering.

2. Experimental

2.1 Materials

Polyoxyethylene sorbitan monolaurate and polyoxyethylene sorbitan monooleate also known as Polysorbate 20 (Tween-20) and Polysorbate 80 (Tween-80) respectively, were purchased from Synth (Brazil). Schematic molecular structure of the surfactant is shown in Figure 1. Chitosan of low molecular weight (150 kDa) and degree of deacetylation of 75 - 85% was obtained from Sigma-Aldrich (St Louis – USA) and used without further purification.

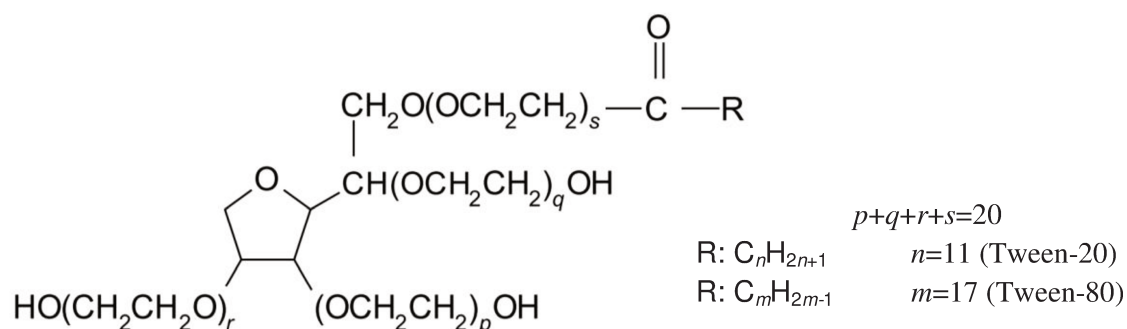


Figure 1. Molecular structure of polysorbates.

2.2. Preparation of systems

Samples were prepared by mixing the surfactant in the aqueous phase for 10 minutes under magnetic stirring and then were stored at 25 °C for 4 days to structure stabilization. The concentration of polysorbates was varied from 0 to 100% (w/v) in steps of 10% (w/v). The role of the length of polysorbate hydrophobic tail was evaluated by samples composed of pure deionized water (pH 6.7) and polysorbate-20 or polysorbate-80. In addition, the effect of the pH of the aqueous phase was determined by the use of 100 mM sodium acetate buffer (pH 3) as aqueous phase in the polysorbate-20 systems.

Chitosan stock solution (2% w/v) was prepared by the dissolution of chitosan powder in 100 mM sodium acetate buffer (pH 3) and stirred overnight at 25 °C. The mixed

samples containing chitosan in the aqueous phase were prepared by magnetic stirring of chitosan stock solution, polysorbate and 100 mM sodium acetate buffer (pH 3) at 25 °C for 10 minutes. The final concentration of chitosan on samples was varied from 0.01 to 1% (w/v). As it was not possible to increase the concentration of chitosan stock solution (due to its high viscosity), the mixed samples containing 0.5 and 1% chitosan and surfactant concentration higher than 80 and 50% polysorbate-20, respectively, could not be prepared.

2.3. Electrical conductivity, zeta potential and particle size distribution

The electrical conductivity, zeta potential and size distribution were measured by dynamic light scattering (DLS) in a Zetasizer Nano-ZS (Malvern Instruments, Herrenberg, Germany) at 25 °C.

2.4. Rheological measurements

The rheological properties of samples were determined in an AR 1500 controlled stress rheometer (TA Instruments, England). A stainless steel cone and plate geometry 60 mm in diameter was used.

2.4.1. Flow curves

Flow curve measurements were carried out with a shear rate ranging from 0 to 300 s⁻¹ at 25 °C. The data obtained in the third sweep were fitted to the power law equation (eq.1) using the software Rheology Advantage Data Analysis v. 5.7.0 (TA Instruments, USA).

$$\sigma = k \cdot \dot{\gamma}^n \quad (1)$$

Where σ is the shear stress (Pa), $\dot{\gamma}$ is the shear rate (s⁻¹), k is the consistency index (Pa.s) and n is the flow behaviour index (dimensionless). The apparent viscosity (η_{100}) of

samples was determined at 100 s^{-1} . Some samples showed structure break-down after 70 s^{-1} , in such cases the apparent viscosity (η_{70}) was determined at 70 s^{-1} .

2.4.2. Oscillatory measurements

The effect of temperature on the samples with gel-like behaviour was evaluated by oscillatory rheological tests. The shear strain was kept in 1% to assure that the measurements were done within the linear viscoelastic region. The samples were gently poured in the rheometer plate and melted at $60 \text{ }^\circ\text{C}$ per 2 minutes and then, cooled down to $25 \text{ }^\circ\text{C}$ at $1 \text{ }^\circ\text{C}/\text{minute}$ and 0.1 Hz . The melt temperature was chosen to be below the cloud point of both polysorbates, 76 and $65 \text{ }^\circ\text{C}$ for polysorbate 20 and 80 respectively [17]. Changes in the slope of complex viscosity (η^*) vs temperature curves were maximized from the derivation of the data using the Savitzky & Golay filter [18]. The gelation point was determined as the temperature of the maximum (absolute) slope of $\log(\eta^*)$.

2.5. Polarizing microscopy

The liquid crystalline structures were identified by polarizing microscopy with an Olympus BX51TF microscope (Olympus Co., Japan).

2.6. Statistical analysis

The results were evaluated from at least three replicates of each sample, using the analysis of variance (ANOVA). The significant differences ($p < 0.05$) between different samples were determined by the Tukey procedure, using the software STATISTICA 5.5 (Statsoft Inc., Tulsa, USA).

3. Results

3.1. Effect of length of polysorbate hydrophobic tail

Table 1 shows the rheological parameters of samples composed of polysorbate-20 and 80. Polysorbate-20 and 80 showed the highest viscosity values in samples composed by 70% (w/v) and 60% (m/v), respectively. Both systems showed a viscosity increasing until such concentrations, followed by a decreasing to values nearest to the samples without water.

Table 1. Rheological parameters of samples composed of polysorbate-20 or polysorbate-80 and water at pH 6.7.

Surfactant	Surfactant concentration (% w/v)	Rheological parameters		
		η_{70} (mPa.s)	k (Pa.s)	n
Polysorbate-20	10	2.0 ^r	-	-
	20	4.5 ^p	-	-
	30	14.0 ⁿ	-	-
	40	57.4 ^l	-	-
	50	221 ^k	-	-
	60	529 ^g	-	-
	70	569 ^f	-	-
	80	473 ^h	-	-
	90	436 ⁱ	-	-
	100	386 ^j	-	-
Polysorbate -80	10	2.1 ^q	-	-
	20	6.1 ^e	-	-
	30	46.9 ^m	-	-
	40	1167 ^d	-	-
	50	4302 ^a	199 ^a	0.17 ^a
	60	6483 ^a	120 ^b	0.36 ^b
	70	3444 ^b	-	-
	80	1489 ^c	-	-
	90	830 ^e	-	-
	100	534 ^g	-	-

Different letters in the same column mean significant differences ($p < 0.05$)

The length of polysorbate hydrophobic tail affected directly the rheological parameters of the samples. Samples with longer polysorbate hydrophobic tail were statistically more viscous, especially that composed of 40 – 80% (w/v) of surfactant as

compared to polysorbate-20. Polysorbate-80 has bulkier side chains which are responsible for different interfacial packing, and thus, these systems show a sharper change in the viscosity [19] due to the formation of more complex structures. In fact, all polysorbate-20 systems showed Newtonian behaviour regardless of surfactant concentration whereas two types of rheological behaviour were observed to polysorbate-80 samples: newtonian and shear thinning. The shear thinning behaviour was observed between 50 - 60% (w/v) polysorbate-80. Such samples showed high consistency index and low flow behaviour index suggesting the formation of structures which tends to self-organize under shearing. As the structure of such sample was extremely sensible to temperature, their rheological behaviour and gel formation were also evaluated by oscillatory measurements (Figure 2 and 3). Samples composed by 70% polysorbate-80 which presented high apparent viscosity were also evaluated.

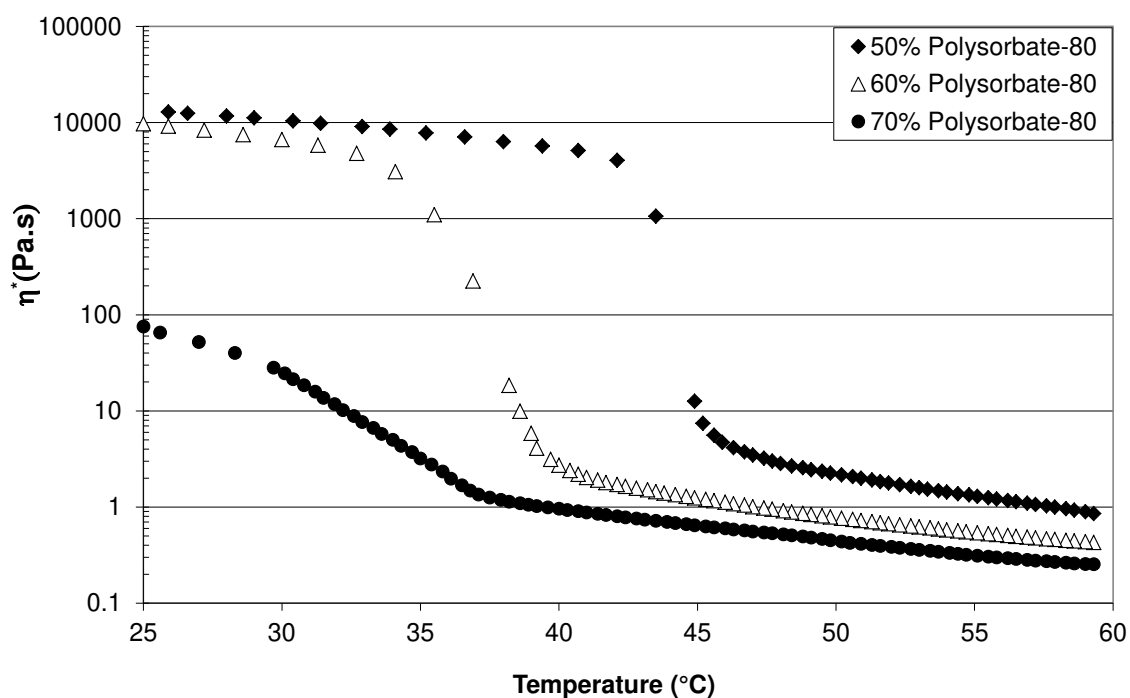


Figure 2. Complex viscosity of polysorbate-80/water systems during cooling from 60 to 25 °C

During cooling, the 50 and 60% polysorbate-80 samples showed a sharp increase in complex viscosity values whilst such increase was smoother for 70% polysorbate-80. As a result, complex viscosity values at 25 °C were considerably lower for 70% polysorbate-80 samples than for other samples. In addition, the increase in polysorbate concentration from 50 to 70% (w/v) decreased the gelation temperature about 10 °C (Table 2).

Table 2. Gelation temperature of polysorbate-80/water samples during cooling.

Polysorbate-80 (% w/v)	Temperature (°C)
50	45.0 ± 0.2 ^a
60	37.0 ± 1.7 ^b
70	35.7 ± 1.8 ^c

Different letters in the same column mean significant differences ($p < 0.05$)

The elastic modulus (G') at 25 °C also decreased with the increase in polysorbate-80 concentration (Figure 3). However, in all the cases the elastic moduli were higher than the loss moduli (G'') at 25 °C. This confirms that at such temperature, the three samples showed gel characteristics. The difference between both moduli ($G' - G''$) were about 3007.3, 1590.0 and 26.8 Pa.s for samples composed of 50, 60 and 70% polysorbate-80, respectively, indicating that the increase in surfactant ratio reduced the elastic character of gels.

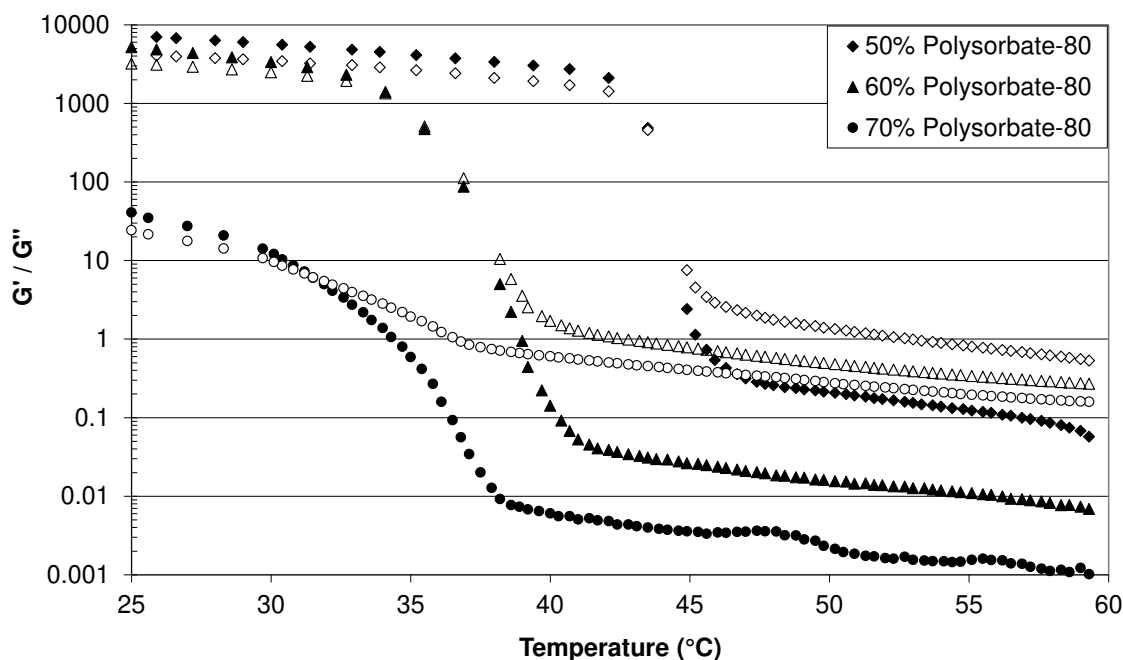


Figure 3. Elastic (G' , full symbols) and loss modulus (G'' , empty symbols) of polysorbate-80/water systems during cooling.

The electrical conductivity can give insights about the structure of surfactant systems since ion mobility is closely related to its structural organization [20], [21], [22], [23]. Figure 4 shows the electrical conductivity of polysorbate systems. Overall polysorbate-80 samples presented lower conductivity values than polysorbate-20 due to its longer hydrophobic tail. The increase in surfactant concentration up to 20% led to an increasing in conductivity for both polysorbates. However whilst the conductivity was constant between 20 – 30% polysorbate-80, it kept increasing for polysorbate-20, achieving the maximum value in 30% polysorbate-20. After this point, polysorbate-20 showed a decreasing in conductivity up to 60% (w/v). Moreover, complex structures formed between 50 - 60% polysorbate-80 resulted in low ion mobility because of higher viscosity, which prevented the conductivity measurements (Figure 4). At polysorbate concentrations higher than 60%, the aqueous phase is the minor phase and thus, reverse

structures were formed. In these systems, the counterions mobility became limited due to the nonionic nature of polysorbates, thus the electrical conductivity could not be measured.

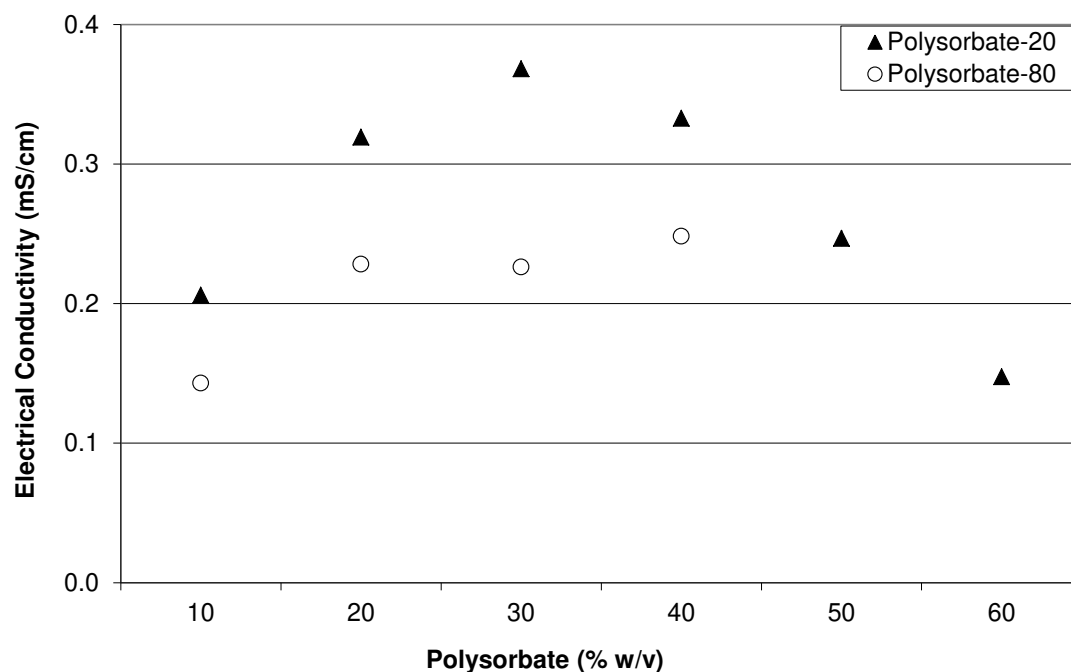


Figure 4. Electrical conductivity (mS/cm) of polysorbate/water systems at 25 °C, pH 6.7.

In ionic micellar systems, two mechanisms of electricity transport are possible: it can be transported by counterions through the continuous aqueous medium; or can move from one micelle to other micelle through the overlapping of diffuse double layers around micelle when two micelles come close together (hopping reaction) [24]. However, the mechanism of electrical conductivity in nonionic micellar systems is still unknown [25]. Theoretically, due to the absence of ionic carriers in nonionic surfactant, the electrical conductivity behaviour would be related only to the counterions of the aqueous phase. Nevertheless, our results indicate that the conductivity of systems enhanced as the number of micellar structures increased up to 20% of polysorbate, suggesting that the micelles play a role in the electrical conduction. Despite the increase in number of micelles from 20 to 30% of polysorbate-20, the increase on conductivity was less intense since the

micelles and their aggregates come near to each other, reducing the aqueous phase channels which restricted the electrical conductance.

In fact, the size distributions confirm an increase in particle size with the increase in surfactant ratio (Table 3, Figure 5). Samples composed of 10% polysorbate showed particle size smaller than 100 nm with one relevant peak near 4 and 4.5 nm for polysorbate-20 and 80, respectively (Figure 5A). Such monomodal distribution is probably related to micelles aggregates, since 10% (w/v) is considerably higher than the critical micellar concentration (CMC) of both polysorbates: 0.07 and 0.015% (w/v) for polysorbate-20 and 80, respectively [26]. This hypothesis was confirmed by increasing polysorbates ratio. As observed in Figure 5, the enhancing in polysorbate-20 concentration led to a multimodal distribution. From 20 to 30% the main peak observed in polysorbate-20 samples started to splint in two peaks which became well defined at 40% surfactant and a small third peak with higher particle size appears at this condition. The main peaks were centered in 1.3 and 12 nm, respectively. The first peak is probably related to free micelles in solution whilst the others, to micelle aggregates. The third peak (above 45 nm) observed at 40% (w/v) polysorbate-20 and beyond (Figure 5) revealed the formation of complex structures, which was partially responsible for the decreasing of electrical conductivity of samples (Figure 4). 20 and 30% polysorbate-80 samples also showed a peak above 45 nm related to the stagnation of the electrical conductivity of systems (Figure 4). At intermediate surfactant concentration, the particle size became larger, as well as its viscosity (Table 3) which limited micelles mobility. From 30 to 40% (w/v) polysorbate-80, a sharp increase in viscosity (Table 3) and a polydisperse size distribution were observed. The size measurements above 40% polysorbate-80 and 70% polysorbate-20 could not be done due to the formation of particles larger than 1 μm . Such particles formed a supramolecular structure resulting in the gel formation between 50 – 70% polysorbate-80.

Table 3. Size range of polysorbate samples at different surfactant concentrations.

	Polysorbate concentration (% w/v)	Peak Intensity (%)		
		1-3 nm	3-45 nm	45-1000 nm
Polysorbate-20 pH 6.7	10	28.6 ± 0.5 ^{bc}	71.0 ± 0.3 ^d	0.0 ± 0.1 ^g
	20	24.0 ± 1.7 ^d	72.9 ± 1.1 ^{bc}	1.7 ± 1.5 ^f
	30	24.8 ± 0.5 ^d	73.9 ± 0.9 ^b	0.9 ± 0.8 ^f
	40	28.8 ± 1.0 ^b	62.9 ± 0.9 ^e	8.3 ± 1.6 ^{de}
	50	27.6 ± 1.0 ^{bc}	51.5 ± 1.6 ^f	20.0 ± 1.9 ^b
	60	25.5 ± 1.9 ^{cd}	30.2 ± 2.5 ^g	43.1 ± 3.1 ^a
Polysorbate-80 pH 6.7	10	14.0 ± 1.1 ^f	86.1 ± 1.0 ^a	0.0 ± 0.0 ^g
	20	23.4 ± 1.6 ^d	70.2 ± 0.7 ^d	6.6 ± 1.8 ^e
	30	20.3 ± 1.6 ^e	70.3 ± 2.8 ^{cd}	10.4 ± 3.6 ^{cd}
	40	35.1 ± 0.5 ^a	53.1 ± 1.6 ^f	12.5 ± 1.3 ^c

Different letters in the same column mean significant differences ($p < 0.05$)

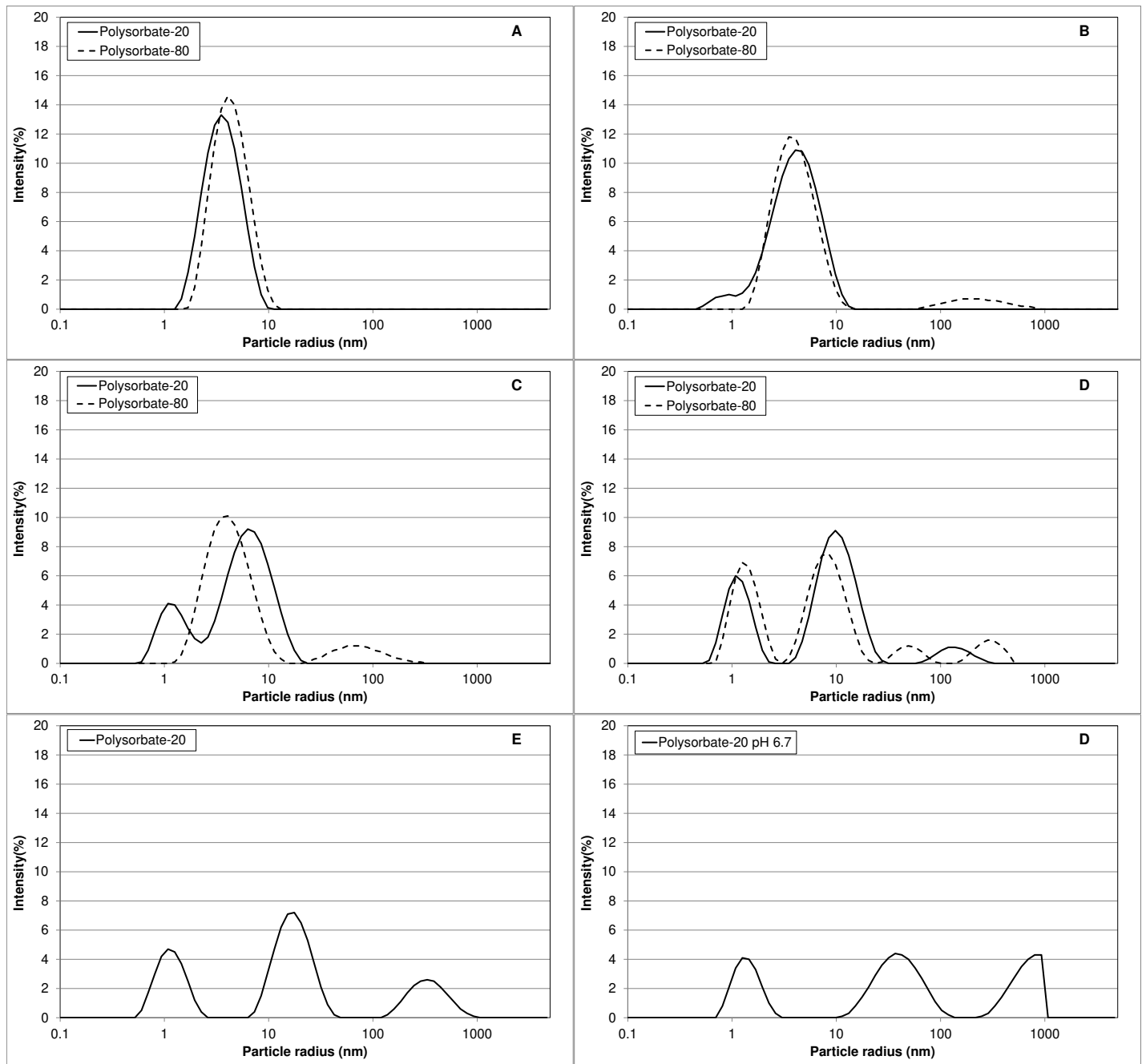


Figure 5. Size distribution by intensity of polysorbate-20 or 80 and water at different surfactant concentration. A) 10% (w/v), B) 20% (w/v), C) 30% (w/v), D) 40% (w/v), E) 50% (w/v) and D) 60% (w/v).

Figure 6 shows the visual appearance of polysorbate/water systems. All polysorbate-20 samples were clear and presented a liquid aspect independently of surfactant concentration. However, significant changes on the appearance of polysorbate-80 samples were observed according to surfactant concentration. From 10 to 40% and 80 - 90% (w/v) polysorbate-80 the systems were clear and liquid-like, similar to polysorbate-20. Nevertheless, systems composed of 50 - 60% (w/v) polysorbate-80 showed a cloudy and gel-like appearance whilst 70% polysorbate-80 were gel-like but clear, confirming rheological results. When observed under polarized light, 50 and 60% (w/v) polysorbate-80 samples were bi-refringent whilst all the others samples were not (Figure 6).

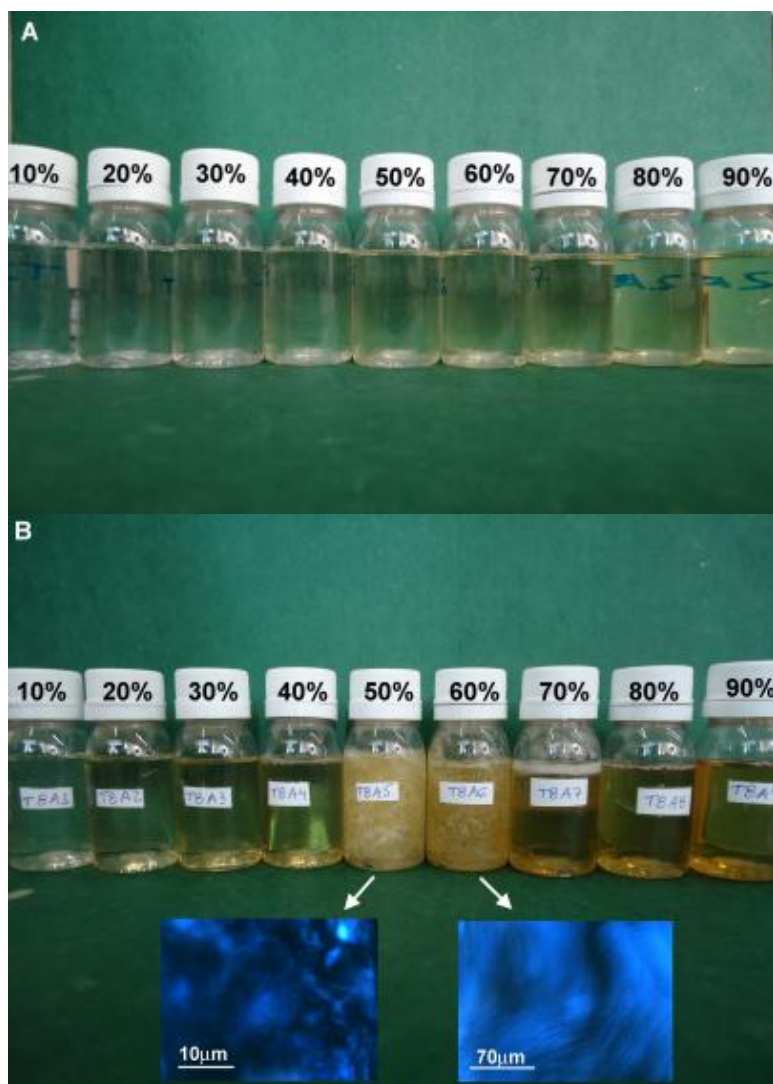


Figure 6. Visual appearance of polysorbate/water systems at 25 °C. A) Polysorbate-20 and B) Polysorbate-80. The micrographies show the birefringence of samples under cross light.

Samples appearance and rheological properties are closely related to the type of assembled structure. Clear, non-birefringent and low viscous solutions are characteristic of micellar phase which is usually formed at surfactant concentration ranging from 0 to 25% [3]. Both polysorbate-20 and 80 presented such characteristics at concentration up to 20% (w/v) (Figure 6 and Table 1), thus suggesting the existence of a micellar phase as also indicated by the size and electrical conductivity results (Figures 4 - 5). Polysorbate micelles are spherical aggregates of the polysorbates with the ethylene oxide subunits

pointing outwards in contact with the surrounding solution and the hydrocarbon tails in the center away from the water [15]. Such type of structure is suitable for either delivery systems or the protection of labile compounds [3]. Clear, non-birefringent but highly viscous samples are typical of bicontinuous cubic phases [3] which fits with the characteristics of 70% polysorbate-80 systems (Figure 6 and Table 1). Typical characteristics of liquid crystalline hexagonal phase were observed only for the polysorbate systems with longer hydrophobic tail length (polysorbate -80) at 50 - 60% (w/v). This type of structure can present a cloudy appearance, birefringent and viscous structures [3] as shown in Figure 6 and Table 1.

Details about morphology of each structure can be further investigated by other techniques, such as small-angle X-ray scattering (SAXS) [27], [28] and NMR spectroscopy [29], [30], [31].

Overall, the length of polysorbate hydrophobic tail was determinant of the type of structure formed. The longer and branched tail of polysorbate-80 resulted in a wide range of structures. However, the high viscosity and gel characteristics of such systems prevented the homogenous mixture and assembly with chitosan. Therefore, the polysorbate-20 was chosen to compose the mixed systems.

3.2. Effect of pH on the self-assembly of polysorbate-20

Chitosan is an anionic polysaccharide insoluble at neutral pH [32]. Thus, the self-aggregation of polysorbate-20 was also studied at the pH of chitosan stock solution (pH 3.0).

The viscosity of polysorbate-20 at pH 3 increased with the enhancing in surfactant concentration and reached a maximum in 70% polysorbate, as well as samples at pH 6.7

(Table 4). All the systems showed Newtonian behaviour and similar viscosity values regardless the pH. The visual appearance of samples was the same, as well.

Table 4. Viscosity at 70 s^{-1} , electrical conductivity and size range of polysorbate-20/water (pH 6.7) and polysorbate-20/acetate buffer (pH 3) at $25 \text{ }^\circ\text{C}$.

Polysorbate-20 (% w/v)	Peak Intensity (%)									
	η_{70} (mPa)		Electrical conductivity (mS/cm)		1 - 3 nm		3 - 45 nm		45 - 1000 nm	
	pH 6.7	pH 3.0	pH 6.7	pH 3.0	pH 6.7	pH 3.0	pH 6.7	pH 3.0	pH 6.7	pH 3.0
10	2.0 ^l	2.4 ^k	0.206 ^h	0.456 ^c	28.6 ^{abc}	12.2 ^e	71.0 ^{df}	87.8 ^a	0.0 ^{ef}	0.0 ^f
20	4.5 ^j	4.9 ⁱ	0.319 ^f	0.475 ^a	24.0 ^d	18.8 ^{de}	72.9 ^{cbe}	81.2 ^{ab}	1.7 ^e	0.0 ^f
30	14.0 ^h	14.2 ^h	0.368 ^d	0.461 ^b	24.8 ^d	18.1 ^e	73.9 ^{cb}	76.9 ^b	0.9 ^e	4.9 ^d
40	57.4 ^g	57.4 ^g	0.333 ^e	0.334 ^e	28.8 ^{ab}	24.4 ^d	62.9 ^g	67.3 ^{efg}	8.3 ^c	9.2 ^c
50	221.6 ^f	212.8 ^f	0.247 ^g	0.242 ^g	27.6 ^{bc}	29.4 ^a	51.5 ^h	53.4 ^h	20.0 ^b	18.1 ^b
60	529.8 ^b	447.6 ^{cd}	0.148 ⁱ	-	25.5 ^{cd}	-	30.2 ⁱ	-	43.1 ^a	-
70	569.8 ^a	519.5 ^a	-	0.085 ^j	-	-	-	-	-	-
80	473.6 ^c	436.0 ^d	-	0.041 ^k	-	-	-	-	-	-
90	436.6 ^d	399.7 ^k	-	0.016 ^l	-	-	-	-	-	-
100	386.3 ^e	386.3 ^e	-	-	-	-	-	-	-	-

Different letters in the same analysis block mean significant differences ($p < 0.05$)

The electrical conductivity measurements also showed similar tendency for both pH values: an increasing in lower surfactant concentration, followed by a decrease in higher polysorbate concentrations (Table 4). Up to 50% of surfactant, the conductivity of samples is mainly determined by the aqueous phase. Thus, up to 30% polysorbate-20 the samples at pH 3 presented higher conductivity than pH 6.7 due to the greater amount of counterions in acetate buffer (pH 3). In addition, despite of the large surfactant concentration, the higher amount of counterions in aqueous phase made it possible to measure the conductivity of systems composed of 70-90% (w/v) polysorbate. The maximum conductivity was observed at 20%-polysorbate (pH 3) instead of 30%-polysorbate (pH 6.7), but no statistically significant differences were observed at surfactant concentrations higher than 40% (w/v) because of the reduced aqueous phase content.

The particle size also increased with pH decrease in samples with polysorbate concentration up to 30% (w/v). From this concentration no significant changes on particle

size were observed (Table 4). Within this concentration range, the changes on electrical conductivity of pH 3 samples were smoother than at pH 6.7, since the main conductance mechanism was by the counterions in aqueous phase instead of hopping reaction (Table 4). The maximum value of electrical conductivity at pH 3 was observed at lower polysorbate concentration because the micelles are larger at such pH and get closer to each other at lower surfactant concentration. Despite the pH does affect the micellar phase, it did not seem to affect the structures formed between 40 - 50% polysorbate-20. Within this concentration range samples presented the same electrical conductivity even with the enhancing in counterions at pH 3 (Table 4). This suggests that the electrical conductivity was determined by the physical barrier of surfactant structures at this concentration range.

Overall, the pH did not affect strongly the polysorbate-20 structures. In both pH values evaluated the structures obtained seem to be promising to association with chitosan.

3.3. Polysorbate-chitosan association

Figure 7 shows the viscosity of chitosan-polysorbate-20 systems at pH 3. Overall the systems showed an increase in viscosity with enhancing polysorbate concentration and reached a maximum at 50 - 60% (w/v). The addition of 0.01% (w/v) chitosan to polysorbate-20 systems did not affect significantly their viscosity, however all the others chitosan concentrations evaluated resulted in more viscous samples. The marked increase in viscosity of mixed samples could be related to the formation of chitosan-surfactant complexes (Grant et al. 2006). Indeed, samples composed of 1% chitosan and 40 - 50% polysorbate-20 or 0.5% chitosan and 50 - 70% polysorbate-20 showed viscosity values higher than the pure chitosan or surfactant solutions, indicating a synergic interaction between both compounds.

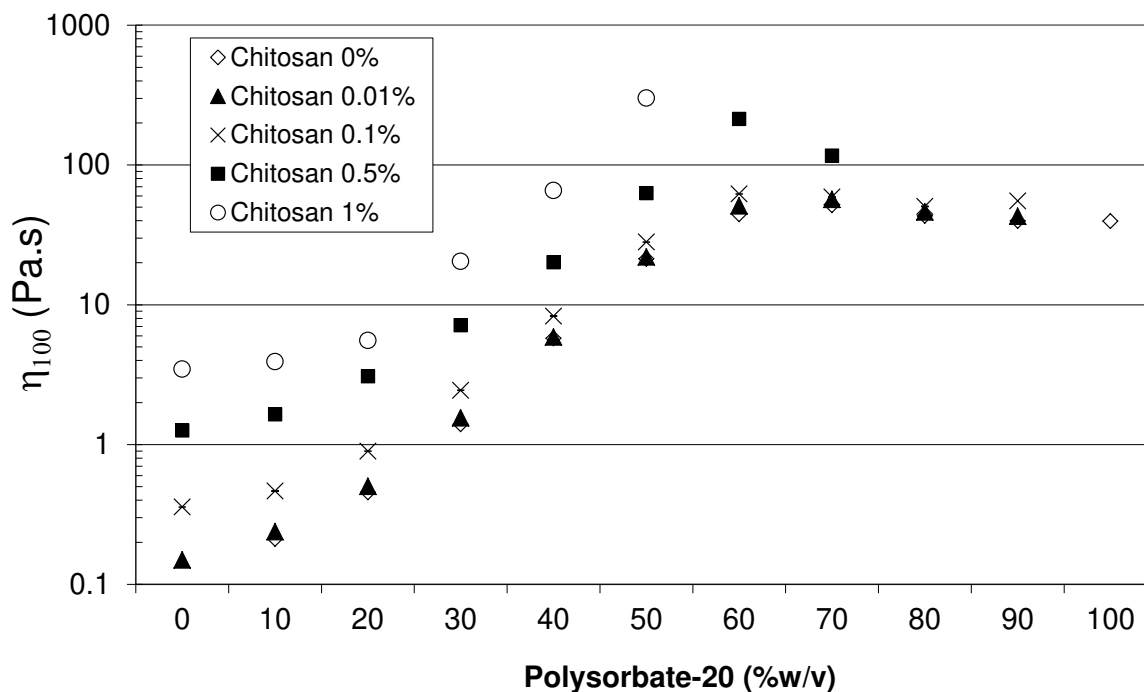


Figure 7. Viscosity at 100 s^{-1} of chitosan-polysorbate-20 systems formed by different chitosan concentrations: \diamond 0% (w/v), \blacktriangle 0.01% (w/v), \times 0.10% (w/v), \blacksquare 0.50% (w/v) and \circ 1.00% (w/v).

Despite all the polysorbate-water systems showed Newtonian behaviour, some of the mixed samples were shear-thinning (Table 5), with a more complex structure.

Table 5. Rheological parameters of non-Newtonian chitosan-polysorbate-20 systems.

Polysorbate-20 (% w/v)	Chitosan (% w/v)	k (Pa.s ⁿ)	n
60	0.50	11.34 ^A	0.64 ^A
70	0.50	2.93 ^B	0.80 ^B
30	1.00	0.36 ^C	0.88 ^C
40	1.00	2.02 ^D	0.76 ^D
50	1.00	71.80 ^E	0.31 ^E

Different letters in the same column mean significant differences ($p < 0.05$)

The electrical conductivity of mixed samples is presented on Figure 8. Two conductance profiles were observed depending on the chitosan concentration. At 0.01% (w/v) chitosan, the electrical conductivity tended to be similar to polysorbate-20-water systems. Overall, the addition of 0.5 - 1.0% (w/v) chitosan increased the conductivity of

samples up to 50% (w/v) polysorbate-20 due to the relevance of aqueous phase to such systems. The polyelectrolyte addition enhanced the charge transport in the aqueous phase and led to an increase in conductivity values. Since beyond that polysorbate concentration, counterions mobility was strongly affected by the formation of reverse structures, hence the conductivity decreased independently of the polysaccharide presence.

A special increase in the electrical conductivity was observed in the samples composed by 40 and 50% (w/v) polysorbate-20 (Zoom, Figure 8) in the presence of 0.01% chitosan. In the absence of the polysaccharide such surfactant concentration marked the point in which the aqueous channels became thinner, constraining counterions mobility and thus electrical conductance.

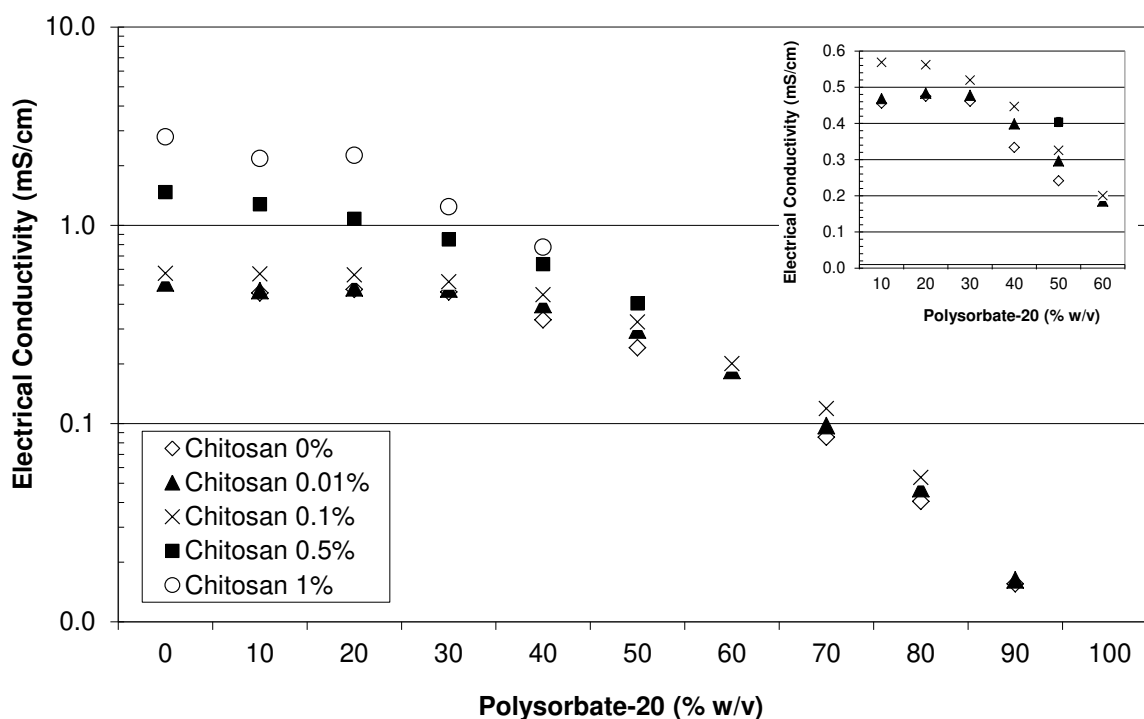


Figure 8. Electrical conductivity (mS/cm) of chitosan-polysorbate-20 assembled systems at 25 °C and different chitosan concentrations: \diamond 0% (w/v), \blacktriangle 0.01% (w/v), \times 0.10% (w/v), \blacksquare 0.50% (w/v) and \circ 1.00% (w/v). The zoom highlights the effect of 0.01% (w/v) in 40 - 50% (w/v) polysorbate mixed systems.

The size measurements revealed that the peak intensity of structures between 45 - 1000 nm formed at 30 – 50% polysorbate-20 tended to increase with the addition of 0.01% chitosan (Table 6). On the other hand, the increase in polysaccharide concentration led to an increase of particles with the lower size range (1 - 3 nm) (Figure 7). The size distributions of mixed samples showed the same tendencies of polysorbate-water systems but the peaks became less polydisperse as the chitosan concentration increased (Figure 9).

Table 6. Size range of polysorbate-chitosan systems.

Chitosan (% w/v)	Polysorbate-20 (% w/v)	Peak Intensity (%)		
		1-3 nm	3-45 nm	45-1000 nm
0.00	10	10.3 ± 4.6 ^{pq}	89.6 ± 4.5 ^c	-
	20	18.8 ± 8.1 ^{ghijklmno}	81.2 ± 8.1 ^{cdefg}	-
	30	18.1 ± 3.6 ^{jkmnop}	76.9 ± 1.7 ^{ghijk}	4.9 ± 2.2 ^f
	40	24.4 ± 2.5 ^{efg}	67.3 ± 4.3 ^{ilmno}	9.2 ± 4.2 ^{de}
	50	29.4 ± 0.7 ^{cd}	53.4 ± 0.9 ^{rs}	18.1 ± 2.1 ^{ab}
0.01	10	21.7 ± 1.2 ^{hijkl}	78.3 ± 1.2 ^{gh}	-
	20	19.3 ± 3.6 ^{ijklm}	78.1 ± 3.1 ^{ghi}	2.5 ± 0.7 ^g
	30	22.9 ± 2.3 ^{ghi}	71.3 ± 1.0 ^{jl}	5.8 ± 1.8 ^{ef}
	40	27.0 ± 1.2 ^{ef}	62.4 ± 0.5 ^{nop}	10.7 ± 1.6 ^d
	50	25.7 ± 1.2 ^{ef}	53.8 ± 1.0 ^{rs}	20.5 ± 2.0 ^a
	60	37.4 ± 0.7 ^a	62.5 ± 0.7 ^{np}	0.1 ± 0.2 ^h
0.10	10	16.4 ± 1.0 ^{kmop}	83.6 ± 1.0 ^{ef}	-
	20	12.0 ± 3.7 ^{kpq}	84.1 ± 4.0 ^{cde}	4.9 ± 0.9 ^f
	30	18.9 ± 1.2 ^{jkno}	70.2 ± 2.3 ^{ilm}	13.8 ± 1.5 ^c
	40	23.6 ± 1.9 ^{fgh}	57.5 ± 3.0 ^q	19.9 ± 1.4 ^{ab}
	50	29.6 ± 0.2 ^{bc}	51.5 ± 0.9 ^f	18.8 ± 0.6 ^{ab}
	60	33.5 ± 3.5 ^b	56.0 ± 5.4 ^{qr}	22.0 ± 10.3 ^a
0.50	10	1.9 ± 1.0 ^f	97.3 ± 1.5 ^b	0.9 ± 1.0 ^h
	20	13.4 ± 1.3 ^{kop}	86.3 ± 1.1 ^{cd}	0.6 ± 1.0 ^h
	30	22.7 ± 5.2 ^{hij}	77.4 ± 5.1 ^{ghijk}	-
1.00	10	-	100.0 ± 0.1 ^a	-
	20	3.7 ± 2.9 ^f	96.4 ± 2.9 ^{ab}	-
	30	22.5 ± 18.7 ^{bdfhijk}	77.5 ± 18.7 ^{cefghij}	-
	40	31.9 ± 5.8 ^{abdf}	68.1 ± 5.7 ^{ilmn}	-

Different letters in the same column mean significant differences ($p < 0.05$)

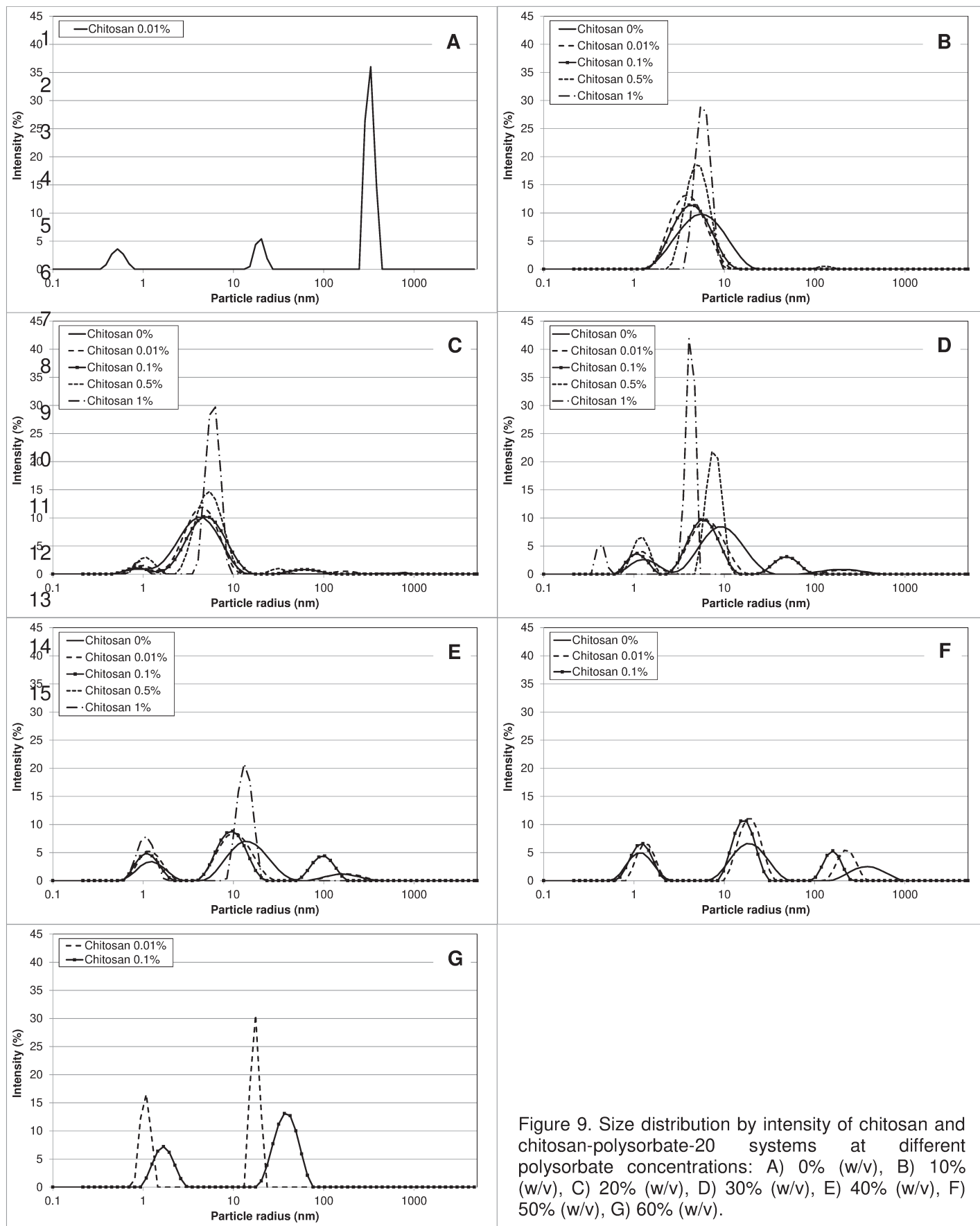


Figure 9. Size distribution by intensity of chitosan and chitosan-polysorbate-20 systems at different polysorbate concentrations: A) 0% (w/v), B) 10% (w/v), C) 20% (w/v), D) 30% (w/v), E) 40% (w/v), F) 50% (w/v), G) 60% (w/v).

The complexation between polymers and surfactants occurs in two distinct modes: the surfactant may adsorb along polymer molecule or it could be adsorbed in the form of discrete micelles [33] (Figure 10). The former mechanism is observed when the polymer-surfactant interaction occurs predominantly by the surfactant tail and the micelles adsorption occurs when the surfactant hydrophilic portion dominates the binding [33]. Chitosan-sorbitan esters complexes are known to be formed by weak interactions: hydrogen bonding between the hydroxyl and carbonyl groups of the sorbitan ester headgroup and the amine, ammonium ions, and hydroxyl groups of chitosan in addition to hydrophobic interactions between the sorbitan ester tails and chitosan hydrophobic sites (Grant et al. 2008). Similar interactions are expected to chitosan-polysorbate complexes which probably present a bottlebrush conformation.

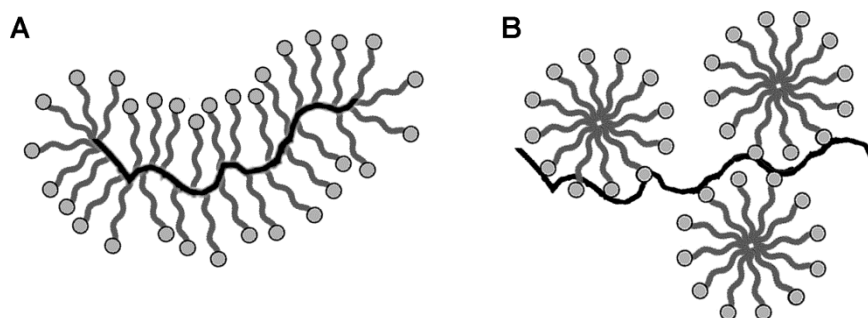


Figure 10. Schematic representation of complexation between polymers and surfactants. A) Surfactant adsorption along polymer molecule and B) Surfactant adsorption in the form of discrete micelles.

The conductivity and size results suggest that at low chitosan concentration (0.01%) all the polysaccharide molecules were involved by surfactant in a bottlebrush conformation (of around 4nm), since if the chitosan molecules were free in aqueous phase, the electrical conductivity would have increased, which did not happened. With the increase in polysorbate concentration up to 50% (w/v), the electrical conductivity also was higher than polysorbate-water systems since chitosan-micelles aggregates come near to each other enhancing the charge transport by the hopping reaction. At polysorbate

concentration higher than 50%, reverse structures were formed with chitosan located in the core, thus its presence was not effective to charge transport and no differences was observed between the polysorbate-chitosan and polysorbate-water systems (Figure 8).

Regarding the samples composed of 0.05% chitosan and 10% polysorbate-20, the amount of surfactant was not enough to completely complex the polysaccharide and an increase in conductivity was observed as compared to polysorbate-water systems (Figure 8). The same behaviour was observed at higher chitosan concentrations. As the polysorbate concentration increased, the number of polysorbate-chitosan aggregates also increased which reduced the chitosan electrical conductance capacity. In addition, the formation of reverse structures contributed to the linear decay in electrical conductivity of samples observed with increasing surfactant concentration (Figure 8).

The intensity of the peak around 1 nm related to un-aggregated micelles, became more intense with the increasing in chitosan concentration. Moreover, the increase in polysaccharide concentration led to size distributions with narrower peaks (Figure 9). This happened because of the marked increase in system viscosity with the enhancing in polysaccharide concentration which reduced the mobility of micelles and micelle aggregates and thus, their clustering. Overall, the increase in viscosity promoted by the increase in polysorbate and chitosan concentration contributed to the formation of nano-sized structures (structures smaller than 100 nm).

The cross polarizing microscopy of mixed samples did not showed birefringence, indicating that the phase behaviour of polysorbate-chitosan and polysorbate-water systems remained similar.

4. Conclusions

The polysorbate hydrophobic tail length was a determinant factor to the type of structures formed. A longer hydrophobic tail resulted in the formation of supramolecular structures such as liquid crystal which presented gel-like properties, leading to inhomogeneous association with chitosan. Thus, polysorbate-20 was selected to compose the mixed systems. Moreover, polysorbate-20 formed nano scale structures in a wider concentration range (10 - 30% (w/v)) than polysorbate-80 (10% (w/v)).

Polysorbate-20 systems showed similar characteristics at pH 3 and 6.7, hence mixed polysorbate-chitosan systems were composed at pH 3 since chitosan presents higher solubility and probably enhanced interaction with the polysaccharide.

The particle size of polysorbate-water and polysorbate-buffer systems was governed by polysorbate concentration. The increase in surfactant concentration enhanced micellar aggregation and increased system polydispersity. In mixed polysorbate-chitosan systems, the size was also determined by the viscosity conferred by chitosan molecules. The higher viscosity values, the lower molecular mobility and smaller structures were obtained due to hindering of particle aggregation. The electrical conductivity results suggested that polysorbate-chitosan complexes present a bottlebrush conformation. Overall, the results of present work suggest that polysorbate-chitosan structures can be modeled by controlling surfactant/aqueous phase ratio and polysaccharide concentration.

5. References

- [1] F. Testard, T. Zemb, C. R. Geosci. 334 (2002) 649.
- [2] G.H. Sagar, M.A. Arunagirinathan, J.R. Bellare, Indian J. Exp. Biol. 45 (2007) 133.
- [3] M.J. Lawrence, Chem. Soc. Rev. 23 (1994) 417.
- [4] Y. Fan, Y. Liu, J. Xi, R. Guo, J. Colloid Interface Sci. 360 (2011) 148.

-
- [5] V. Tomašić, A. Tomašić, I. Šmit, N. Filipović-Vinceković, J. Colloid Interface Sci. 285 (2005) 342.
- [6] R. Jayakumar, D. Menon, K. Manzoor, S.V. Nair, H. Tamura, Carbohydr. Polym. 82 (2010) 227.
- [7] M. Dash, F. Chiellini, R.M. Ottenbrite, E. Chiellini, Prog. Polym. Sci. 36 (2011) 981.
- [8] I. Pepić, J. Filipović-Grčić, I. Jalšenjak, Colloids Surf., A 336 (2009) 135.
- [9] B. Nyström, A.-L. Kjøniksen, C. Iversen, Adv. Colloid Interface Sci. 79 (1999) 81.
- [10] M.L. Tsaih, R.H. Chen, Int. J. Biol. Macromol. 20 (1997) 233.
- [11] R. Barreiro-Iglesias, C. Alvarez-Lorenzo, A. Concheiro, 258 (2003)
- [12] A. Kellarakis, V. Castelletto, M.J. Krysmann, V. Havredaki, K. Viras, I.W. Hamley, Langmuir 24 (2008) 3767.
- [13] J. Desbrieres, C. Bousquet, V. Babak, Cellul. Chem. Technol. 44 (2010) 395.
- [14] J. Jim, Adv. Drug Delivery Rev. 60 (2008) 1663.
- [15] B.A. Kerwin, J. Pharm. Sci. 97 (2008) 2924.
- [16] S. Petersen, J. Ulrich, Chem. Eng. Technol. 34 (2011) 1869.
- [17] M. Donbrow, E. Azaz, A. Pillersdorf, J. Pharm. Sci. 67 (1978) 1676.
- [18] A. Savitzky, M.J.E. Golay, Anal. Chem. 36 (1964) 1627.
- [19] S. Mehta, G. Kaur, K. Bhasin, AAPS PharmSciTech 11 (2010) 143.
- [20] A. Maldonado, R. Ober, T. Gulik-Krzywicki, W. Urbach, D. Langevin, J. Colloid Interface Sci. 308 (2007) 485.
- [21] L. Zhai, J. Zhang, Q. Shi, W. Chen, M. Zhao, J. Colloid Interface Sci. 284 (2005) 698.
- [22] M.J. Lawrence, G.D. Rees, Adv. Drug Delivery Rev. 45 (2000) 89.
- [23] L. Djordjevic, M. Primorac, M. Stupar, D. Krajisnik, Int. J. Pharm. 271 (2004) 11.
- [24] Y. Moroi, K. Matsuoka, Bull. Chem. Soc. Jpn. 67 (1994) 2057.
- [25] D. Vijayaraghavan, J. Mol. Liq. 166 (2012) 76.

- [26] T. Cottrell, J.V. Peij, in: R.J. Whitehurst, (Ed.), *Emulsifiers in Food Technology*, Blackwell Publishing 2007, p. 162-185.
- [27] D. Varade, K. Ushiyama, L.K. Shrestha, K. Aramaki, *J. Colloid Interface Sci.* 312 (2007) 489.
- [28] C. Richards, G. Tiddy, S. Casey, *Colloid Polym. Sci.* 286 (2008) 31.
- [29] U. Olsson, K. Shinoda, B. Lindman, *J. Phys. Chem.* 90 (1986) 4083.
- [30] F. Nilsson, O. Söderman, I. Johansson, *Langmuir* 12 (1996) 902.
- [31] G.T. Dimitrova, T.F. Tadros, P.F. Luckham, M.R. Kipps, *Langmuir* 12 (1996) 315.
- [32] V. Kjell, S. Olav, in: A.M. Stephen, G.O. Phillips, P.A. Williams, (Eds.), *Food Polysaccharides and Their Applications*, CRC Press, 2006, p. 497-520.
- [33] R.D. Groot, *Langmuir* 16 (2000) 7493.

– CAPÍTULO 5 –

Chitosan-Gellan electrostatic complexes

**CHITOSAN-GELLAN ELECTROSTATIC COMPLEXES: INFLUENCE OF POLYSACCHARIDE RATIO,
PREPARATION CONDITIONS AND SURFACTANT PRESENCE**

PICONE, Carolina Siqueira Franco¹ & CUNHA, Rosiane Lopes^{1*}

¹ Department of Food Engineering, Faculty of Food Engineering, University of Campinas (UNICAMP), 13083-862, Campinas-SP, Brazil

* Phone: +55 19 3521- 4047 FAX: +55 19 3521-4027 email: rosiane@fea.unicamp.br

Submitted to “Carbohydrate Polymers”

Abstract

Nanoparticles were obtained by electrostatic complexation between chitosan and gellan gum at different polysaccharide ratios. The effect of the chitosan (0.001 - 0.005% w/v):gellan ratio (0.005 - 0.009 %w/v) on the particle charge and particle size distribution was determined by Dynamic Light Scattering measurements. The particle stability was studied during storage in an aqueous medium at 25 °C for 100 hours. The effect of the preparation procedure (mixing steps) on the characteristics of the complexes was also determined. In addition, the influence of different concentrations (0.00005 – 0.001% (w/v) of a nonionic surfactant (polysorbate-20) on the chitosan:gellan electrostatic complexes (PECs) was evaluated. The charge of the PECs depended on the polysaccharide ratio but a neutral zeta potential was observed at 2C:8G chitosan:gellan ratio. The low electrostatic repulsion of such a system resulted in particle aggregation, confirmed by the decrease in count rate and increase in particle size. During storage, structural reorganization of the complexes was observed, especially for the systems with 2C:8G and 3C:7G chitosan:gellan ratios, due to a decreased zeta potential. Only the 3C:7G systems presented size stability for 100 hours, while the other particles increased in size up to values greater than 6 µm. The mixture protocol was a determinant factor for PEC size. Multilayered particles formed by a 2-step mixing of polysaccharide solutions showed a

considerable increase in size as compared to the complexes formed by a 1-step mixing. The PEC size, count rate and zeta potential were not affected by the presence of polysorbate-20.

Keywords: Chitosan, gellan gum, electrostatic complexes, nanoparticles

1. Introduction

Many techniques have been used for the production of nanoparticles, such as solvent evaporation (Desgouilles et al., 2003), interfacial polymerization (Ibrahim, Bindschaedler, Doelker, Buri & Gurny, 1992) and emulsification methods (Battaglia, Trotta, Gallarate, Carlotti, Zara & Bargoni, 2007; Lv, Zheng & Tung, 2005; Qi, Chen, Huang, Jin & Wang, 2012). However, most of these approaches involve the use of organic solvents, high temperatures and elevated shear rate, which limit their application in the encapsulation of labile compounds. Thus the electrostatic complexation shows relevant advantages, since it is a biocompatible process, requires low energy and does not use cross-linking agents (Jintapattanakit, Junyaprasert, Mao, Sitterberg, Bakowsky & Kissel, 2007; Lankalapalli & Kolapalli, 2009). The electrostatic complexes (PECs) are formed by the association of oppositely charged polyelectrolytes (Amaike, Senoo & Yamamoto, 1998) and lead to particles with dimensions on a colloidal level, generating optically homogeneous and stable nano-dispersions (Mao, Bakowsky, Jintapattanakit & Kissel, 2006; Sun, Mao, Mei & Kissel, 2008).

The most common food PEC is formed from sodium alginate and chitosan. Chitosan is a nontoxic, bioadhesive and biocompatible cationic polysaccharide obtained by the partial deacetylation of chitin. Its linear structure is composed of three reactive functional groups, an amino group and primary and secondary hydroxyl groups at the C-2, C-3 and C-6 positions, respectively (Claesson & Ninham, 1992; Shahidi, Arachchi & Jeon, 1999). When positively charged, the amino groups are promising sites for electrostatic

interactions (Gomez, Ramirez, Neira-Carrillo & Villalonga, 2006). The molecular weight of chitosan varies from 1 to 1000 kDa depending on its degree of acetylation (DA) (George & Abraham, 2006) and is 10 times higher than that of globular proteins (Payne & Raghavan, 2007). This polysaccharide is widely used to form PECs due to its abundance and mucoadhesive properties which, enhance absorption of the bioactive in the intestine. However, nanoparticles composed of chitosan alone are unstable to low pH values and may release the bioactive earlier than expected due to its fast dissolution in the stomach (Hamman, 2010). Such instability can be overcome by complexing the chitosan with sodium alginate or another anionic polysaccharide resistant to low pH values, such as gellan gum (Norton, Cox & Spyropoulos, 2011; Picone & Cunha, 2011).

Gellan gum is a heteropolysaccharide produced by *Pseudomonas elodea* (Jansson, Lindberg & Sandford, 1983) which has received increasing attention due to its capacity to form strong gels, even at concentrations as low as 0.2% (w/v) (Moritaka, Nishinari, Taki & Fukuba, 1995; Picone & Cunha, 2011; Yamamoto & Cunha, 2007). Its structure presents a wormlike shape (Dentini, Coviello, Burchard & Crescenzi, 1988) and consists of tetrasaccharide repeating units of D-glucose, D-glucuronic acid, D-glucose and L-rhamnose (Jansson, Lindberg & Sandford, 1983). Gellan shows a coiled conformation at high temperatures and aggregates into double helices as the temperature decreases (Picone & Cunha, 2011). The helical conformation shows substantial stiffness (Dentini, Coviello, Burchard & Crescenzi, 1988) and its persistence length is reported as 98 nm at 25 °C (Takahashi et al., 2004). The main factor that distinguishes gellan gum from other polysaccharides is its gel forming capacity at low pH values. It makes chitosan-gellan complexes a promising enteric delivery system: the gellan gum protecting the bioactive from the low pH of the stomach whilst the chitosan would promote mucoadhesion of the complex to the intestinal tissues and the controlled release of the bioactive component.

Several variables affect the formation mechanisms and stability of the polyelectrolyte complexes in water, such as the ionic strength, pH, polyelectrolyte concentrations and their characteristics such as molecular weight, charge density, flexibility and the presence of hydrophilic or hydrophobic moieties in the polymers (Lima Vidal, Pereira Fagundes, Cabral de Menezes, Machado da Silva Ruiz & Balaban Garcia, 2005). Surfactants are amphiphilic molecules that readily adsorb at surfaces, thereby decreasing the interfacial tension. Despite intensive research aimed at understanding surfactant-polymer interactions (Grant, Cho & Allen, 2006; Grant, Lee, Liu & Allen, 2008; Groot, 2000; Naderi, Claesson, Bergström & Dédinaite, 2005; Pepić, Filipović-Grčić & Jalšenjak, 2008, 2009; Ziani, Henrist, Jerome, Aqil, Mate & Cloots, 2011), their influence in the complexation mechanisms of biopolymer systems is still not clear.

The aim of this work was to evaluate the complexation between chitosan and gellan gum and to investigate the characteristics of the PECs obtained. The stability of the complexes was evaluated with time. The effects of the preparation conditions and of the presence of a nonionic surfactant on the final characteristics of the PECs were also studied.

2. Materials

Deacylated gellan gum powder (Kelcogel® F) (250 kDa, 3.42% w/w moisture content) was kindly donated by Kelco Biopolymers (San Diego, CA). Low molecular weight chitosan (150 kDa, 75 - 85% deacetylated) was purchased from Sigma-Aldrich Co. (St Louis, EUA) and polyoxyethylene sorbitan monolaurate, also known as polysorbate-20 or Tween-20, was obtained from Synth (Brazil).

3. Methods

3.1. Preparation of stock solutions

The chitosan (C) stock solution (1% w/v) was prepared by the dissolution of chitosan powder in 100 mM sodium acetate buffer (pH 3) and stirred overnight at 25 °C. The 0.7% (w/w) gellan gum (G) stock solution (pH 5.3) was prepared by stirring the gellan powder in deionized water at 80 °C for 30 min in a jacketed vessel, followed by cooling to 10 °C in an ice bath. Each stock solution was diluted in deionized water to a final concentration of 0.01% (w/v).

3.2. Sample preparation

The 0.01% (w/v) polysaccharide solutions were mixed by magnetic stirring at the final concentrations presented in Table 1, and the pH adjusted to 4.5 by the addition of 0.1 M HCl. After adjustment of the pH, samples were stirred for 2 hours at 25 °C before analysis.

Table 1. Composition of chitosan (CH):gellan (GN) systems.

System (Chitosan:Gellan)	Chitosan (%w/v)x10 ³	Gellan (%w/v)x10 ³	Total polysaccharide concentration (%w/v)
0C:1G	0.0	10.0	0.01
1C:9G	1.0	9.0	0.01
2:C8G	2.0	8.0	0.01
3C:7G	3.0	7.0	0.01
4C:6G	4.0	6.0	0.01
5C:5G	5.0	5.0	0.01
1C:0G	10.0	0.0	0.01

The protocol of particle formation was tested by preparing multilayered systems (M1C:9G and M2C0:80G). The pre-mixtures were first prepared by the conventional method mentioned above. After 2 hours, extra volumes of 0.01% (w/v) chitosan or gellan solutions were added to the pre-mixtures to change their concentration ratio from 1C:9G to

M2C:8G and from 2C:8G to M1C:9G, respectively. The pH of the samples was readjusted and the samples stirred for a further 2 hours at 25 °C before analysis.

The effect of the surfactant concentration on the chitosan-gellan interactions was studied using the 3C:7G and 2C:8G systems. The samples were prepared by the conventional method at the surfactant concentrations presented in Table 2, as detailed before.

Table 2. Composition of the chitosan (CH):gellan (GN):surfactant (ST) ternary systems.

System (Chitosan:Gellan:Surfactant)	Chitosan % (w/v)x10 ³	Gellan % (w/v) x10 ³	Surfactant % (w/v) x10 ³
3C:7G:0.05S			0.05
3C:7G:0.1S			0.1
3C:7G:0.2S	3.0	7.0	0.2
3C:7G:0.5S			0.5
3C:7G:1S			1.0
2C:8G:0.05S			0.05
2C:8G:0.1S			0.1
2C:8G:0.2S	2.0	8.0	0.2
2C:8G:0.5S			0.5
2C:8G:1S			1.0

3.3. Particle size, zeta potential and quantity of particles

The size distribution and zeta potential of the samples were determined by dynamic light scattering (DLS) using a Zetasizer Nano-ZS (Malvern Instruments, Herrenberg, Germany) with a detection angle of 173°, equipped with a MPT-2 Autotitrator (Malvern Instruments, Herrenberg, Germany). For data analysis, the viscosity (0.88 mPa·s) and refractive index (1.33) of distilled water at 25 °C were used. All measurements were carried out at 25 °C and at least 6 replicates of each sample were taken to check repeatability. The zeta potentials of the 0.01% (w/v) polysaccharide solutions at different pH values were determined using titration curves from pH 2.5 to 7.0 (in 0.5 ± 0.2 steps) by

adding 0.25 M NaOH or 0.5 M HCl. The curves were evaluated in triplicate. The quantity of particles was considered proportional to the sample count rates (Mao, Bakowsky, Jintapattanakit & Kissel, 2006; Sun, Mao, Mei & Kissel, 2008).

3.4. Particle stability

The zeta potential, size distribution and quantity of particles in the 3C:7G, 2C:8G and 1C:9G samples were evaluated immediately after mixing the polysaccharides and during storage at 25 °C for 100 hours (at rest).

3.5. Statistical analysis

The significant differences ($p < 0.05$) amongst the different samples were determined by the Tukey procedure, using the software STATISTICA 5.5 (Statsoft Inc., Tulsa, USA).

4. Results

4.1. Effect of polysaccharide concentration on chitosan-gellan complexation

Since complex formation between polyelectrolytes is primarily driven by coulombic interactions, the pH of the polysaccharide solution influences its charge density and therefore the complexation mechanisms and properties of the resulting PECs (Lima Vidal, Pereira Fagundes, Cabral de Menezes, Machado da Silva Ruiz & Balaban Garcia, 2005; Sun, Mao, Mei & Kissel, 2008). The charge densities of the gellan and chitosan solutions at the different pH values are presented in Figure 1.

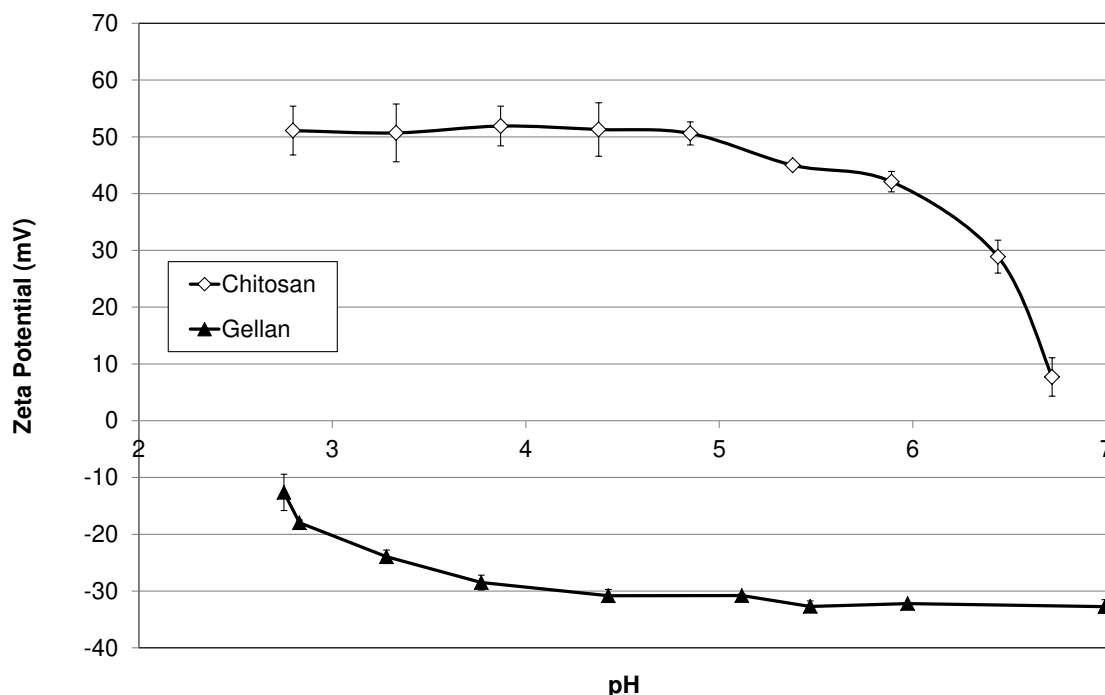


Figure 1. Zeta potential of 0.01% (w/v) gellan and 0.01% (w/v) chitosan solutions at different pH values.

Between pH 2.8 and 5.4 the zeta potential of chitosan was statistically constant at +51 mV and decreased to +7.7 mV as the pH increased to 6.7. Such a reduction is associated with the closeness of the pH value to the pKa of chitosan (6.2 – 7.0 depending on its degree of acetylation (Arrascue, Garcia, Horna & Guibal, 2003)). The amino groups of chitosan are deprotonated below the pKa of the polysaccharide, which confers a cationic character to the chitosan.

The gellan gum was negatively charged throughout the whole pH range studied. A decrease in zeta potential was observed between pH 2.7 and 4.0, and from this point the zeta potential remained constant at -31 mV. Gellan gum is an anionic polysaccharide because of its low pKa (3.5) which is determined by gluconic acid, a weak acid present in the gellan structure (de Jong & van de Velde, 2007). At low pH values the anionic character of gellan is reduced, due to dissociation of the carboxylic groups of gluconic acid (Horinaka, Kani, Hori & Maeda, 2004).

To form PEC, both polymers have to be ionized and bear opposite charges (Berger, Reist, Mayer, Felt & Gurny, 2004), since the reaction can only proceed at pH values in the vicinity of the pKa interval of the two polymers. Therefore the systems were prepared at pH 4.5.

Figure 2 shows the zeta potential of each system. Chitosan concentrations higher than 0.002% (w/v) resulted in systems with a positive zeta potential, suggesting that the amount of gellan was not enough to neutralize all the chitosan amino groups. At a chitosan concentration below 0.002% (w/v), the opposite behavior was observed, the samples showing a negative character due to the excess of gellan. The 2C:8G samples showed a zeta potential near neutrality.

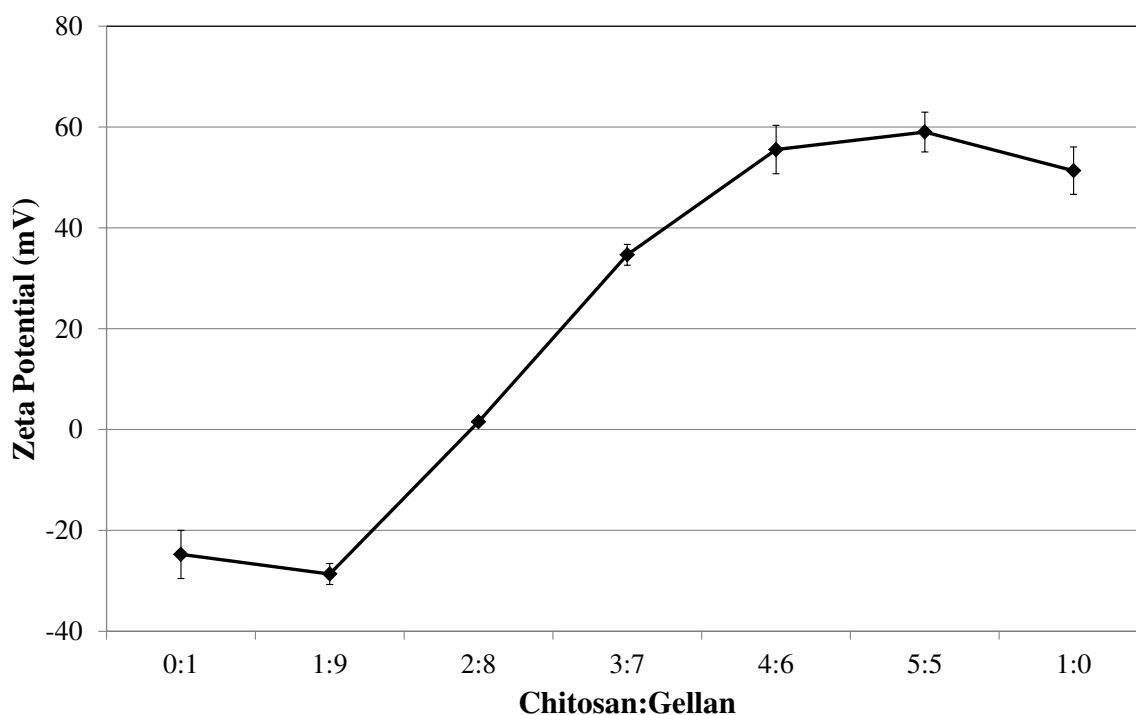


Figure 2. Zeta potential of chitosan:gellan systems at pH 4.5 and different polysaccharide ratios

The charge density of gellan gum is relatively low as compared with other anionic polysaccharides such as pectin and the carrageenans. Gellan gum has an average charge density of 0.25 mol negative charge/mol of monosaccharide in the form of a carboxylic

acid group (de Jong & van de Velde, 2007). Besides the low charge density of the gellan gum, the pH of the samples (4.5) was closer to the pKa of the gellan (3.5) than to that of the chitosan (6.5), i.e., the chitosan was more dissociated than the gellan. Other parameters that could affect the stoichiometry of complexation are the charge distribution over the polysaccharide chains, the position of the ionic groups on the chains and the chain flexibility (Hamman, 2010).

The chitosan:gellan ratio markedly affected the particle size distribution (Table 3, Figure 3). Chitosan (sample 100:0) showed a monomodal size distribution centered at 2.43 nm. The dimensions of chitosan depend on the semi-rigid character of the polysaccharide chains. Since chitosan is a polyelectrolyte in an acid medium, these properties are influenced by the concentration of the ions and especially by the degree of acetylation (DA) (Rinaudo, 2006). Thus different persistence lengths have been described in the literature. Chitosan was reported to measure 9 nm without acetyl groups (DA = 0.0%) (Rinaudo, 2006), 4.2 nm for DA = 0.15% (Rinaudo & Domard, 1989), 22 nm for DA ~ 0.42% (Terbojevich, Cosani, Conio, Marsano & Bianchi, 1991) and 12.5 nm for DA = 60% (Rinaudo, 2006).

The gellan gum also presented a monomodal distribution (Figure 3) centered at 3.15 nm. A similar value was found by Okamoto, Kubota and Kuwahara (1993), who found a diameter of 2.4 nm.

Table 3. Range of diameters of the particles formed with different chitosan:gellan ratios

System (Chitosan:Gellan)	Peak Volume (%)		
	1-10 nm	10-100 nm	100-3000 nm
1C:0G	99.9 ± 0.2 ^a	-	-
5C:5G	-	75.7 ± 1.2 ^a	24.1 ± 1.6 ^d
4C:6G	-	57.8 ± 0.7 ^b	42.4 ± 0.4 ^c
3C:7G	-	4.9 ± 2.9 ^d	84.0 ± 1.8 ^b
2C:8G	-	-	100.0 ± 0.0 ^a
1C:9G	-	19.7 ± 1.4 ^c	80.2 ± 2.1 ^b
0C:1G	99.9 ± 0.1 ^a	-	-

Different letters in the same column mean significant differences ($p < 0.05$)

The peaks related to the pure polysaccharides (between 1-10 nm) were not observed in any of the chitosan:gellan samples, suggesting that all the polysaccharide molecules were aggregated (Figure 3).

The systems composed of both polysaccharides showed a bimodal distribution, except for the sample 2C:8G (Figure 3). Overall, the first peak was observed between 10 – 100 nm followed by a second one between 100 – 1000 nm. An increase in the amount of gellan in the ratio enhanced the number of particles between 100 - 1000 nm and decreased the number of particles between 10 - 100 nm (Table 3). This fact suggests the existence of two different types of complex (Figure 3). Despite the fact that chitosan has a semi-rigid structure, its persistence length, 4.2 nm for DA = 15% (Rinaudo & Domard, 1989), is much shorter than that of gellan, 98 nm (Okamoto, Kubota & Kuwahara, 1993). Since chain stiffness is proportional to polymer persistence length, the chitosan chain is more flexible than the gellan helix. The illustrations shown in Figure 3, present hypothetical PEC structures for both polysaccharides. The first peak, observed near 30 nm, is probably related to PECs formed from gellan molecules surrounded by chitosan chains, whereas in the second peak (200 – 300 nm), the gellan molecules bridge the chitosan chains, leading to larger aggregates.

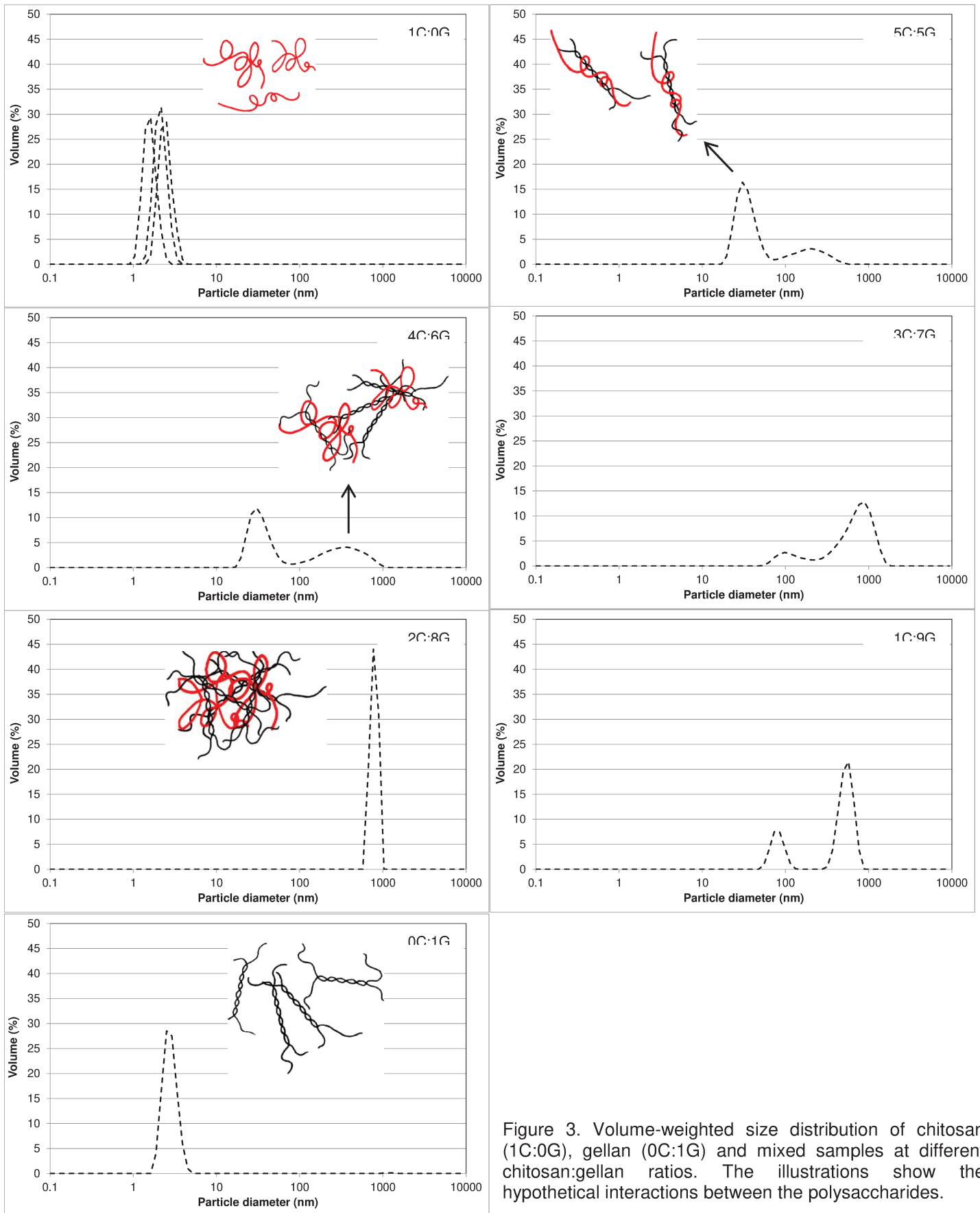


Figure 3. Volume-weighted size distribution of chitosan (1C:0G), gellan (0C:1G) and mixed samples at different chitosan:gellan ratios. The illustrations show the hypothetical interactions between the polysaccharides.

The 2C:8G samples showed a single and relatively low polydispersed peak (Figure 3). The zeta potential of such samples was near zero, i.e., at this polysaccharide ratio there was a balance between the positive and negative charges. Therefore, the absence of repulsive interactions in such a system resulted in aggregation of the PECs. With the increase in the proportion of gellan to a 1C:9G chitosan:gellan ratio, there was an excess in the negative charge of the systems such that repulsive interactions prevailed. Again, the particles presented a bimodal size distribution (Figure 3).

4.2. Particle stability

Overall, the PECs formed at 3C:7G, 2C:8G and 1C:9G (chitosan:gellan ratios) were stable for 100 hours during storage at 25 °C, i.e., no disintegration was observed.

The changes in zeta potential, count rate and size distribution of the 1C:9G, 2C:8G and 3C:7G systems with time are presented in Figures 4 and 5 and Table 4, respectively.

The three systems showed charge stability between 1.5 and 24 hours after mixing of the polysaccharides, but different charge profiles were observed after this period (Figure 4). The average charge of the 3C:7G samples was +40 mV in the first 24 hours. From this time on, the zeta potential showed a reduction, and reached +31 mV after 73 hours. The 2C:8G sample also presented a decrease in charge with time, the statistically neutral zeta potential observed up to 4 hours decreasing to -13.15 mV after 73 hours. This suggests that the chitosan:gellan interactions rearrange themselves with time, leading to the exposition of the negative gellan charge on the particle surface.

The only system which presented a statistically constant zeta potential with time was the 1C:9G one (Figure 4), which also presented a constant count rate with time (Figure 5).

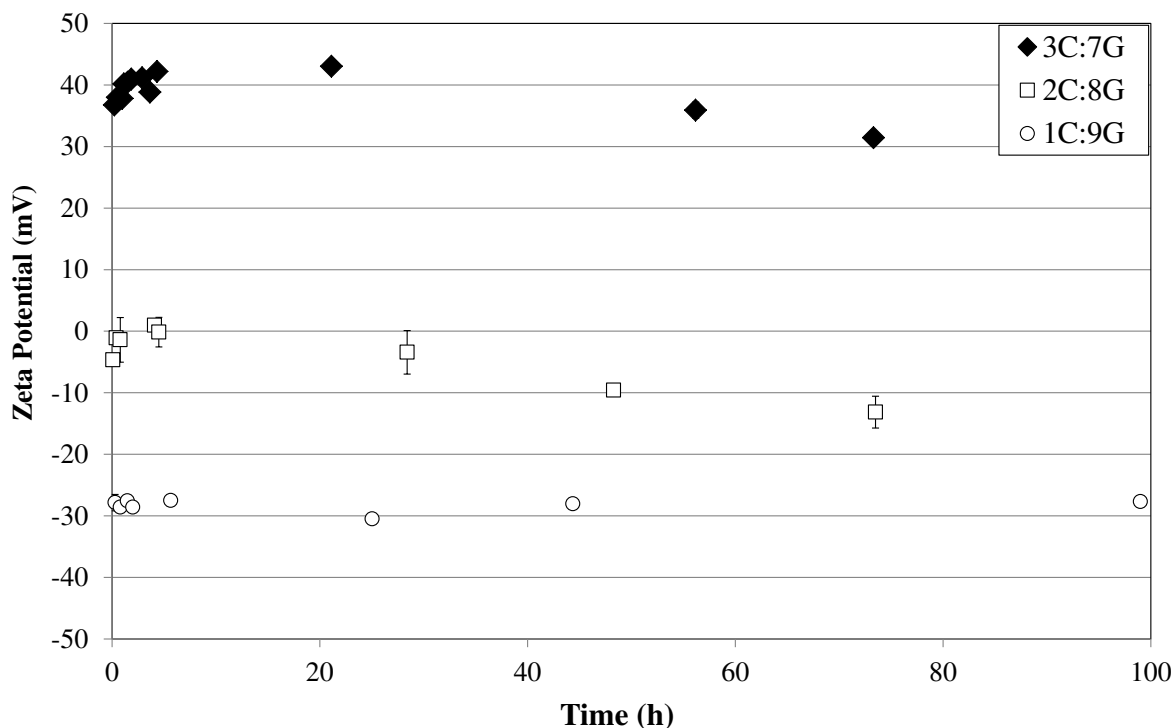


Figure 4. Zeta potential of the samples 1C:9G, 2C:8G and 3C:7G during storage at 25 °C

The count rate is related to the number of particles in the samples (Mao, Bakowsky, Jintapattanakit & Kissel, 2006; Sun, Mao, Mei & Kissel, 2008). Overall, a marked variation in the count rate of the samples was observed in the first hour (Figure 5), during which time complexation occurred simultaneously with aggregation of the PECs. The count rate of the samples 3C:7G and 1C:9G stabilized after 1.7 and 0.5 hours, respectively, but the time was shorter for the 1C:9G sample due to the excess of gellan (Figure 4), which enhanced complexation. The sample 2C:8G showed no significant changes in count rate with time, since considerable aggregation occurred during storage promoted by the neutral zeta potential. This aggregation was confirmed by the low count rate values and large particle diameters (Figure 4, Table 3).

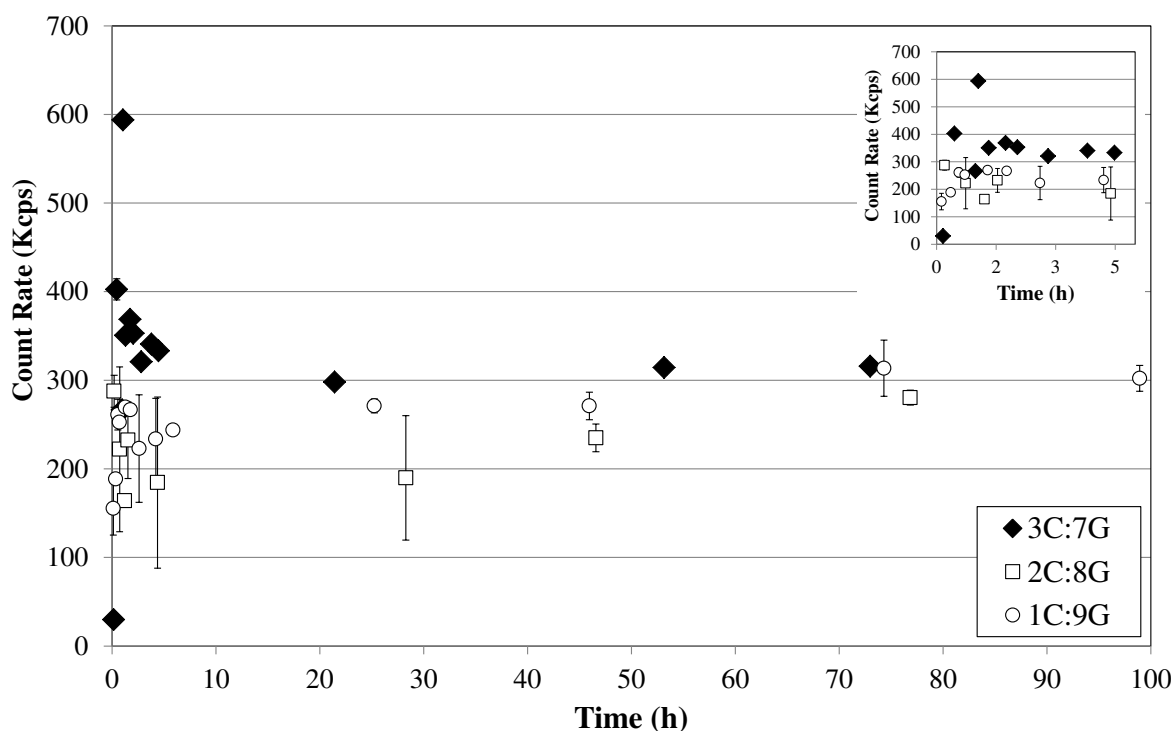


Figure 5. Count rate of the 3C:7G, 2C:8G and 1C:9G samples during storage at 25 °C. The inset graph shows the count rate in the first 5 hours after mixing the polysaccharides

Therefore, the number of particles is related not only to the polysaccharide ratio but also to the aggregation rate of the complexes. An adequate polysaccharide concentration favors polyelectrolyte complexation but the neutrally charged PECs tend to aggregate, leading to larger sizes and a small number of particles, as observed in the 2C:8G samples (Figures 3, 4 and 5). In the first 24 hours after sample preparation, the charge of the 2C:8G samples was statistically neutral, favoring particle aggregation (Figure 4). After longer storage times, the structure of the 2C:8G aggregates reorganized, and gellan carboxylic groups were probably exposed on the surface of the complexes, which reduced the particle zeta potential (Figure 4). Electrostatic interactions usually prevail in systems composed of oppositely charged polyelectrolytes (Dublier, Garnier, Renard & Sanchez, 2000). However, the hydrophobic interactions may overlap the electrostatic interactions

when the polymer presents apolar segments (Borrega, Tribet & Audebert, 1999; Kumar, Dixit, Zhou & Fraunhofer, 2011; Mizusaki, Morishima & Dubin, 1998; Tsianou, Kjøniksen, Thuresson & Nyström, 1999). In chitosan:gellan systems, the long range electrostatic interactions overcome other interactions in the early hours after mixing the polysaccharides, and are responsible for PEC formation. After charge screening, the electrostatic repulsion is reduced and, consequently, so are the intermolecular distances. Thus, short range interactions, such as hydrophobic interactions, are favored with time, and may cause molecular reorganization. The zeta potential results (Figure 5) suggested that reorganization of the chitosan:gellan systems with time resulted in protection of the chitosan hydrophobic groups in the PEC core, and hence the gellan became more exposed on the PEC surface leading to a decrease in zeta potential after 48h (Figure 5). This reorganization was more intense in the 2C:8G system since the zeta potential of these samples was neutral in the early hours after PEC formation. In the 1C:9G systems, the structural reorganization did not affect the zeta potential, since the gellan molecules were already the major constituent on the PEC surface, due to their greater concentration with respect to chitosan.

Despite the decrease in the 2C:8G zeta potential, PEC size was enhanced with time (Figures 4 and 6), indicating that the charge changes were not sufficient to prevent aggregation of the complexes. The size distribution in these samples (Figure 6) showed that the particles doubled in size after 24 hours. It was not possible to measure the particle size after 48 hours, because the particles were larger than 6 μm (above the measuring range of the equipment). The same tendency was observed for the 1C:9G samples, but 3C:7G showed the opposite behaviour. During storage at 25 °C the 3C:7G samples decreased in size. The same bimodal distribution was observed but the number of particles between 10 - 100 nm increased considerably, whilst the number of particles

between 100 - 3000 nm decreased (Table 4, Figure 6), although the count rate remained constant (Figure 6). This suggests that desaggregation had not occurred. In fact, the decrease in size may be related to PEC maturation. In this case the reorganization of structure of the complexes may have intensified the electrostatic interactions, which led to PEC shrinkage.

Table 4. Range in diameter of the chitosan:gellan particles with storage time at 25 °C

Size range (nm)	Time (h)	Volume (%)		
		3C:7G	2C:8G	1C:9G
1-10	2	-	-	-
	24	-	-	-
	48	-	-*	-*
10 - 100	2	4.9 ± 2.9 ^{Bd}	-	19.7 ± 1.4 ^{Ad}
	24	13.6 ± 1.8 ^{Bc}	-	29.6 ± 2.3 ^{Ac}
	48	50.3 ± 2.4 ^{Ab}	-*	-*
100 - 3000	2	84.0 ± 3.4 ^{Ba}	100.0 ± 0.0 ^{Aa}	80.2 ± 1.8 ^{Ba}
	24	86.0 ± 1.2 ^{Ba}	100.0 ± 0.0 ^{Aa}	70.3 ± 1.2 ^{Cb}
	48	49.5 ± 1.5 ^{Ab}	-*	-*

* Above the measuring range of the equipment (6 μm);

Different capital letters in the same row and small letters in the same column mean statistically significant differences (p < 0.05).

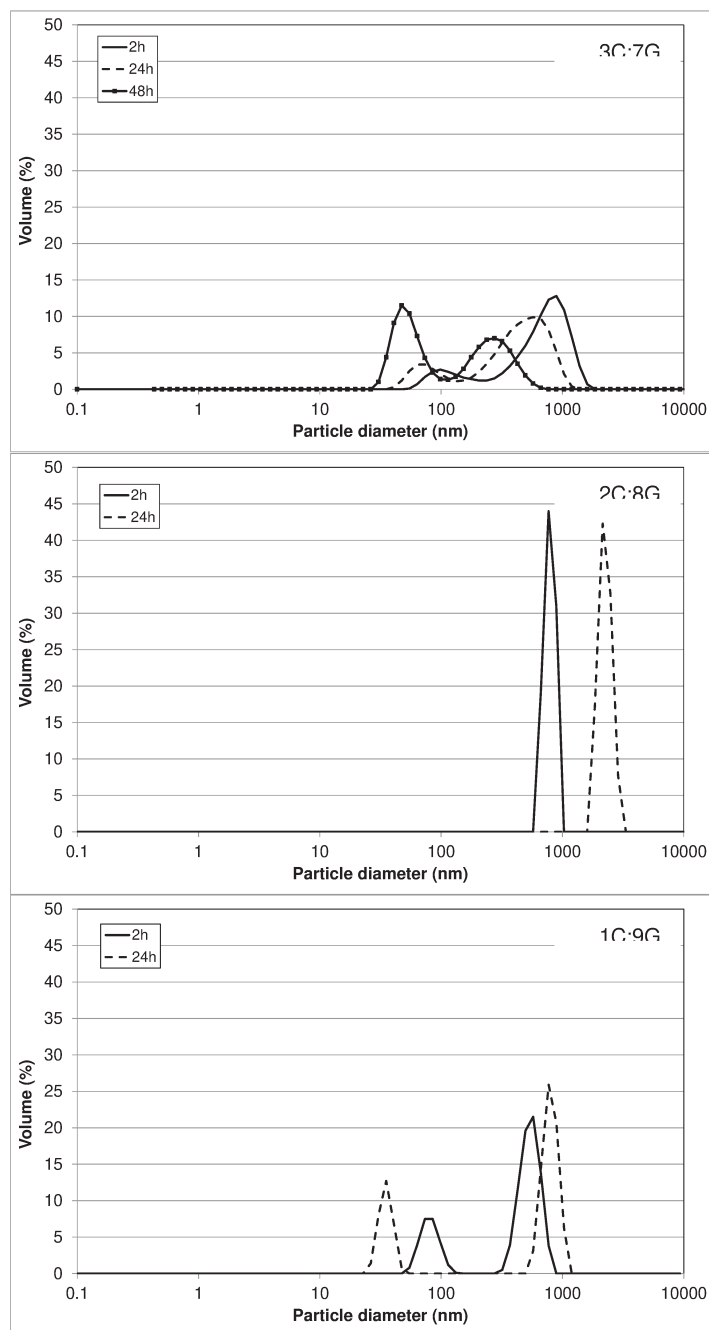


Figure 6. Volume-weighted size distribution of the 3C:7G, 2C:8G and 1C:9G samples during storage at 25 °C

4.3. Effect of PEC preparation on its properties

The effect of sample preparation on the properties of the PECs was studied in uncharged (2C:8G) and charged (1C:9G) systems. As described in item 3.2, the final

concentration of the M2C:8G and M1C:9G samples (prepared in two mixing steps) matched the concentration of the 1C:9G and 2C:8G samples (prepared by the traditional mixing), respectively.

Table 5 shows the count rate and zeta potential during each preparation step of the multilayered systems, i.e., the characteristics of the M2C:8G system during mixing step 1 were the same as for system 1C:9G, prepared by traditional mixing (all together). Although no statistical changes were observed in the count rate of the samples between the first and second mixing steps, they showed different tendencies and zeta potential values (Table 5). Moreover, the samples prepared in two steps presented a marked increase in size when compared to those prepared in a single mixing step (data not shown). The final particle diameters of the samples prepared in two steps were above the limit of the equipment (6 μm), whilst all the samples prepared in one step were smaller than 3000 nm.

Table 5. Count rate and zeta potential of the samples prepared in 2 steps: properties of the samples during the first and second mixing steps

Multilayered systems	Mixture step	Count rate (kcps)	Zeta potential (mV)
M2C:8G	1	233.6 \pm 46 ^{ab}	-28.6 \pm 2.1 ^c
	2	178.2 \pm 61 ^b	-3.1 \pm 0.5 ^b
M1C:9G	1	196.1 \pm 92 ^{ab}	1.4 \pm 0.7 ^a
	2	262.6 \pm 17 ^{ab}	-33.0 \pm 3.5 ^d

Different letters in the same column mean statistically significant differences ($p < 0.05$).

Besides the increase in size, the sample M2C:8G showed slightly lower values for the final count rate (178.2 kcps) and zeta potential (-3.1 mV) than the samples prepared in a single step (which showed 196.1 kcps and 1.4 mV, respectively) (Table 5). As expected, in the first preparation step the zeta potential of the M2C:8G samples was negative (-28.6 mV), which prevented particle aggregation, leading to greater count rate values (233.6 kcps). With the addition of more chitosan in the second mixing step, the negative charge decreased to -3.1 mV, and the electrostatic repulsion between the particles decreased

favoring particle aggregation, which was confirmed by the slight decrease in count rate value. Particle aggregation led to a size increase, but the increase was much greater than expected from the count rate values. As previously commented, the diameter of such particles was more than two times that of the same particles prepared in a single step. This confirms that the sample preparation does affect their properties.

After the first mixing step, the surface of the M2C:8G PECs was formed mainly by gellan molecules, which conferred a negative zeta potential to the particles. In the second mixing step more chitosan was added in the system, and this cationic polysaccharide was attracted to the PEC surface, forming a multilayered particle. As both the gellan and chitosan present relatively stiff structures (Okamoto, Kubota & Kuwahara, 1993; Rinaudo & Domard, 1989) and were already bound during the first step, polysaccharide mobility was lower in the second step, and hence the particles showed a considerable increase in size (Figure 7).

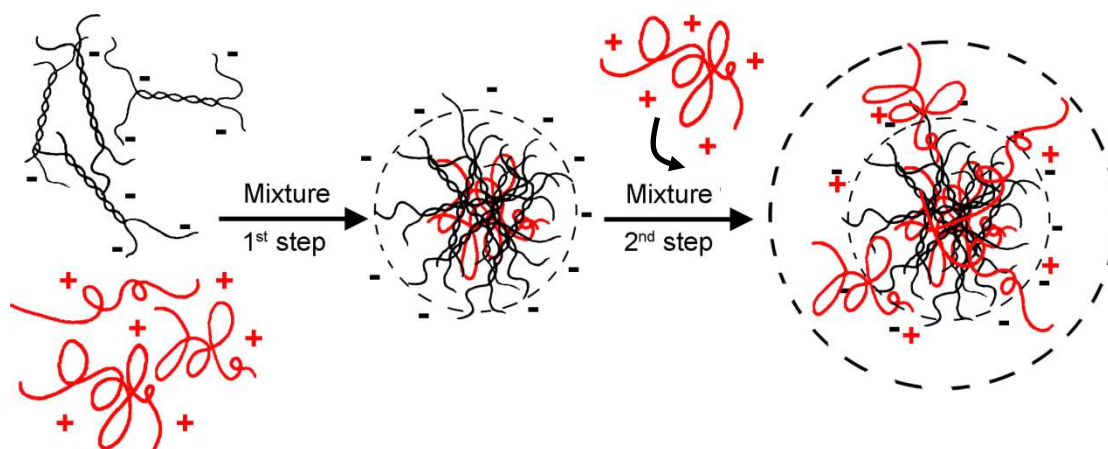


Figure 7. Illustration of PEC formation in the M2C:8G sample

The M1C:9G samples presented a nearly neutral charge in the first mixing step and a low count rate due to particle aggregation (Table 5). With the addition of more gellan the particle acquired a negative charge, which led to partial disaggregation and a slight

increase in count rate. A considerable increase in particle size was observed once again, suggesting that the aggregation in the second mixing step formed a multilayered particle.

4.4. Influence of surfactant

The influence of polysorbate-20 on chitosan:gellan systems was studied for the 3C:7G and 2C:8G samples. Overall, the samples with the addition of 0.0001% (w/v) polysorbate-20 showed no significant changes in size (Figure 8), zeta potential (Figure 9) or count rate (results not shown) during 48 hours, when compared to the pure chitosan:gellan systems (Figures 4 and 6). Thus the effect of the surfactant concentration on the count rate and particle size of systems was evaluated 2 hours after their preparation (Figure 10).

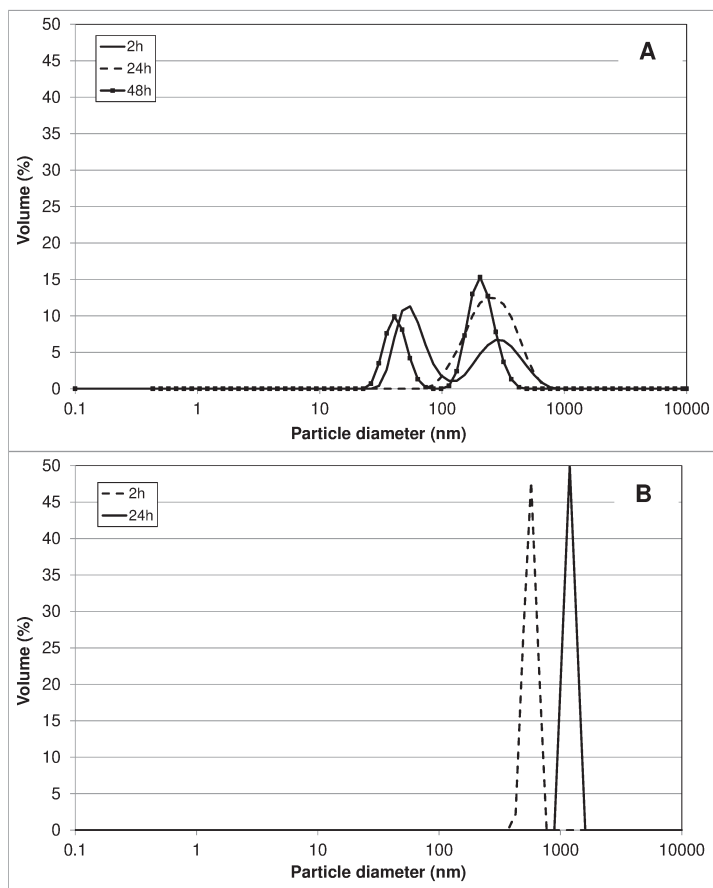


Figure 8. Volume-weighted size distribution of the 3C:7G and 2C:8G samples with added 0.0001% (w/v) polysorbate-20 during 48 hours of storage at 25 °C. A) 3C:7G:0.1S and B) 2C:8G:0.1S

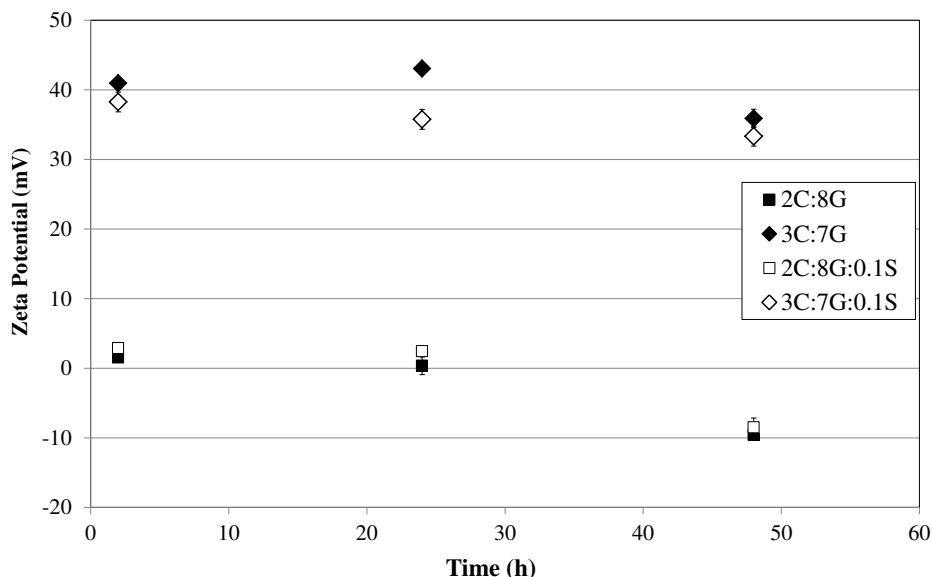


Figure 9. Influence of the addition of polysorbate (0.0001% w/v) on the zeta potential of the 3C:7G and 2C:8G samples during 48 hours of storage at 25 °C

The presence of surfactants may change the behavior of a polymer in solution (Silva, Antunes, Sousa, Valente & Pais, 2011). This can be exemplified by surfactant-induced thickening (Antunes, Marques, Miguel & Lindman, 2009; Barreiro-Iglesias, Alvarez-Lorenzo & Concheiro, 2003a), surfactant-induced swelling (Barreiro-Iglesias, Alvarez-Lorenzo & Concheiro, 2003b) or compaction (Dias, Pais, Miguel & Lindman, 2004), and surfactant-induced phase separation (Holmberg, Jönsson, Kronberg & Lindman, 2003), amongst other effects. However, in the present study the count rate of the samples was statistically constant independent of surfactant concentration (data not shown). The size distribution also showed no significant changes (Figure 10), except for a slight reduction in sample polydispersity at surfactant concentrations above 0.0005% (w/v).

Chitosan-nonionic surfactant interactions are known to be of a weak nature. The chitosan-sorbitan ester for example may interact by hydrogen bonding between the hydroxyl and carbonyl groups of the sorbitan ester head group and the amine, ammonium ions and hydroxyl groups of the chitosan, in addition to hydrophobic interactions between

the sorbitan ester tails and chitosan hydrophobic sites (Grant, Lee, Liu & Allen, 2008). Similar interactions are expected for chitosan-polysorbate complexes. However, in the presence of an oppositely charged polysaccharide such interactions were suppressed, due to its weak nature as compared to the strong electrostatic attraction between the two oppositely charged polyelectrolytes. At high surfactant concentrations, the hydrophobic interactions between the polysorbate tail and the chitosan hydrophobic sites probably enhanced PEC shrinkage, which resulted in a decrease in sample polydispersity. Nonetheless, no significant improvement in PEC formation and stability was achieved by the addition of surfactant.

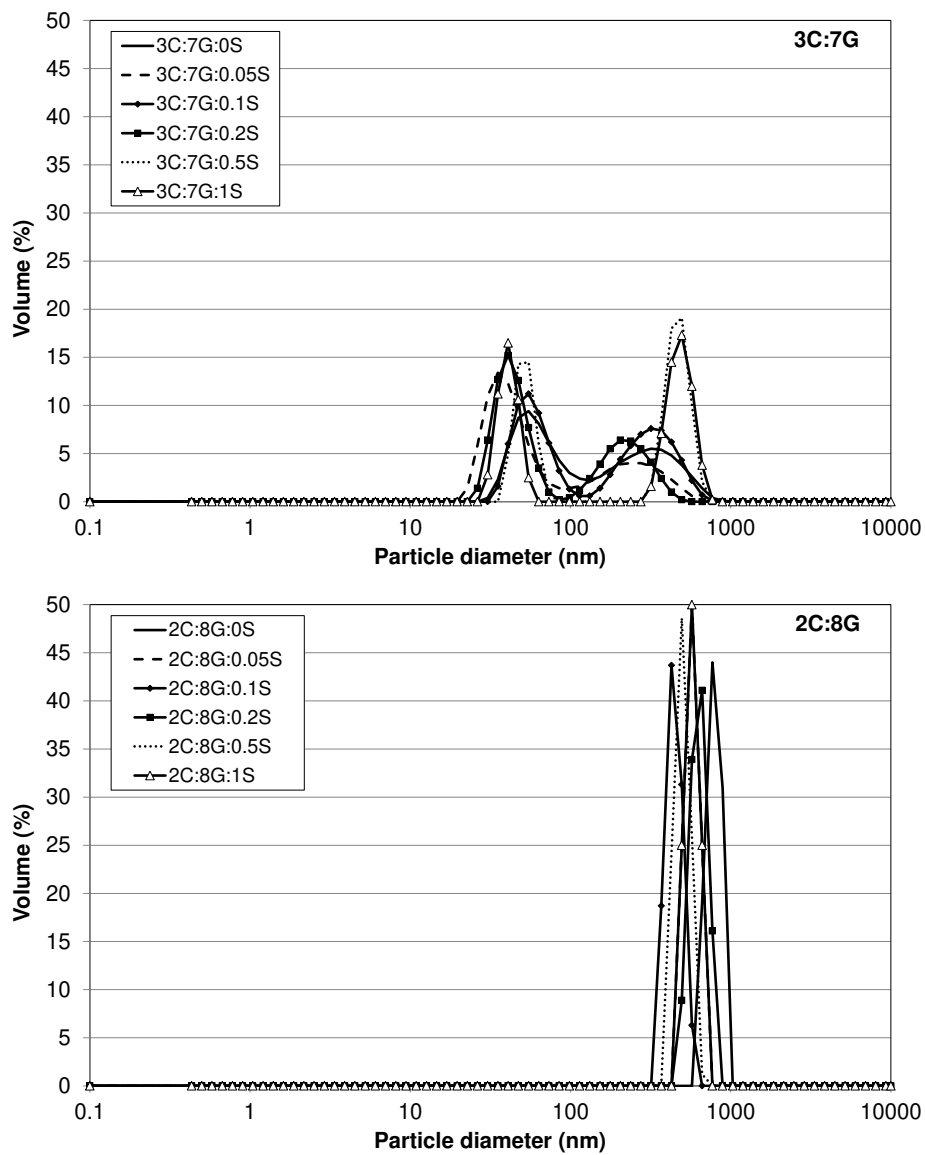


Figure 10. Volume-weighted size distribution of the 3C:7G and 2C:8G samples with added polysorbate-20: 0.00005, 0.0001, 0.0002, 0.0005 and 0.0010% (w/v)

5. Conclusion

Chitosan:gellan interactions led to nano scale PECs of different sizes. Depending on the polysaccharide ratio, the particles presented different charge characteristics, which determined particle aggregation and hence the final PEC diameter. Samples composed of 2C:8G and 3C:7G (chitosan:gellan ratio) exhibited structural reorganization during storage at 25 °C, which reduced the zeta potential of the samples. This reorganization specially affected the sample 2C:8G, which showed a decrease in particle aggregation and consequent increase in the number of dispersed particles. However, the particle size continued to increase and doubled in size after 24 hours. Similar increases were observed in the 1C:9G systems and both samples formed particles larger than 6 µm after 48 hours. The sample 3C:7G was the only one which presented a stable size throughout the period evaluated. The mixing protocol was essential to determine PEC size. The multilayered particle was considerably larger than the one formed in the traditional way (1 - step mixing). However, no significant changes in the PEC characteristics were observed in the presence of a non-ionic surfactant, since the driving force of PEC formation (electrostatic forces) was markedly higher than the hydrophobic and hydrogen bonding of the surfactant-polysaccharide interactions. The results presented in this paper show that it is possible to control the characteristics of chitosan:gellan PECs by changing the polysaccharide ratio and mixing methodology.

6. References

- Amaike, M., Senoo, Y., & Yamamoto, H. (1998). Sphere, honeycomb, regularly spaced droplet and fiber structures of polyion complexes of chitosan and gellan. *Macromolecular Rapid Communications*, 19(6), 287-289.
- Antunes, F. E., Marques, E. F., Miguel, M. G., & Lindman, B. (2009). Polymer-vesicle association. *Advances in Colloid and Interface Science*, 147-148(0), 18-35.

- Arrascue, M. L., Garcia, H. M., Horna, O., & Guibal, E. (2003). Gold sorption on chitosan derivatives. *Hydrometallurgy*, 71(1-2), 191-200.
- Barreiro-Iglesias, R., Alvarez-Lorenzo, C., & Concheiro, A. (2003a). Poly(acrylic acid) microgels (carbopol® 934)/surfactant interactions in aqueous media: Part I: Nonionic surfactants. *International Journal of Pharmaceutics*, 258(1-2), 165-177.
- Barreiro-Iglesias, R., Alvarez-Lorenzo, C., & Concheiro, A. (2003b). Poly(acrylic acid) microgels (carbopol® 934)/surfactant interactions in aqueous media: Part II: Ionic surfactants. *International Journal of Pharmaceutics*, 258(1-2), 179-191.
- Battaglia, L., Trotta, M., Gallarate, M., Carlotti, M. E., Zara, G. P., & Bargoni, A. (2007). Solid lipid nanoparticles formed by solvent-in-water emulsion-diffusion technique: Development and influence on insulin stability. *Journal of Microencapsulation*, 24(7), 672-684.
- Berger, J., Reist, M., Mayer, J. M., Felt, O., & Gurny, R. (2004). Structure and interactions in chitosan hydrogels formed by complexation or aggregation for biomedical applications. *European Journal of Pharmaceutics and Biopharmaceutics*, 57(1), 35-52.
- Borrega, R., Tribet, C., & Audebert, R. (1999). Reversible Gelation in Hydrophobic Polyelectrolyte/Protein Mixtures: An Example of Cross-Links between Soft and Hard Colloids. *Macromolecules*, 32(23), 7798-7806.
- Claesson, P. M., & Ninham, B. W. (1992). Ph-Dependent Interactions between Adsorbed Chitosan Layers. *Langmuir*, 8(5), 1406-1412.
- de Jong, S., & van de Velde, F. (2007). Charge density of polysaccharide controls microstructure and large deformation properties of mixed gels. *Food Hydrocolloids*, 21(7), 1172-1187.
- Dentini, M., Coviello, T., Burchard, W., & Crescenzi, V. (1988). Solution Properties of exocellular microbial polysaccharides. 3. Light-scattering from gellan and from the exocellular polysaccharide of *Rhizobium-Trifolii* (Strain-TA-1) in the ordered state. *Macromolecules*, 21(11), 3312-3320.
- Desgouilles, S., Vauthier, C., Bazile, D., Vacus, J., Grossiord, J.-L., Veillard, M., & Couvreur, P. (2003). The Design of Nanoparticles Obtained by Solvent Evaporation: A Comprehensive Study. *Langmuir*, 19(22), 9504-9510.
- Dias, R. S., Pais, A. A. C. C., Miguel, M. G., & Lindman, B. (2004). DNA and surfactants in bulk and at interfaces. *Colloids and Surfaces A: Physicochemical and Engineering Aspects*, 250(1-3), 115-131.
- Doublier, J. L., Garnier, C., Renard, D., & Sanchez, C. (2000). Protein-polysaccharide interactions. *Current Opinion in Colloid & Interface Science*, 5(3-4), 202-214.

- George, M., & Abraham, T. E. (2006). Polyionic hydrocolloids for the intestinal delivery of protein drugs: Alginate and chitosan — a review. *Journal of Controlled Release*, 114(1), 1-14.
- Gomez, L., Ramirez, H. L., Neira-Carrillo, A., & Villalonga, R. (2006). Polyelectrolyte complex formation mediated immobilization of chitosan-invertase neoglycoconjugate on pectin-coated chitin. *Bioprocess Biosyst Eng*, 28(6), 387-395.
- Grant, J., Cho, J., & Allen, C. (2006). Self-assembly and physicochemical and rheological properties of a polysaccharide–surfactant system formed from the cationic biopolymer chitosan and nonionic sorbitan esters. *Langmuir*, 22(9), 4327-4335.
- Grant, J., Lee, H., Liu, R. C. W., & Allen, C. (2008). Intermolecular Interactions and Morphology of Aqueous Polymer/Surfactant Mixtures Containing Cationic Chitosan and Nonionic Sorbitan Esters. *Biomacromolecules*, 9(8), 2146-2152.
- Groot, R. D. (2000). Mesoscopic simulation of polymer–surfactant aggregation. *Langmuir*, 16(19), 7493-7502.
- Hamman, J. H. (2010). Chitosan based polyelectrolyte complexes as potential carrier materials in drug delivery systems. *Marine Drugs*, 8(4), 1305-1322.
- Holmberg, K., Jönsson, B., Kronberg, B., & Lindman, B. (2003). Surfactant–Protein Mixtures. *Surfactants and Polymers in Aqueous Solution* (pp. 305-315): John Wiley & Sons, Ltd.
- Horinaka, J., Kani, K., Hori, Y., & Maeda, S. (2004). Effect of pH on the conformation of gellan chains in aqueous systems. *Biophysical Chemistry*, 111(3), 223-227.
- Ibrahim, H., Bindschaedler, C., Doelker, E., Buri, P., & Gurny, R. (1992). Aqueous nanodispersions prepared by a salting-out process. *International Journal of Pharmaceutics*, 87(1–3), 239-246.
- Jansson, P.-E., Lindberg, B., & Sandford, P. A. (1983). Structural studies of gellan gum, an extracellular polysaccharide elaborated by *Pseudomonas elodea*. *Carbohydrate Research*, 124(1), 135-139.
- Jintapattanakit, A., Junyaprasert, V. B., Mao, S., Sitterberg, J., Bakowsky, U., & Kissel, T. (2007). Peroral delivery of insulin using chitosan derivatives: A comparative study of polyelectrolyte nanocomplexes and nanoparticles. *International Journal of Pharmaceutics*, 342(1-2), 240-249.
- Kumar, V., Dixit, N., Zhou, L., & Fraunhofer, W. (2011). Impact of short range hydrophobic interactions and long range electrostatic forces on the aggregation kinetics of a monoclonal antibody and a dual-variable domain immunoglobulin at low and high concentrations. *International Journal of Pharmaceutics*, 421(1), 82-93.

- Lankalapalli, S., & Kolapalli, V. R. M. (2009). Polyelectrolyte complexes: A review of their applicability in drug delivery technology. *Indian Journal of Pharmaceutical Sciences*, 71(5), 481-487.
- Lima Vidal, R. R., Pereira Fagundes, F., Cabral de Menezes, S. M., Machado da Silva Ruiz, N., & Balaban Garcia, R. (2005). Solution properties of partially hydrolysed polyacrylamide and chitosan mixed solutions. *Macromolecular Symposia*, 229(1), 118-126.
- Lv, F.-F., Zheng, L.-Q., & Tung, C.-H. (2005). Phase behavior of the microemulsions and the stability of the chloramphenicol in the microemulsion-based ocular drug delivery system. *International Journal of Pharmaceutics*, 301(1-2), 237-246.
- Mao, S. R., Bakowsky, U., Jintapattanakit, A., & Kissel, T. (2006). Self-assembled polyelectrolyte nanocomplexes between chitosan derivatives and insulin. *Journal of Pharmaceutical Sciences*, 95(5), 1035-1048.
- Mizusaki, M., Morishima, Y., & Dubin, P. L. (1998). Interaction of Pyrene-Labeled Hydrophobically Modified Polyelectrolytes with Oppositely Charged Mixed Micelles Studied by Fluorescence Quenching. *The Journal of Physical Chemistry B*, 102(11), 1908-1915.
- Moritaka, H., Nishinari, K., Taki, M., & Fukuba, H. (1995). Effects of pH, potassium chloride, and sodium chloride on the thermal and rheological properties of gellan gum gels. *Journal of Agricultural and Food Chemistry*, 43(6), 1685-1689.
- Naderi, A., Claesson, P. M., Bergström, M., & Dédinaité, A. (2005). Trapped non-equilibrium states in aqueous solutions of oppositely charged polyelectrolytes and surfactants: effects of mixing protocol and salt concentration. *Colloids and Surfaces A: Physicochemical and Engineering Aspects*, 253(1-3), 83-93.
- Norton, A. B., Cox, P. W., & Spyropoulos, F. (2011). Acid gelation of low acyl gellan gum relevant to self-structuring in the human stomach. *Food Hydrocolloids*, 25(5), 1105-1111.
- Okamoto, T., Kubota, K., & Kuwahara, N. (1993). Light scattering study of gellan gum. *Food Hydrocolloids*, 7(5), 363-371.
- Payne, G. F., & Raghavan, S. R. (2007). Chitosan: a soft interconnect for hierarchical assembly of nano-scale components. *Soft Matter*, 3(5), 521-527.
- Pepić, I., Filipović-Grčić, J., & Jalšenjak, I. (2008). Interactions in a nonionic surfactant and chitosan mixtures. *Colloids and Surfaces A: Physicochemical and Engineering Aspects*, 327(1-3), 95-102.
- Pepić, I., Filipović-Grčić, J., & Jalšenjak, I. (2009). Bulk properties of nonionic surfactant and chitosan mixtures. *Colloids and Surfaces A: Physicochemical and Engineering Aspects*, 336(1-3), 135-141.

-
- Picone, C. S. F., & Cunha, R. L. (2011). Influence of pH on formation and properties of gellan gels. *Carbohydrate Polymers*, 84(1), 662-668.
- Qi, C., Chen, Y., Huang, J.-H., Jin, Q.-Z., & Wang, X.-G. (2012). Preparation and characterization of catalase-loaded solid lipid nanoparticles based on soybean phosphatidylcholine. *Journal of the Science of Food and Agriculture*, 92(4), 787-793.
- Rinaudo, M. (2006). Chitin and chitosan: Properties and applications. *Progress in Polymer Science*, 31(7), 603-632.
- Rinaudo, M., & Domard, A. (1989). Solution properties of chitosan. In G. Skjak-Braek, T. Anthonsen & P. Sandford (Eds.). *Chitin and chitosan. Sources, chemistry, biochemistry, physical properties and applications* (pp. 71-86). London: Elsevier.
- Shahidi, F., Arachchi, J. K. V., & Jeon, Y. J. (1999). Food applications of chitin and chitosans. *Trends in Food Science & Technology*, 10(2), 37-51.
- Silva, S. M. C., Antunes, F. E., Sousa, J. J. S., Valente, A. J. M., & Pais, A. A. C. C. (2011). New insights on the interaction between hydroxypropylmethyl cellulose and sodium dodecyl sulfate. *Carbohydrate Polymers*, 86(1), 35-44.
- Sun, W., Mao, S., Mei, D., & Kissel, T. (2008). Self-assembled polyelectrolyte nanocomplexes between chitosan derivatives and enoxaparin. *European Journal of Pharmaceutics and Biopharmaceutics*, 69(2), 417-425.
- Takahashi, R., Tokunou, H., Kubota, K., Ogawa, E., Oida, T., Kawase, T., & Nishinari, K. (2004). Solution properties of gellan gum: Change in chain stiffness between single- and double-stranded chains. *Biomacromolecules*, 5(2), 516-523.
- Terbojevich, M., Cosani, A., Conio, G., Marsano, E., & Bianchi, E. (1991). Chitosan: chain rigidity and mesophase formation. *Carbohydrate Research*, 209(0), 251-260.
- Tsianou, M., Kjøniksen, A.-L., Thuresson, K., & Nyström, B. (1999). Light Scattering and Viscoelasticity in Aqueous Mixtures of Oppositely Charged and Hydrophobically Modified Polyelectrolytes. *Macromolecules*, 32(9), 2974-2982.
- Yamamoto, F., & Cunha, R. L. (2007). Acid gelation of gellan: Effect of final pH and heat treatment conditions. *Carbohydrate Polymers*, 68(3), 517-527.
- Ziani, K., Henrist, C., Jerome, C., Aqil, A., Mate, J. I., & Cloots, R. (2011). Effect of nonionic surfactant and acidity on chitosan nanofibers with different molecular weights. *Carbohydrate Polymers*, 83(2), 470-476.

-CAPÍTULO 6 -
Conclusões Gerais

Nanopartículas com diferentes tamanhos e propriedades superficiais foram obtidas pela associação de surfactantes e polissacarídeos de origem alimentar. O estudo de soluções puras de gelana e quitosana revelou uma grande dependência do processo de agregação e propriedades reológicas dos polissacarídeos em relação ao pH e temperatura do meio, principalmente no caso da gelana. Em pH 3,5 e temperaturas inferiores a 31,4 °C, a elevada agregação da gelana levou à formação de rede de gel com característica rígida e pouco deformável. Além disso, a gelana apresentou transição conformacional hélice-enovelada reversível com o aumento da temperatura. Já a quitosana apresentou insolubilidade em valores de pH superiores a 4,5 pois a desprotonação dos grupos amino reduziu a repulsão eletrostática intra e intermolecular levando à compactação das cadeias. A redução da temperatura de 80 para 10 °C intensificou o comportamento pseudoplástico da quitosana devido à maior agregação molecular, porém a agregação não foi suficiente para promover a formação de gel em nenhuma das condições estudadas. Os ensaios reológicos oscilatórios sugerem que a quitosana não apresenta transição conformacional significativa com a temperatura.

O estudo da formação de nanopartículas por complexação eletrostática revelou que devido à menor flexibilidade e densidade de carga da gelana, é necessário maior quantidade deste polissacarídeo que de quitosana para formação de complexos eletrostáticos neutros. Na razão 20:80 (quitosana:gelana) os complexos apresentaram carga total neutra e conseqüentemente elevada agregação, o que resultou em uma menor quantidade de partículas, porém de maior tamanho. Ao longo do tempo as amostras 20:80 e 30:70 apresentaram reorganização molecular que reduziu a carga superficial das partículas, sugerindo que a baixa densidade de carga e flexibilidade estrutural da gelana faz com que sua interação com a quitosana seja dependente do tempo. A adição de polissorbato não afetou significativamente as propriedades das partículas, porém o

tamanho das partículas mostrou-se fortemente dependente do método de preparo das amostras. Partículas multicamadas formadas pela mistura dos polissacarídeos em duas etapas apresentaram tamanho consideravelmente maior que as partículas formadas pela mistura em um único passo.

O estudo das partículas formadas pela associação de polissorbato e quitosana confirmou que o comprimento da cadeia hidrofóbica do polissorbato tem papel fundamental no processo de agregação e na diversidade de estruturas formadas. Quanto maior a quantidade de átomos de carbono na cauda do surfactante, maior a complexidade das estruturas. A variação da razão de concentração água/polissorbato-80 resultou desde partículas com dimensões manométricas, como as micelas, até macroestruturas anisotrópicas ou cristais líquidos, com características de gel. Já os sistemas compostos por polissorbato-20 apresentaram aspecto líquido e comportamento newtoniano, independente da razão água/surfactante empregada. A variação de pH (6,7 - 3,0) da fase aquosa não afetou significativamente as características das estruturas formadas assim como a adição de pequenas concentrações de quitosana. No entanto, quando adicionada em altas concentrações, a quitosana diminuiu a polidispersão das amostras devido ao aumento de viscosidade que impediu a agregação das partículas.

Assim, os resultados obtidos sugerem que a associação de biopolímeros e surfactantes é um processo promissor e versátil para a produção de nanopartículas a partir de ingredientes alimentícios. Além de envolver baixa energia de formação, a associação controlada dos ingredientes permitiu a formação de nanopartículas com diferentes características estruturais e químicas a partir do controle das condições de processo e composição dos sistemas. Isso demonstra que é possível modelar as características das nanopartículas, de forma a torná-las um veículo eficiente para a entrega controlada e encapsulação de compostos funcionais em alimentos.

– APÊNDICE 1 –

***Ensaaios preliminares de dissolução dos
polissacarídeos***

1. Objetivos

Determinar as condições de temperatura e pH para a dissolução da gelana e da quitosana.

2. Métodos

Os ensaios de dissolução da gelana e da quitosana foram realizados pela dispersão do pó em água deionizada sob agitação magnética. Foram avaliadas diferentes concentrações de polissacarídeo (de 0,1 a 2% (m/v)), temperaturas (25 – 80 °C), tempo de tratamento térmico (10 - 30 minutos) e valores de pH. O tratamento térmico foi realizado em béquer encamisado acoplado a um banho de circulação externa. O pH foi ajustado pela adição de ácido láctico, um ácido fraco, de forma a se evitar a degradação dos polissacarídeos. Além disso, sua utilização é permitida em alimentos. Também foi utilizado tampão acetato de sódio 100 mM (pH 3).

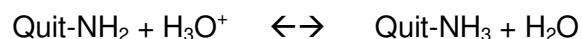
A avaliação da dissolução foi feita visualmente 1 e 24 horas após a dispersão do pó. Nas amostras tratadas termicamente, a avaliação foi realizada após resfriamento em banho de gelo até a temperatura ambiente (25 °C).

3. Resultados

Tanto a gelana como a quitosana apresentaram insolubilidade em água após agitação magnética por 12 horas à temperatura ambiente. Nesta temperatura a goma gelana apresenta-se em forma de duplas hélices, com baixa área superficial disponível para interagir com a água. No entanto, estudos indicam que a gelana é solúvel entre 70 e 90 °C (Evageliou et al., 2010; Moritaka et al., 2002; Yamamoto & Cunha, 2007), visto que nesta faixa de temperatura suas moléculas apresentam conformação enovelada e com maior número de sítios hidrofílicos disponíveis. Diferentes temperaturas e tempos de

tratamento térmico foram testados e a completa dissolução do pó de gelana foi observada após tratamento de 80 °C por 30 minutos em pH natural da solução (5,3). Portanto, determinou-se como metodologia padrão de preparação da solução estoque de gelana a dissolução do pó em água deionizada em béquer encamisado sob agitação magnética a 80 °C por 30 minutos. Nestas condições, dependendo da concentração da solução foi observada gelificação durante o resfriamento. A maior concentração em que a solução apresentou características líquidas a 25 °C foi 0,7% (m/v).

A quitosana também se mostrou insolúvel à dispersão em água à temperatura ambiente, apesar do seu alto grau de desacetilação (80% de acordo com o fornecedor). Quanto maior o grau de acetilação, maior o tamanho e a rigidez das moléculas, o que reduz sua solubilidade. Usualmente, a dissolução deste polissacarídeo é feita em meio ácido (Claesson & Ninham, 1992; George & Abraham, 2006; Peng et al., 2010). A dissolução em diferentes concentrações de ácido foi avaliada tanto a temperatura ambiente, como sob aquecimento. Como no Capítulo 3 o ajuste do pH da solução de gelana foi feito com ácido láctico, optou-se por utilizá-lo também na dissolução da quitosana de forma a se manter o mesmo padrão. A condição de melhor dissolução foi obtida com ácido láctico 0,1% (v/v) e tratamento térmico de 80 °C por 30 minutos, resultando em uma solução de quitosana com pH final igual a 4,4. O aumento da solubilidade da quitosana em meio ácido ocorre devido à protonação dos grupos amino (-NH₂) formando grupos catiônicos (-NH₃⁺) levando a uma forte repulsão eletrostática intra e inter-molecular que resulta na expansão das cadeias e consequente aumento da solubilidade (Peng et al., 2010; Thongngam & McClements, 2004).



O pH do meio irá determinar não só a dissolução dos polissacarídeos, mas também as possíveis interações entre eles e consequentemente as características do

sistema formado (Berger et al., 2004). Dessa maneira, no Capítulo 3 o efeito do pH na transição conformacional e propriedades reológicas da gelana foi avaliado ajustando-se o pH da solução de gelana para 3,5, ou 7,0 com a adição de ácido láctico 0,22 M ou NaOH 1 M. Um estudo similar seria realizado para a quitosana, porém não foi possível realizar o ajuste de pH da solução de quitosana devido à formação de aglomerados mesmo com uso de reagentes diluídos e alta agitação. Portanto, a caracterização reológica da quitosana (Apêndice 2) foi feita apenas no pH natural de dissolução (pH 4,4).

Nos Capítulos 4 e 5 soluções mistas foram formadas. Para que o pH permanecesse constante ao longo dos experimentos, foi necessário o uso de solução tampão. A quitosana apresentou insolubilidade em tampão lactato de sódio (pH 4), porém mostrou-se totalmente solúvel em tampão acetato de sódio 100 mM (pH 3), o qual foi utilizado no restante do trabalho.

4. Referências Bibliográficas

- Berger, J., Reist, M., Mayer, J. M., Felt, O., & Gurny, R. (2004). Structure and interactions in chitosan hydrogels formed by complexation or aggregation for biomedical applications. *European Journal of Pharmaceutics and Biopharmaceutics*, 57(1), 35-52.
- Claesson, P. M., & Ninham, B. W. (1992). Ph-Dependent Interactions between Adsorbed Chitosan Layers. *Langmuir*, 8(5), 1406-1412.
- Evageliou, V., Mazioti, M., Mandala, I., & Komaitis, M. (2010). Compression of gellan gels. Part II: Effect of sugars. *Food Hydrocolloids*, 24(4), 392-397.
- George, M., & Abraham, T. E. (2006). Polyionic hydrocolloids for the intestinal delivery of protein drugs: Alginate and chitosan — a review. *Journal of Controlled Release*, 114(1), 1-14.
- Moritaka, H., Takeuchi, M., Okoshi, H., & Fukuba, H. (2002). Particle and matrix gels of gellan gum: effects of filler particles on rheological properties of matrix gels. *Food Hydrocolloids*, 16(2), 175-182.
- Peng, B., Hao, Y., Kang, H., Han, X., Peng, C., & Liu, H. (2010). Aggregation behavior of N-carboxyethylchitosan in aqueous solution: effects of pH, polymer concentration, and presence of a gemini surfactant. *Carbohydrate Research*, 345(1), 101-107.

- Thongngam, M., & McClements, D. J. (2004). Characterization of Interactions between Chitosan and an Anionic Surfactant. *Journal of Agricultural and Food Chemistry*, 52(4), 987-991.
- Yamamoto, F., & Cunha, R. L. (2007). Acid gelation of gellan: Effect of final pH and heat treatment conditions. *Carbohydrate Polymers*, 68(3), 517-527.

– APÊNDICE 2 –

***Caracterização reológica da quitosana a
diferentes temperaturas***

1. Objetivo

O objetivo desta parte do trabalho foi determinar as propriedades reológicas da quitosana e compreender seu comportamento frente a diferentes temperaturas, visando facilitar o estudo das suas interações com a gelatina.

2. Métodos

2.1. Preparação das soluções

Para a preparação da solução de quitosana, o pó foi disperso em ácido láctico 0,1% (m/m) em béquer encamisado e aquecido a 80 °C por 30 minutos, resultando em uma solução final com concentração 0,2% (m/m) de biopolímero e pH 4,4. Após o tratamento térmico, as soluções foram resfriadas em banho de gelo e analisadas quanto ao comportamento reológico.

2.2. Ensaio reológicos

O comportamento reológico das soluções de quitosana foi avaliado em um reômetro modular compacto de tensão controlada AR 1500 - TA Instruments Ltd. (Inglaterra) equipado com uma geometria cone placa de 60 mm de diâmetro e 1,59°.

2.2.1. Curvas de escoamento

Foram realizadas curvas de escoamento no intervalo de taxas de deformação de 0 a 90 Pa em três rampas (ciclo crescente, decrescente e crescente, respectivamente) para a eliminação da possível tixotropia das amostras. Os dados da última rampa que correspondem ao estado estacionário de escoamento foram ajustados segundo a lei da potência (Equação 1) com o auxílio do software Rheology Advantage Data Analysis v. 5.7.0 (TA Instruments Ltd, Estados Unidos).

$$\sigma = k \dot{\gamma}^n \quad (1)$$

onde σ é a tensão de cisalhamento (Pa), $\dot{\gamma}$ é a taxa de cisalhamento (s^{-1}), k é o índice de consistência (Pa.s) e n é o índice de escoamento.

Para verificar a influência da temperatura no comportamento reológico do fluido, foram realizados ensaios a 10, 20, 30, 50 e 80 °C. Os dados obtidos foram ajustados ao modelo de Arrhenius que relaciona a viscosidade aparente do fluido com a temperatura (Equação 2).

$$\ln \eta_{ap} = \left(\frac{E_a}{R} \right) \cdot T^{-1} + B \quad (2)$$

Onde η_{ap} é a viscosidade aparente (Pa.s), E_a é a energia de ativação ($\text{kJ}\cdot\text{mol}^{-1}$), R é a constante universal dos gases ($8,314 \text{ J}\cdot\text{mol}^{-1}\cdot\text{K}^{-1}$), T é a temperatura absoluta (K) e B um parâmetro de ajuste.

2.2.2. Ensaios oscilatórios

As amostras foram colocadas no equipamento a 5 °C com uma fina camada de óleo de silicone ao redor da geometria para se evitar evaporação da amostra. Então, as amostras foram pré-cisalhadas por 1 minuto a uma taxa de deformação de 100 s^{-1} para completa homogeneização. Posteriormente, realizou-se uma varredura de aquecimento de 5 a 90 °C seguida por uma de resfriamento de 90 a 5 °C, ambas a $1 \text{ }^\circ\text{C}\cdot\text{min}^{-1}$ e 0,1 Hz de frequência. As varreduras foram realizadas utilizando-se valores de tensão determinados em ensaios prévios de varredura de tensão (0,05 Pa no aquecimento e 0,01 Pa no resfriamento) de forma a assegurar que os experimentos estivessem sempre na região de viscoelasticidade linear das amostras.

3. Resultados e Discussão

3.1. Curvas de escoamento

A Figura 1 apresenta uma curva típica de tensão de cisalhamento versus taxa de deformação de soluções de quitosana 0,2% (m/m) avaliada a diferentes temperaturas (10, 20, 30, 50 e 80 °C). Nos ensaios realizados de 10 a 30 °C, as amostras não apresentaram diferenças significativas entre as curvas de subida e descida. Porém, a partir de 50 °C observa-se que as curvas de subida ocorrem em valores de tensão superiores a da primeira descida, provavelmente devido a algum ressecamento da amostra com a temperatura apesar do uso de silicone. Para uma dada tensão de cisalhamento, a taxa de deformação das amostras aumenta significativamente com a temperatura, refletindo a maior fluidez das soluções de quitosana a temperaturas elevadas.

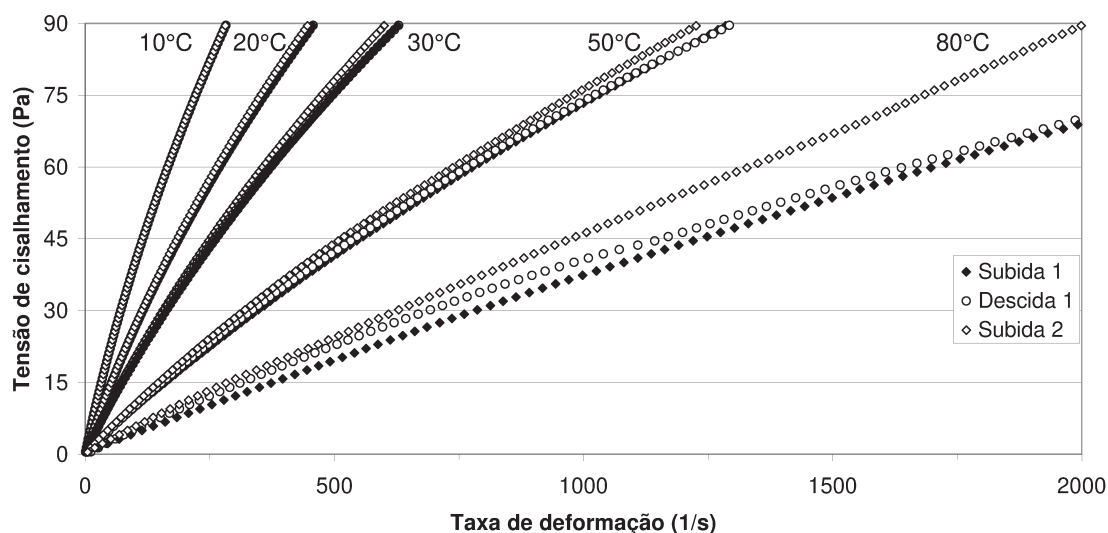


Figura 1. Curva de escoamento típica de uma solução de quitosana 0,2% (m/m) a 10, 20, 30, 50 e 80 °C.

A Figura 2 apresenta a variação da viscosidade com a taxa de deformação e temperatura. Perfis parecidos foram observados por Hwang e Shin (2000) que estudaram a variação do comportamento reológico da quitosana de acordo com a concentração da solução. Os valores de viscosidade obtidos por estes autores foram um pouco maiores

que os da Figura 2, o que pode estar relacionado ao grau de desacetilação da quitosana utilizada. Enquanto no presente trabalho o grau de desacetilação é de 80%, a quitosana avaliada por (Hwang & Shin, 2000) era 91% desacetilada e não comercial. Como já explicado anteriormente, maiores graus de desacetilação estão relacionadas à maior agregação entre as moléculas de quitosana, o que explica os maiores valores de viscosidade.

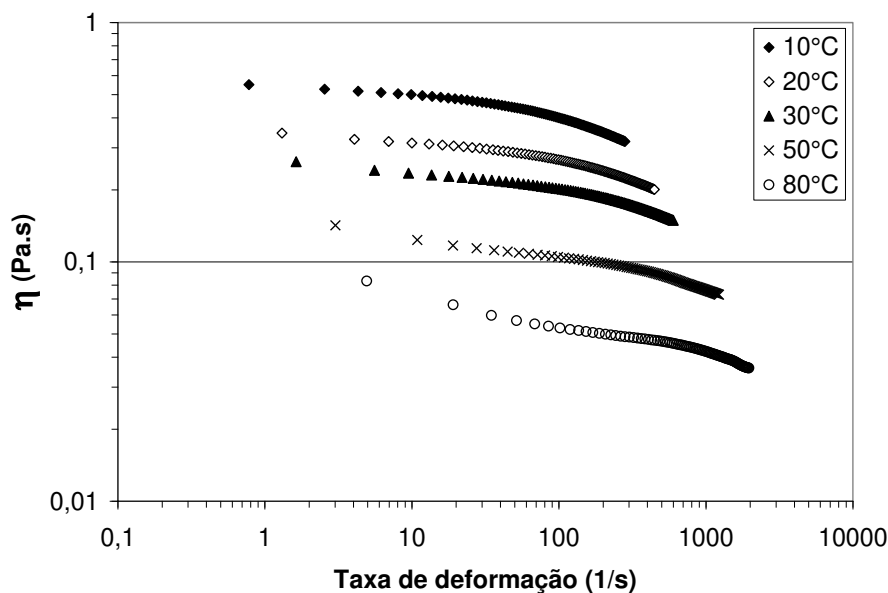


Figura 2. Viscosidade em estado estacionário (η) versus taxa de deformação de soluções de quitosana 0,2% (m/m) em diferentes temperaturas.

As curvas a 10 e 20 °C apresentaram duas regiões distintas. Até aproximadamente 4 s^{-1} a viscosidade observada para estas curvas é praticamente constante e independente da taxa de deformação enquanto que acima de 4 s^{-1} a viscosidade cai com o aumento da taxa de deformação (Figura 2). A primeira região corresponde à região de escoamento newtoniano que apresenta uma viscosidade constante (η_0) a taxas de deformação tendendo a zero. Nesta região o fluido apresenta comportamento newtoniano e a viscosidade permanece constante, pois a taxa de desentrelaçamento entre as moléculas devido às forças cisalhantes é a mesma que a de

novos entrelaçamentos (Graessley, 1974). A viscosidade inicial (η_0) tem sido frequentemente relacionada à estrutura de sistemas biopoliméricos (Hwang & Kokini, 1991), sendo uma representação da natureza microestrutural dos biopolímeros (Hwang & Shin, 2000). A Figura 2 mostra que a região de viscosidade constante tende a ser menor a altas temperaturas.

A partir de aproximadamente 4 s^{-1} , a viscosidade diminui com a taxa de deformação, indicando um comportamento típico de fluidos pseudoplásticos. Nesta região a taxa de desentrelaçamento entre as moléculas devido às forças cisalhantes é maior que a de entrelaçamento (Graessley, 1974) e a viscosidade é denominada viscosidade aparente, pois é uma função da taxa de deformação. Outros autores afirmam que nesta região há uma quebra estrutural irreversível e a queda da viscosidade estaria relacionada ao alinhamento molecular do biopolímeros (Glicksman, 1969; Marcotte et al., 2001).

O ajuste das curvas para a lei da potência (Equação 1) resultou nos valores de índice de consistência (k) e de escoamento (n) apresentados na Tabela 1.

Tabela 1. Parâmetros reológicos da lei da potência para solução de quitosana 0,2% (m/m) em diferentes temperaturas.

Temperatura (°C)	k (Pa s ^{n})	n	Erro padrão
10	0,965	0,804	8,39
20	0,626	0,816	7,43
30	0,482	0,825	7,45
50	0,264	0,827	6,61
80	0,118	0,867	5,53

Todas as amostras apresentaram índice de comportamento menor que 1, confirmando que as soluções de quitosana se comportam como um fluido pseudoplástico, principalmente a baixas temperaturas onde os valores observados de n foram ainda menores (Tabela 5). Já o índice de consistência (k), que é proporcional à viscosidade das amostras (Bae et al., 2008), aumentou com a redução da temperatura. A influência da

temperatura na viscosidade aparente das amostras pode ser melhor avaliada pela equação de Arrhenius (Equação 2). A Figura 3 mostra a variação da viscosidade aparente da solução de quitosana com a temperatura considerando a taxa de deformação de 50-s^{-1} .

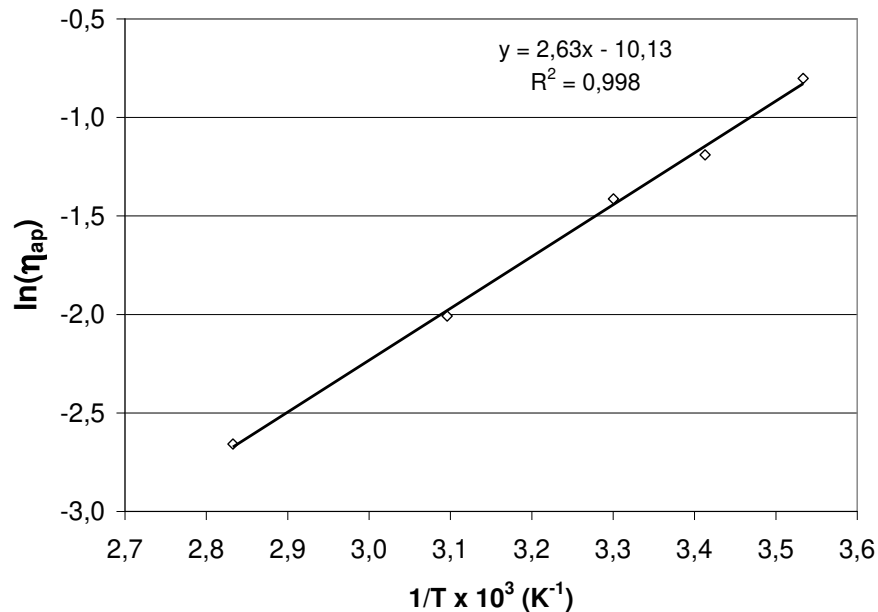


Figura 3. Efeito da temperatura sobre a viscosidade aparente (50-s^{-1}) de solução de quitosana 0,2 % (m/m).

Pelo ajuste dos pontos experimentais, tem-se que a energia de ativação (E_a) corresponde a $21,88 \text{ kJ}\cdot\text{mol}^{-1}$. Segundo de Paula et al. (2001), uma baixa energia de ativação ($E_a \leq 17 \text{ kJ}\cdot\text{mol}^{-1}$) indica o estabelecimento de poucas interações inter e intramoleculares entre as cadeias de polissacarídeos. Outros trabalhos relacionam a energia de ativação à forma estrutural dos polissacarídeos, sendo que baixos valores de E_a ($15 - 17 \text{ kJ}\cdot\text{mol}^{-1}$) estariam relacionados a polissacarídeos ramificados enquanto que polissacarídeos lineares apresentariam alta energia de ativação ($27 \text{ kJ}\cdot\text{mol}^{-1}$) (Bae et al., 2008; de Paula et al., 2001). Além disso, baixas energias de ativação também foram reportadas como tendo relação com fluidos cujas propriedades reológicas são pouco dependentes da temperatura (Chun & Yoo, 2004; Holdsworth, 1971). Portanto, a relativa

alta energia de ativação observada para a quitosana pode estar relacionada ao seu alto grau de desacetilação (80%) que favorece as interações intermoleculares na solução.

O valor da constante B, que corresponde à viscosidade à temperatura infinita (Bae et al., 2008; Togrul & Arslan, 2003) foi aproximadamente zero, confirmando a diminuição da viscosidade das soluções de quitosana a altas temperaturas.

3.2. Ensaio oscilatórios

A Figura 4 apresenta a viscosidade complexa (η^*) da solução de quitosana durante o aquecimento e resfriamento dentro do intervalo de viscoelasticidade linear das amostras. De forma geral, a viscosidade complexa das amostras diminuiu com o aquecimento até 80 °C da mesma forma que a viscosidade aparente, porém um rápido aumento da viscosidade foi observado entre 85 – 90 °C associado a uma grande histerese entre as curvas de aquecimento e resfriamento. Isso indica a ocorrência de uma reorganização molecular da quitosana com a temperatura. A histerese normalmente está relacionada à associação molecular ou grau de agregação em transições sol - gel de biopolímeros (Lai et al., 2000; Picone & Cunha, 2010), porém a formação de hidrogéis de quitosana só foi anteriormente reportada na presença de agentes reticulantes (George & Abraham, 2006). No valor de pH estudado (4,4) o aumento de temperatura não interfere no grau de desacetilação da quitosana, mas pode aumentar o grau de protonação dos grupos amino ($-NH_2$) aumentando a repulsão eletrostática intra e inter-molecular da quitosana que resulta na expansão das cadeias (Peng et al., 2010; Thongngam & McClements, 2004) e redução da mobilidade molecular da solução. No entanto, mais estudos são necessários para elucidar este comportamento.

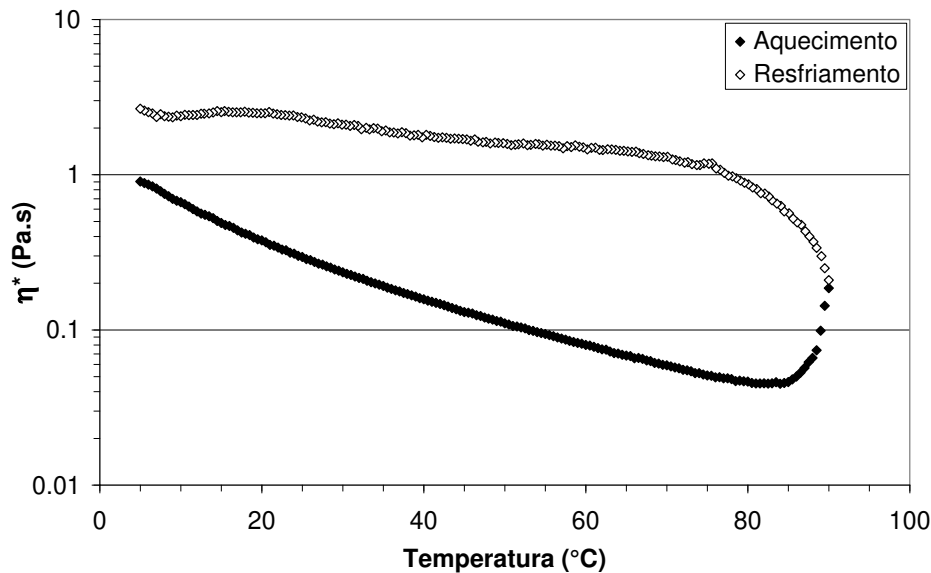


Figura 4. Viscosidade Complexa (η^*) durante o aquecimento (símbolos fechados) e resfriamento (símbolos abertos) de soluções de quitosana 0,2 % (m/m).

4. Conclusões

As soluções de quitosana apresentaram comportamento pseudoplástico dependente da temperatura. Em altas temperaturas a viscosidade das soluções diminui e tende a zero a temperaturas infinitas. Uma alta energia de ativação foi observada nos ensaios de escoamento, refletindo a linearidade das moléculas de quitosana devido ao seu alto grau de desacetilação. Os ensaios oscilatórios de varredura de temperatura confirmaram que não houve estruturação das soluções de quitosana nas condições estudadas, porém a alta histerese revelou uma mudança da organização molecular provavelmente associada à maior protonação da quitosana a altas temperaturas.

5. Referências Bibliográficas

- Bae, I. Y., Oh, I.-K., Lee, S., Yoob, S.-H., & Lee, H. G. (2008). Rheological characterization of levan polysaccharides from *Microbacterium laevaniformans*. *International Journal of Biological Macromolecules*, 42(1), 10-13.
- Chun, S. Y., & Yoo, B. (2004). Rheological behavior of cooked rice flour dispersions in steady and dynamic shear. *Journal of Food Engineering*, 65(3), 363-370.

- de Paula, R. C. M., Santana, S. A., & Rodrigues, J. F. (2001). Composition and rheological properties of *Albizia lebbek* gum exudate. *Carbohydrate Polymers*, 44(2), 133-139.
- George, M., & Abraham, T. E. (2006). Polyionic hydrocolloids for the intestinal delivery of protein drugs: Alginate and chitosan — a review. *Journal of Controlled Release*, 114(1), 1-14.
- Glicksman, M. (1969). Rheology, texture and gums. In Glicksman, M. *Gum technology in the food industry* pp. 56-93. New York and London: Academic Press.
- Graessley, W. W. (1974). *The entanglement concept in polymer rheology*. Berlin: Springer-Verlag.
- Holdsworth, S. D. (1971). Applicability of rheological models to the interpretation of flow and processing behaviour of fluid food products. *Journal of Texture Studies*, 2(4), 393-418.
- Hwang, J., & Kokini, J. L. (1991). Structure and rheological function of side branches of carbohydrate polymers. *Journal of Texture Studies*, 22(2), 123-167.
- Hwang, J. K., & Shin, H. H. (2000). Rheological properties of chitosan solutions. *Korea-Australia Rheology Journal*, 12(3/4), 175-179.
- Lai, V. M. F., Wong, P. A. L., & Lii, C. Y. (2000). Effects of cation properties on sol-gel transition and gel properties of kappa-carrageenan. *Journal of Food Science*, 65(8), 1332-1337.
- Marcotte, M., Taherian Hoshahili, A. R., & Ramaswamy, H. S. (2001). Rheological properties of selected hydrocolloids as a function of concentration and temperature. *Food Research International*, 34(8), 695-703.
- Peng, B., Hao, Y., Kang, H., Han, X., Peng, C., & Liu, H. (2010). Aggregation behavior of N-carboxyethylchitosan in aqueous solution: effects of pH, polymer concentration, and presence of a gemini surfactant. *Carbohydrate Research*, 345(1), 101-107.
- Picone, C. S. F., & Cunha, R. L. (2010). Interactions between milk proteins and gellan gum in acidified gels. *Food Hydrocolloids*, 24(5), 502-511.
- Thongngam, M., & McClements, D. J. (2004). Characterization of Interactions between Chitosan and an Anionic Surfactant. *Journal of Agricultural and Food Chemistry*, 52(4), 987-991.
- Togrul, H., & Arslan, N. (2003). Production of carboxymethyl cellulose from sugar beet pulp cellulose and rheological behaviour of carboxymethyl cellulose. *Carbohydrate Polymers*, 54(1), 73-82.